

AD-A050 477

NAVAL SURFACE WEAPONS CENTER WHITE OAK LAB SILVER SP--ETC F/G 17/9
COMPUTING R.O.C. FOR QUADRATIC DETECTORS.(U)
OCT 76 L E MILLER

UNCLASSIFIED

NSWC/WOL/TR-76-148

NL

1 OF 2

AD
A050 477



AD A 050477

NSWC/WOL TR 76-148

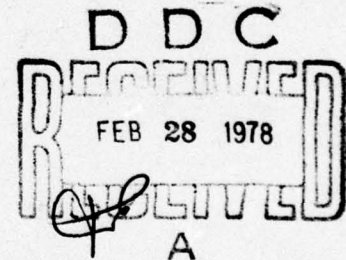
**COMPUTING R.O.C. FOR
QUADRATIC DETECTORS**

BY L. E. MILLER

ORDNANCE SYSTEMS DEVELOPMENT DEPARTMENT

OCTOBER 1976

Approved for public release; distribution unlimited.



NAVAL SURFACE WEAPONS CENTER

Dahlgren, Virginia 22448 • Silver Spring, Maryland 20910

AD No. —
DDC FILE COPY

UNCLASSIFIED

SECURITY CLASSIFICATION OF THIS PAGE (When Data Entered)

REPORT DOCUMENTATION PAGE		READ INSTRUCTIONS BEFORE COMPLETING FORM
1. REPORT NUMBER NSWC/WOL/TR-76-148	2. GOVT ACCESSION NO.	3. RECIPIENT'S CATALOG NUMBER
4. TITLE (and Subtitle) COMPUTING R.O.C. FOR QUADRATIC DETECTORS.		5. TYPE OF REPORT & PERIOD COVERED Final rept.
7. AUTHOR(s) 10 Dr. L. E. Miller		6. PERFORMING ORG. REPORT NUMBER
9. PERFORMING ORGANIZATION NAME AND ADDRESS Naval Surface Weapons Center White Oak Laboratory White Oak, Silver Spring, Maryland 20910		8. CONTRACT OR GRANT NUMBER(s)
11. CONTROLLING OFFICE NAME AND ADDRESS		10. PROGRAM ELEMENT, PROJECT, TASK AREA & WORK UNIT NUMBERS 62711N; A03S370B/001B; 7F11/100/000; WU65BB;
14. MONITORING AGENCY NAME & ADDRESS (if different from Controlling Office)		12. REPORT DATE 10 Oct 76
		13. NUMBER OF PAGES 106
		15. SECURITY CLASS. (of this report) Unclassified
16. DISTRIBUTION STATEMENT (of this Report) Approved for public release. Distribution unlimited.		15a. DECLASSIFICATION/DOWNGRADING SCHEDULE
17. DISTRIBUTION STATEMENT (of the abstract entered in Block 20, if different from Report)		
18. SUPPLEMENTARY NOTES		
19. KEY WORDS (Continue on reverse side if necessary and identify by block number) detection nonlinear analysis quadratic correlator detector probability		
20. ABSTRACT (Continue on reverse side if necessary and identify by block number) After defining a broad class of nonlinear detectors--those whose outputs are quadratic forms in terms of their inputs, exact probability distributions are derived when time samples are independent for three important sub-classes: coherent power (sum and square), correlator, and incoherent power (square and sum) detectors. An asymptotic method is used to obtain the distributions of the more general class of		

DD FORM 1 JAN 73 1473

EDITION OF 1 NOV 65 IS OBSOLETE
S/N 0102-014-6601

UNCLASSIFIED

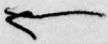
SECURITY CLASSIFICATION OF THIS PAGE (When Data Entered)

391596

12

UNCLASSIFIED

SECURITY CLASSIFICATION OF THIS PAGE(When Data Entered)

detector, including dependent time samples. Computer programs, example calculations, and many graphical results are included; the emphasis is on imparting a methodology which has been successful in computing R.O.C. for the detectors modeled, for both Gaussian and deterministic signals. 

UNCLASSIFIED

SECURITY CLASSIFICATION OF THIS PAGE(When Data Entered)

NSWC/WOL/TR 76-148

10 October 1976

Preface

This report demonstrates how receiver operating characteristics may be calculated for a broad class of nonlinear detectors, those whose outputs are quadratic forms of the inputs. Of particular interest is the capability to perform these calculations for arbitrary bandwidth-integration time products and dependent time samples. The work documented by this report was performed in the Signal and Digital Processing Branch under Task No. A03S370B/001B/7F11/100-000.

*Edward C. Whitman*EDWARD C. WHITMAN
By direction

ACCESSION INT	
HTS	White Section <input checked="" type="checkbox"/>
ZSC	Buff Section <input type="checkbox"/>
UNANNOUNCED	<input type="checkbox"/>
JUSTIFICATION	
BY	
DISTRIBUTION/AVAILABILITY CODES	
DATE	AVAIL. AND/OR SPECIAL
A	

TABLE OF CONTENTS

Title	Page
1. Introduction	5
PART I. SELECTED CASES INVOLVING INDEPENDENT SAMPLES	
2. Coherent Power Detector	13
3. Correlation Detector	30
4. Incoherent Power Detector	49
PART II. THE MORE GENERAL CASE	
5. Approximation to the Distribution of Quadratic Forms	62
6. ROC for General Quadratic Forms	71
References	91
APPENDICES	
A. Approximation to the Noncentral χ^2 Distribution	A-1
B. Derivation of Correlator PDF	B-1
C. Derivation of Square-And-Sum PDF	C-1
D. Equivalence of Lowpass and Narrowband Distributions	D-1

LIST OF FIGURES

Title	Page
1-1 Detector Model	12
2-1 Coherent Power Detector Model	14
2-2 Procedure for Computing ROC	18
2-3 Program to Compute the Chi-Squared Probability Integral	22
2-4 ROC for Gaussian Signal, $\alpha = 10^{-2}$	23
2-5 ROC for Gaussian Signal, $\alpha = 10^{-4}$	24
2-6 ROC for Deterministic Signal, $\alpha = 10^{-2}$	28
2-7 ROC for Deterministic Signal, $\alpha = 10^{-4}$	29
3-1 Correlation Detector Model	31
3-2 Program to Compute Correlation Detector Probabilities	38
3-3 Procedure to Compute False Alarm Thresholds	39
3-4 Method for Computing P_D	41
3-5 ROC for Deterministic Signal, $\alpha = 10^{-2}$	42
3-6 ROC for Deterministic Signal, $\alpha = 10^{-4}$	43
3-7 ROC for Gaussian Signal, $\alpha = 10^{-2}$	45
3-8 ROC for Gaussian Signal, $\alpha = 10^{-4}$	46
4-1 Incoherent Power Detector Model	50
4-2 Program to Compute Square and Sum Detector Probabilities	54
4-3 ROC for Deterministic Signal, $\alpha = 10^{-2}$	56
4-4 ROC for Deterministic Signal, $\alpha = 10^{-4}$	57
4-5 System Comparison: MDS vs WT, Deterministic Signal	58
4-6 ROC for Gaussian Signal, $\alpha = 10^{-2}$	59
4-7 ROC for Gaussian Signal, $\alpha = 10^{-4}$	60
4-8 System Comparison: MDS vs WT, Gaussian Signal	61
6-1 Outline of Computational Procedures	71
6-2 Program to Construct Matrices	73
6-3 Example of Computed Matrices	74
6-4 Program to Compute Narrowband Coefficients	76
6-5 Example Correlator Output PDF for M Varied ($\psi = .1$)	80
6-6 Example Correlator Output Probability Int. (M varied, $\psi = .1$)	81
6-7 Program to Compute PDF and Probability Integral	83
6-8 Example Incoherent Power Detector Prob. Int. (ψ varied)	84
6-9 Example Incoherent Power Detector Prob. Int. (ρ varied)	85
6-10 Four-Input Detectors	87
6-11 System Comparison, Gaussian Signal ($\alpha = 10^{-2}$)	89
6-12 System Comparison, Gaussian Signal ($\alpha = 10^{-4}$)	90

LIST OF TABLES

	Page
2-1 False Alarm Thresholds, Square-Law Detector	20
2-2 Gaussian Probability Integral	26
3-1 False Alarm Thresholds, Correlation Detector	40
3-2 Normalized False Alarm Thresholds, Correlation Detector	40
3-3 Detector Performance Comparison	48
4-1 False Alarm Thresholds, Square-And-Sum Detector	55
6-1 Example Expansion Coefficients for Narrowband Correlator	77
6-2 Example Square-Law Coefficients	72

COMPUTING R.O.C. FOR QUADRATIC DETECTORS

Prepared by:

L. E. Miller

CHAPTER 1

COMPUTING RECEIVER OPERATING CHARACTERISTICS
FOR QUADRATIC DETECTORS

1. INTRODUCTION

For comparing performances of different signal detector configurations, the functions known as receiver operating characteristics (ROC) are a standard tool. A given detector's ROC may be expressed

$$P_D = \gamma(h^2; \alpha) \quad (1-1)$$

where

$\gamma \equiv P_D$ = probability of detection

$\alpha \equiv P_{FA}$ = probability of false alarm

h^2 = input signal-to-noise ratio (SNR). (1-2)

The probabilities are computed on the assumption that the detector output undergoes a statistical test to decide between the hypotheses

H_0 : no signal is present

H_1 : a signal is present

The test is performed by comparing the value of the detector output z to a number τ called a threshold. If $z \geq \tau$, H_1 is accepted; if $z < \tau$, H_0 is accepted.

If there actually is no signal ($h^2 = 0$) and $z \geq \tau$, then the test yields an error of Type I or false alarm, with the probability

$$\alpha = \int_{\tau}^{\infty} dz p_z(z|h^2=0) \quad (1-4)$$

where $p_z(z|h^2=0)$ is the probability density function (pdf) of the detector output subject to the condition that there is no signal. If the value of τ is chosen to keep α at a particular value, then α is known as the "level" of the test.

If there actually is a signal present but $z < \tau$, the test yields an error of Type II, with the probability

$$\beta = \int_{-\infty}^{\tau} dz p_z(z|h^2 \neq 0). \quad (1-5)$$

Conversely, if $z \geq 0$ when there is a signal present, the test result is correct with the probability

$$\gamma = 1 - \beta = \int_{\tau}^{\infty} dz p_z(z|h^2 \neq 0). \quad (1-6)$$

If τ has been constrained by α so that $\tau = \tau(\alpha)$, then $\gamma = \gamma(h^2; \alpha)$ and is known as the "power function" of the test.

It is clear that to compute the ROC for a given detector requires knowledge of the probability distribution of the detector output. Often the functional form of this distribution is very difficult to obtain analytically.

The purpose of this report is to document methods for calculating the ROC of a class of detectors. Attention is first paid, in

Chapters 2-4, to cases in which samples of the detector inputs are considered independent, thus allowing direct calculation of the ROC. In Chapters 5 and 6, the more general case is treated, using an approximation method.

1.1 Channel Model.

It is assumed that the detector has one or more inputs $x_i(t)$, where

$$x_i(t) = s_i(t) + n_i(t), \quad i=1,2,\dots,L. \quad (1-7)$$

and the noise terms $n_i(t)$ are jointly Gaussian, stationary random processes with zero means and $L \times L$ covariance matrix \sum_n , with elements

$$E\{n_i^2(t)\} = \sigma_i^2$$

$$E\{n_i(t)n_j(t)\} = \rho_{ij}\sigma_i\sigma_j, \quad i \neq j. \quad (1-8)$$

Two types of signals will be considered, deterministic and random. Random signals will be considered to be from jointly Gaussian, stationary random processes with zero means and $L \times L$ covariance matrix \sum_s , with elements

$$E\{s_i^2(t)\} = d_i^2$$

$$E\{s_i(t)s_j(t)\} = r_{ij}d_id_j, \quad i \neq j. \quad (1-9)$$

Bandwidth and spectra. Two categories of detector bandwidth will be treated, low-pass and narrowband. In either case, a (two-sided) bandwidth of W hertz and ideal (flat) response is assumed. This

bandwidth is lumped with the signal and noise models, so that, assuming flat spectra over the bandwidth, we have

$$\sigma_1^2 = N_1 W, d_1^2 = P_1 W \quad (1-10)$$

for the random waveforms. Deterministic signals are modeled as

$$s_1(t) = S_1(t) \cos[\omega_0 t - \theta_1(t)] \quad (1-11)$$

in which the envelope S_1 and phase θ_1 are slowly varying, so that signal power is given by

$$s_1^2(t) = s_1^2, \text{ lowpass signal}$$

$$s_1^2(t) = S_1^2/2, \text{ narrowband signal.} \quad (1-12)$$

Thus input SNR's are taken to be

$$h^2 = \begin{cases} s^2/\sigma^2, & \text{lowpass deterministic signal} \\ S^2/2\sigma^2, & \text{narrowband deterministic signal} \\ d^2/\sigma^2, & \text{random signal.} \end{cases} \quad (1-13)$$

An alternate form for the information represented in a detector's ROC is to write

$$h^2 = h^2(\gamma, \alpha), \quad (1-14)$$

a function which answers the question, "What SNR is required to produce $P_D = \gamma$ when the false alarm probability is α ?" Often this

relationship is abbreviated by giving its value for specified $(\gamma, \alpha) = (\gamma_1, \alpha_1)$, say $(\gamma, \alpha) = (.5, 10^{-4})$, and calling it "minimum detectable signal (MDS):

$$\text{MDS} = h^2(\gamma_1, \alpha_1). \quad (1-15)$$

Also, for deterministic signals a number called "detection threshold" (DT) is often quoted and is the MDS referred to a one-hertz bandwidth:

$$\text{DT} = W h^2(\gamma_1, \alpha_1). \quad (1-16)$$

In the case of narrowband signals and noise, the detector inputs can be written

$$\begin{aligned} x_i(t) &= X_i(t) \cos[\omega_0 t - \phi_i(t)] \\ &= x_{ic}(t) \cos \omega_0 t + x_{is}(t) \sin \omega_0 t \\ &= (n_{ic} + s_{ic}) \cos \omega_0 t + (n_{is} + s_{is}) \sin \omega_0 t. \end{aligned} \quad (1-17)$$

Under this expansion, n_{ic} and n_{is} are independent and each set $\{n_{ic}\}$ and $\{n_{is}\}$ has covariance matrix Σ_n . A similar statement is true of the signal terms if they are Gaussian.

The envelopes of the random inputs' correlation functions have the factors

$$\begin{aligned} \sin(\pi W \Delta t) / \pi W \Delta t, & \text{ narrowband} \\ \sin(2\pi W \Delta t) / \pi W \Delta t, & \text{ lowpass.} \end{aligned} \quad (1-18)$$

Therefore, if samples of the inputs are taken $1/W$ and $1/2W$ seconds apart, respectively, the samples are uncorrelated and, being Gaussian, independent.

1.2 Detector Model.

Let M samples of the L detector inputs be assembled to form a vector:

$$\xi' \triangleq [x_1(t_1), \dots, x_L(t_1); x_1(t_2), \dots, x_L(t_2); \dots; x_1(t_M), \dots, x_L(t_M)], \quad (1-19)$$

where the prime (') indicates transpose. Detectors will be considered which produce as an output decision variable or statistic the quadratic form

$$z = \xi' Q_M \xi; \quad Q_M \text{ LMxLM}, \quad (1-20)$$

and therefore termed "quadratic detectors." In Part II (Chapters 5,6), expressions will be developed at this level of generality in order to treat correlated input samples. However, in Part I (Chapters 2-4) and in calculations based on the more general cases, it will be assumed that

$$z = \frac{1}{M} \sum_{j=1}^M \xi'_j Q \xi_j, \quad Q \text{ LxL} \quad (1-21)$$

where

$$\xi'_j = [x_1(t_j), x_2(t_j), \dots, x_L(t_j)]. \quad (1-22)$$

Effectively, this is the same as saying that Q_M is a block diagonal matrix with identical $L \times L$ diagonals Q/M .

The detector form (1-21) is illustrated in Figure 1-1. The "quadratic processor" is assumed memoryless, so that the sampling operation can be placed after the processor for convenience. This model is of interest because it is an idealized representation of the non-sampled case with post-detection integration. That is,

$$\frac{1}{M} \sum_{j=1}^M z(j\Delta t) \leftrightarrow \frac{1}{T} \int_0^T dt z(t). \quad (1-23)$$

If $\Delta t = 1/W$, then the equivalence $M = WT$ is made, and is commonly referred to as the "time-bandwidth product" in communications theory.

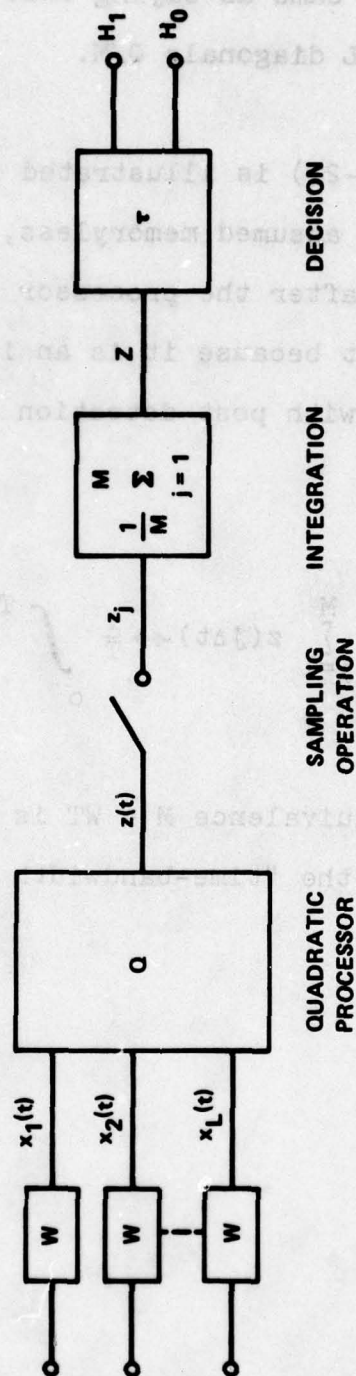


FIG. 1-1 DETECTOR MODEL.

CHAPTER 2

COHERENT POWER DETECTOR

In this chapter, and in the two which follow, three types of quadratic detector of frequent interest are treated for the case in which time samples $\{z_j\}$ of the processor output are independent, allowing us to compute ROC exactly.

2.1 Detector Configuration.

A great variety of practical detectors can be modeled by the configuration of Figure 2-1, in which the detector inputs $x_i(t)$ are summed and then squared. Commonly it is called the "square-law detector", and sometimes the "conventional detector."

Let the sum of inputs be

$$x(t_j) = \sum_{i=1}^L x_i(t_j) \quad (2-1)$$

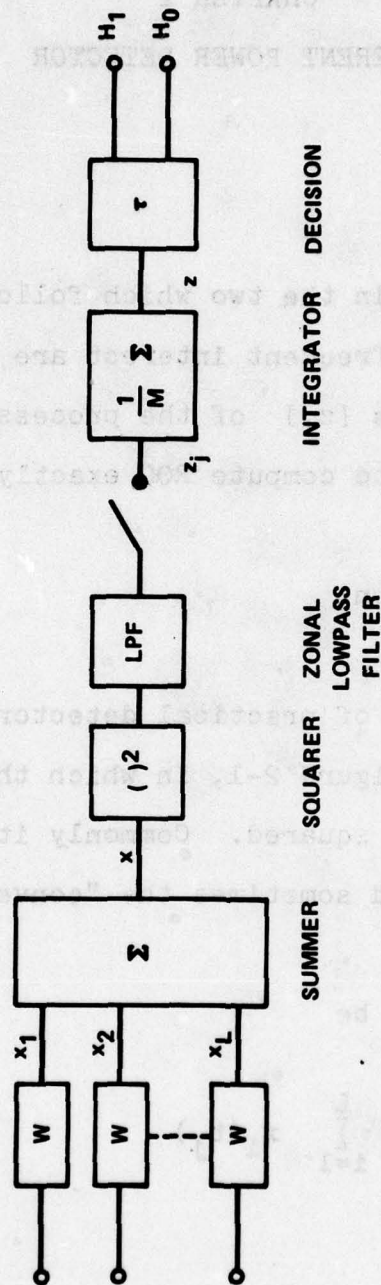


FIG. 2-1. COHERENT POWER DETECTOR MODEL

so that

$$E\{x\} = \begin{cases} s = \sum s_1 & \text{DS*} \\ 0 & \text{RS} \end{cases} \quad (2-2)$$

and

$$\text{Var}\{x\} = \begin{cases} \sigma^2 = \sum \rho_{1j} \sigma_1 \sigma_j & \text{DS} \\ \sigma^2 + d^2 = \sigma^2 + \sum r_{1j} d_1 d_j & \text{RS} \end{cases} \quad (2-3)$$

Thus, for example, $\sigma^2 = \sigma_1^2 + 2\rho\sigma_1\sigma_2 + \sigma_2^2$ for $L=2$ and a deterministic signal.

In the lowpass input case, the detector output is

$$z = \frac{1}{M} \sum_{j=1}^M x_j^2, \quad M=2WT. \quad (2-4)$$

Now, the sum of the squares of v independent Gaussian random variables with unit variances and means μ_1 is a noncentral chi-squared variable (χ'^2) with v degrees of freedom and noncentrality parameter $\lambda = \sum \mu_1^2$. Therefore, we have

$$\frac{2WTz}{\sigma^2} \text{ is } \chi'^2\{2WT, 2WT\lambda\} \quad \text{DS}$$

and

$$\frac{2WTz}{\sigma^2 + d^2} \text{ is } \chi^2\{2WT\}, \quad \text{RS} \quad (2-5)$$

where χ^2 denotes a (central) chi-squared variable - one for which $\lambda=0$.

*Using "DS" for deterministic signal and "RS" for random signal.

In the narrowband input case the detector output is

$$z = \frac{1}{M} \sum_{j=1}^M \frac{x_{cj}^2 + x_{sj}^2}{2}, \quad M=WT \quad (2-6)$$

Since $E\{x_{c1}\} = S_1 \cos \theta_1$ and $E\{x_{s1}\} = S_1 \sin \theta_1$ for deterministic signals, we have

$$\begin{aligned} \frac{2WTz}{\sigma^2} & \text{ is } \chi'^2\{2WT, 2WTh^2\} \quad \text{DS} \\ \frac{2WTz}{\sigma^2 + d^2} & \text{ is } \chi^2\{2WT\}, \quad \text{RS} \end{aligned} \quad (2-7)$$

the same result as for the lowpass case.

2.2 Receiver Operating Characteristics

From (1-6) we have

$$\begin{aligned} P_D \equiv \gamma &= \int_{\tau}^{\infty} dz p_z(z) \\ &= \int_{2WT\tau/\sigma^2}^{\infty} dv p_{\chi'^2}(v|2WT, 2WTh^2) \\ &\equiv Q(2WT\tau/\sigma^2 | 2WT, 2WTh^2), \quad \text{DS} \end{aligned} \quad (2-8)$$

where $Q(\chi'^2|v, \lambda)$ is the noncentral chi-squared probability integral.

Similarly, we have

$$\gamma = Q[2WT\tau/(\sigma^2 + d^2) | 2WT], \quad \text{RS} \quad (2-9)$$

where $Q(\chi^2|v)$, the chi-squared probability integral, is widely tabulated.

EXAMPLE 2-1. Problem: What is the probability that a chi-squared random variable with 18 degrees of freedom exceeds the value 30?

Solution: Using Table 26.7 of [1], we find that $Q(30|18) = .03745$.

Setting $h^2=0$ in (2-8) or $d^2=0$ in (2-9) yields

$$P_{FA} \equiv \alpha = Q(2WT\tau/\sigma^2 | 2WT). \quad (2-10)$$

EXAMPLE 2-2. Problem: Find the threshold value τ necessary to maintain a false alarm probability of 10^{-4} when $WT = 100$.

Solution: In Table II of [2], the function $P(a,c) \equiv 1-Q(2a/2c)$ is tabulated. Under $P=.9999$ and $c=100$ we find that $a=141.530$ or $\tau=2\sigma^2 a/2WT=1.4153\sigma^2$.

The procedure for obtaining ROC is diagrammed in Figure 2-2. For either type of signal, the process begins with the selection of a false alarm probability α . Using the identity

$$\alpha \equiv Q(\chi_{1-\alpha}^2 | v) \quad (2-11)$$

and (2-10), the false alarm threshold is found to be

$$\tau_\alpha = \frac{\sigma^2}{2WT} \chi_{1-\alpha}^2(2WT). \quad (2-12)$$

We may speak also of a normalized false alarm threshold d_α , given by

$$d_\alpha = \frac{\tau_\alpha - E\{z\}}{\sqrt{\text{Var}\{z\}}} = \frac{\chi_{1-\alpha}^2(2WT) - 2WT}{2\sqrt{WT}}, \quad (2-13)$$

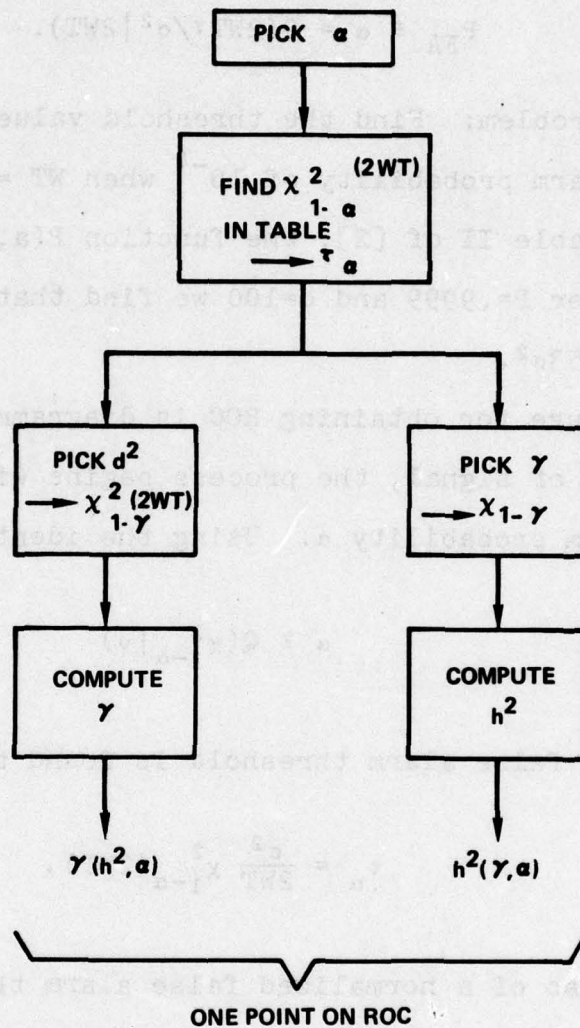


FIG. 2-2. PROCEDURE FOR COMPUTING ROC

since $E\{\chi^2(v)\} = v$ and $\text{Var}\{\chi^2(v)\} = 2v$. The quantity d_α is interpreted as the number of detector output noise standard deviations above the mean at which the threshold τ must be set to produce a false alarm probability α .

EXAMPLE 2-3. Problem: Find d_α for $WT=10$ and $\alpha=.01$.

Solution: The table on page 252 of [3] gives $P=Q(\chi^2|v)$. For $P=.01$ and $v=20$, we find $\chi^2_{.99}(20)=37.566$. Therefore $d_\alpha=(37.566-20)/2\sqrt{10}=2.777$.

For convenience, values of $\chi^2_{1-\alpha}(2WT)$ and d_α are given in Table 2-1 for various values of α and WT . Also d_α is plotted vs α for $WT=1, 10, 50, \infty$ in Figure 4 of [4].

Having fixed the value of τ_α , the ROC is a plot of $P_D=\gamma(h^2)$ or, if it is more convenient, $h^2=h^2(\gamma)$. For Gaussian signals, from (2-9) and (2-12) we have

$$\gamma = Q[\chi^2_{1-\alpha}(2WT)/(1+h^2)|2WT]. \quad \text{RS} \quad (2-14)$$

One approach is to interpolate in a chi-squared table to find the value of $Q(\chi^2|v)$ corresponding to the number

$$\chi^2_{1-\gamma}(2WT) = \frac{\chi^2_{1-\alpha}(2WT)}{1+h^2}. \quad (2-15)$$

However, it is simpler to calculate Q , since it is given by the finite sum [1]

$$\begin{aligned} Q(\chi^2|2v) &= e^{-\chi^2/2} \sum_{k=0}^{v-1} (\chi^2/2)^k / k! \\ &= e^{-\chi^2/2} e_{v-1}(\chi^2/2), \end{aligned} \quad (2-16)$$

α	10^{-1}	10^{-2}	10^{-3}	10^{-4}	10^{-6}
WT					
	$\chi^2_{1-\alpha} (2WT)^*$				
1	4.60517	9.21034	13.816	18.421	27.64
2	7.77944	13.2767	18.467	25.513	33.38
5	15.9871	23.2093	29.588	35.564	46.86
10	28.4120	37.5662	45.315	52.386	65.42
20	51.8050	63.6907	73.402	82.062	97.66
50	118.498	135.807	149.449	161.319	182.12
100	226.0210	249.446	267.458	283.060	309.84
	$d\alpha$, NORMALIZED FALSE ALARM THRESHOLD**				
1	1.3026	3.6052	5.9080	8.2105	12.82
2	1.3362	3.2798	5.1149	6.8989	10.3874
5	1.3388	2.9537	4.3800	5.7163	8.2421
10	1.3301	2.7775	4.0027	5.1207	7.1815
20	1.3198	2.6487	3.7345	4.7027	6.4466
50	1.3080	2.5319	3.4966	4.3359	5.8068
100	1.3011	2.4723	3.3729	4.1530	5.4920
∞	1.28155	2.32635	3.09023	3.71902	4.7534

NOTES:

*VALUES FOR WT = 100 AND/OR $\alpha = 10^{-6}$ TAKEN FROM TABLE II OF [2];
THE REMAINDER FROM TABLE 26.8 OF [1].

**COMPUTED USING VALUES OF $\chi^2_{1-\alpha} (2WT)$ FROM TABLE II OF [2].

TABLE 2-1. FALSE ALARM THRESHOLDS.

using the program of Figure 2-3. This calculation was performed for a number of cases, and the results are plotted in Figures 2-4 and 2-5 for $\alpha=10^{-2}$ and 10^{-4} , respectively.

EXAMPLE 2-4. Problem: - What integration time T is required to achieve 90% detection and 1% false alarm probabilities when the input SNR is zero dB, if the bandwidth is 0.25 Hz?

Solution: From Figure 2-4, $\gamma=.9$ and $h^2=0$ dB correspond approximately to $WT=25$. Thus about 100 seconds of integration time is required.

For deterministic signals, from (2-8) and (2-12) we have

$$\gamma = Q[\chi^2_{1-\alpha}(2WT)|2WT, 2WTh^2]. \quad (2-17)$$

Here, direct calculation is not as simple since the noncentral chi-squared probability integral is given by the infinite sum [1]

$$Q(\chi'^2|v, \lambda) = e^{-\lambda/2} \sum_{k=0}^{\infty} \frac{(\lambda/2)^k}{k!} Q(\chi'^2|v+2k). \quad (2-18)$$

Tables for this function are relatively rare [5,6], of which [6] is fairly extensive for $2WT \leq 100$ and $\alpha \geq 10^{-3}$. For $WT=1$, Q is well known to communications engineers as Marcum's Q -function, thoroughly tabulated in [7] and given by nomograph in [8]. Urkowitz [9] uses a nomograph for the (central) chi-squared probability integral [10] and an approximation technique due to Patnaik [11].

In order to avoid both the labor of interpolating tables and the inherent inaccuracy of nomographs, an excellent Gaussian approximation

76/09/10. 14.22.33.

PROGRAM CHI534

```

10 READ A, X, M
20 PRINT "M = "M,"A ="A,"X = "X
30 PRINT
40 PRINT "SNR(DB)","PD"
50 FOR V=2.5 TO 3 STEP .1
60 H=10^V
70 Y=.5* X/(1+H)
80 S1=S2=1
90 FOR K=1 TO M-1
100 S2=S2*Y/K
110 S1=S1+S2
120 NEXT K
130 S1=S1*EXP(-Y)
140 PRINT 10*V,S1
150 NEXT V
160 STOP
170 DATA .0001
175 DATA 23.513,2
180 END

```

$$H \equiv h^2$$

$$X \equiv \chi^2_{1-\alpha}$$

$$Y \equiv \chi^2_{1-\gamma}$$

$$S1 \equiv Q(\chi^2_{1-\gamma} | 2M)$$

FIGURE 2-3

Program to Compute the Chi-Squared Integral

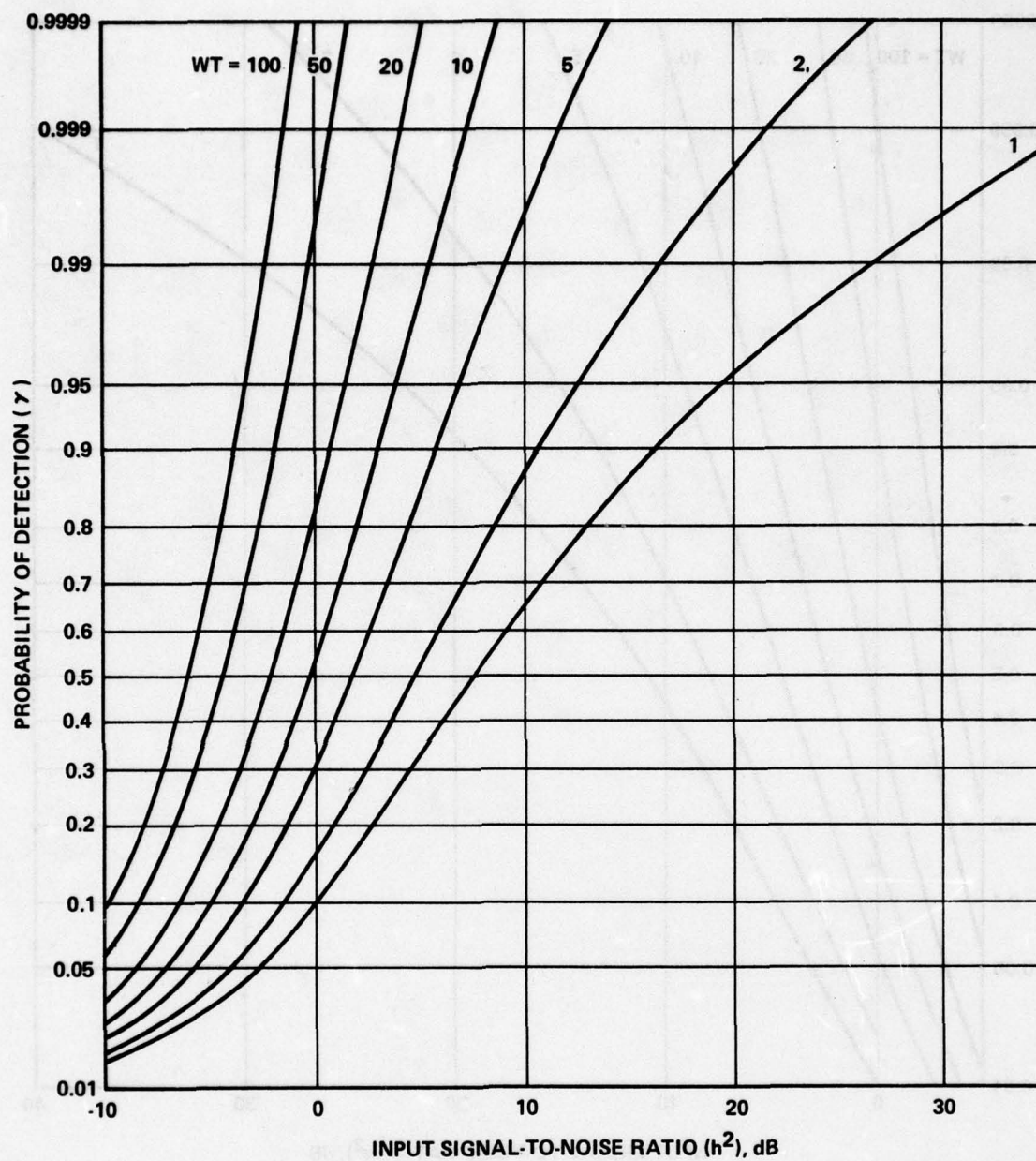


FIG. 2-4 RECEIVER OPERATING CHARACTERISTICS, SQUARE-LAW DETECTOR, FOR $PFA = 0.01$ AND WT VARIED (RANDOM SIGNAL)

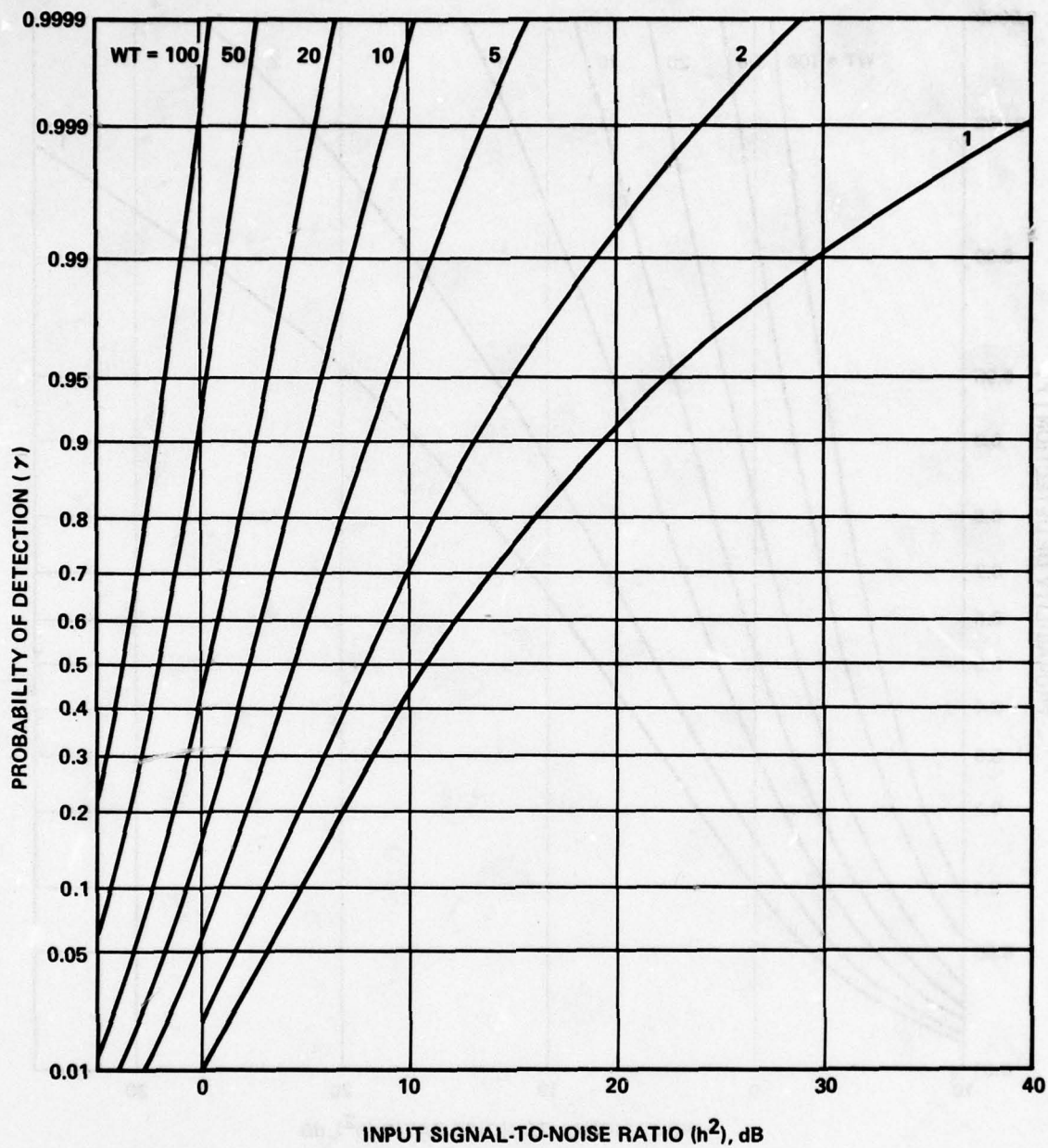


FIG. 2-5 RECEIVER OPERATING CHARACTERISTICS, SQUARE-LAW DETECTOR, FOR PFA = 0.0001 AND WT VARIED (RANDOM SIGNAL)

to the noncentral chi-squared distribution, due to Sankaran [12], was used to obtain h^2 in terms of γ . In Appendix A it is shown that

$$h^2(\gamma) = \frac{d_\alpha}{\sqrt{WT}} + \frac{d_\gamma^2 + 1}{2WT} - \frac{d_\gamma}{\sqrt{WT}} \sqrt{\frac{2d_\alpha}{\sqrt{WT}} + \frac{2WT+1}{2WT}}, \quad (2-19)$$

where d_γ is defined by

$$\gamma \equiv Q(d_\gamma) = \frac{1}{2}[1 - \text{erf}(d_\gamma/\sqrt{2})], \quad (2-20)$$

$Q(x)$ being the Gaussian probability integral* and $\text{erf}(x)$ the error function, both universally known and tabulated. For reference, Table 2-2 provides several values of d_γ .

It is interesting to note that if the value of h^2 yielding $\gamma=.5$ is taken to be the minimum detectable signal (MDS), then from (2-19) it is given simply as

$$\text{MDS} = \frac{d_\alpha}{\sqrt{WT}} + \frac{1}{2WT}. \quad (2-21)$$

This is to be compared with the heuristic value of $\text{MDS} = d_\alpha/\sqrt{WT}$ in [4], which is based on distributional properties when WT is very large (i.e., the central limit theorem).

EXAMPLE 2-5. Problem: Find the MDS for $\alpha=10^{-4}$ and $WT=50$.

Solution: Since no table of γ is available for this value of α , we use the approximation (2-21), yielding $\text{MDS} = 4.3359/\sqrt{50} + .01 = .6232 = -2.05$ dB, where d_α was obtained from Table 2-1. If $W=.1$ Hz, the

*One of the spinoffs from this study is the discovery that Marcum's Q-function is rather easily and accurately approximated by

$$Q(\alpha, \beta) \approx Q(\sqrt{\beta-1/2} - \sqrt{\alpha+1/2}).$$

γ	$d\gamma$
10^{-6}	4.75342
10^{-5}	4.26489
10^{-4}	3.71902
.0002	3.54008
.0005	3.29053
.001	3.09023
.002	2.87816
.005	2.57583
.01	2.32635
.02	2.05375
.05	1.64485
.1	1.28155
.2	0.84162
.3	0.52440
.4	0.25335
.5	0

$$\gamma = Q(d\gamma)$$

NOTES:

(1) $d_1\gamma = -d\gamma$

(2) VALUES TAKEN FROM TABLES 26.5
AND 26.6 OF [1].

TABLE 2-2. GAUSSIAN PROBABILITY INTEGRAL.

corresponding detection threshold is

$$DT = (.1) \text{ MDS} = -12.05 \text{ dB.}$$

Using (2-19), ROC were computed for the square-law detector with deterministic input signal, and are displayed in Figures 2-6 and 2-7 for $\alpha = 10^{-2}$ and 10^{-4} , respectively.

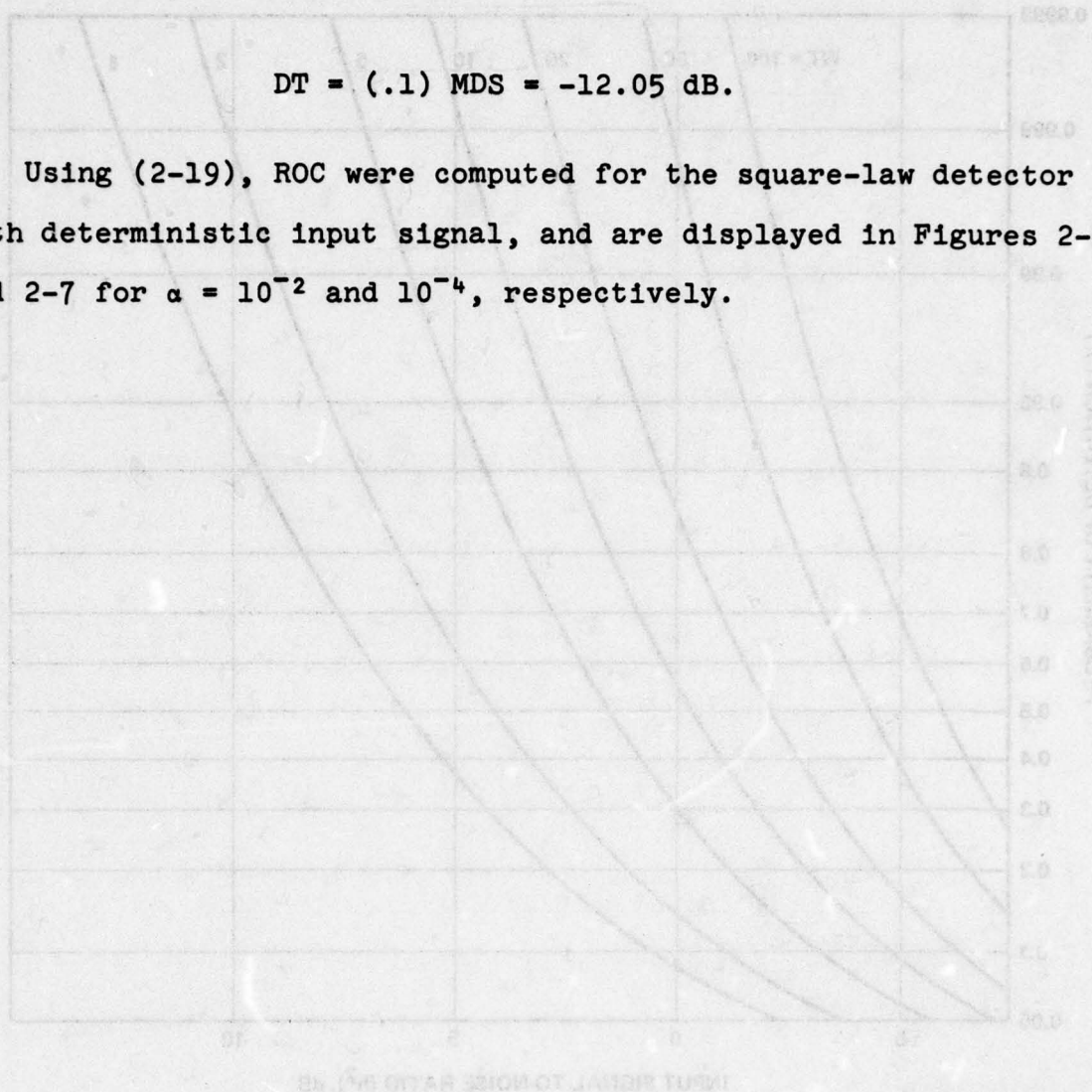


FIG. 2-8 RECEIVER OPERATING CHARACTERISTICS, SQUARE-LAW DETECTOR, FOR $\alpha = 10^{-2}$ AND $\alpha = 10^{-4}$ AND VARIOUS DETECTION THRESHOLDS

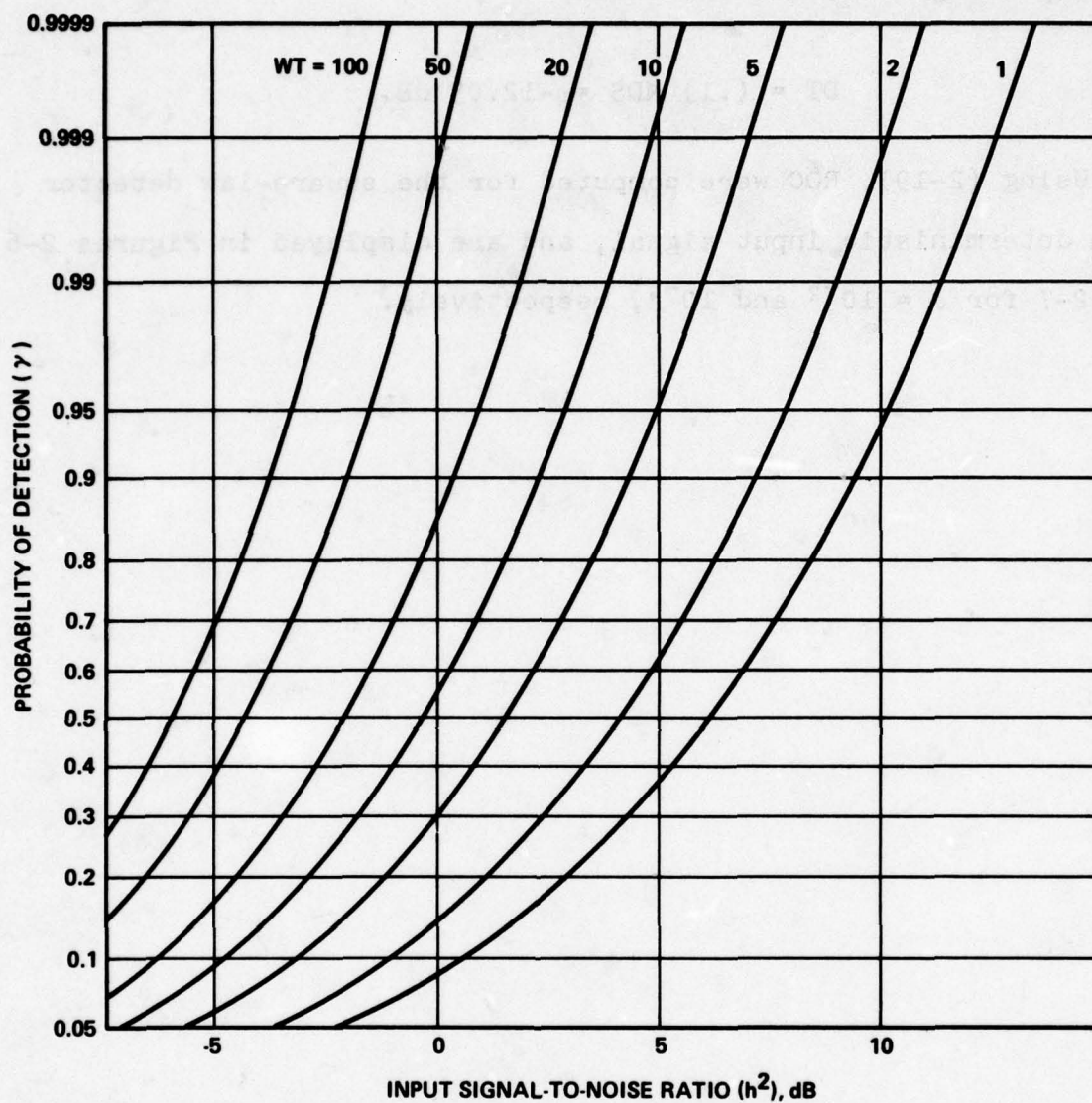


FIG. 2-6 RECEIVER OPERATING CHARACTERISTICS, SQUARE-LAW DETECTOR, FOR PFA = 0.01 AND WT VARIED (DETERMINISTIC SIGNAL)

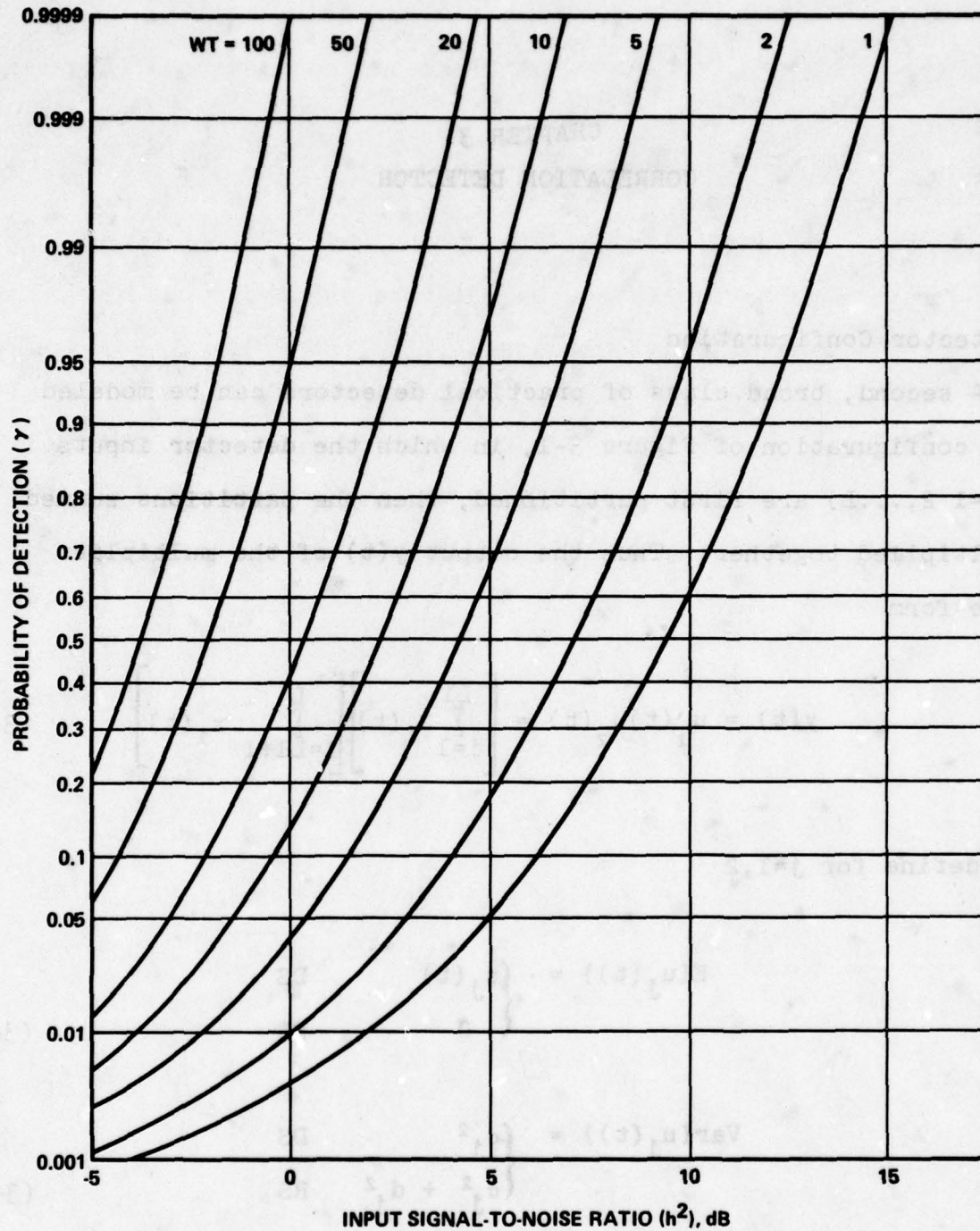


FIG. 2-7. RECEIVER OPERATING CHARACTERISTICS, SQUARE-LAW DETECTOR, FOR PFA = 0.0001 AND WT VARIED (DETERMINISTIC SIGNAL)

CHAPTER 3

CORRELATION DETECTOR

3.1 Detector Configuration

A second, broad class of practical detectors can be modeled by the configuration of Figure 3-1, in which the detector inputs $\{x_i; i=1,2,\dots,L\}$ are first partitioned, then the partitions summed and multiplied together. Thus the output $y(t)$ of the multiplier has the form

$$y(t) = u_1(t)u_2(t) = \left[\sum_{i=1}^{L1} x_i(t) \right] \left[\sum_{i=L1+1}^L x_i(t) \right] \quad (3-1)$$

Let us define for $j=1,2$

$$E\{u_j(t)\} = \begin{cases} s_j(t) & \text{DS} \\ 0 & \text{RS} \end{cases} \quad (3-2)$$

$$\text{Var}\{u_j(t)\} = \begin{cases} \sigma_j^2 & \text{DS} \\ \sigma_j^2 + d_j^2 & \text{RS} \end{cases} \quad (3-3)$$

and

$$\text{Cov}\{u_1(t), u_2(t)\} = \begin{cases} \rho\sigma_1\sigma_2 & \text{DS} \\ \rho\sigma_1\sigma_2 + rd_1d_2 & \text{RS} \end{cases} \quad (3-4)$$

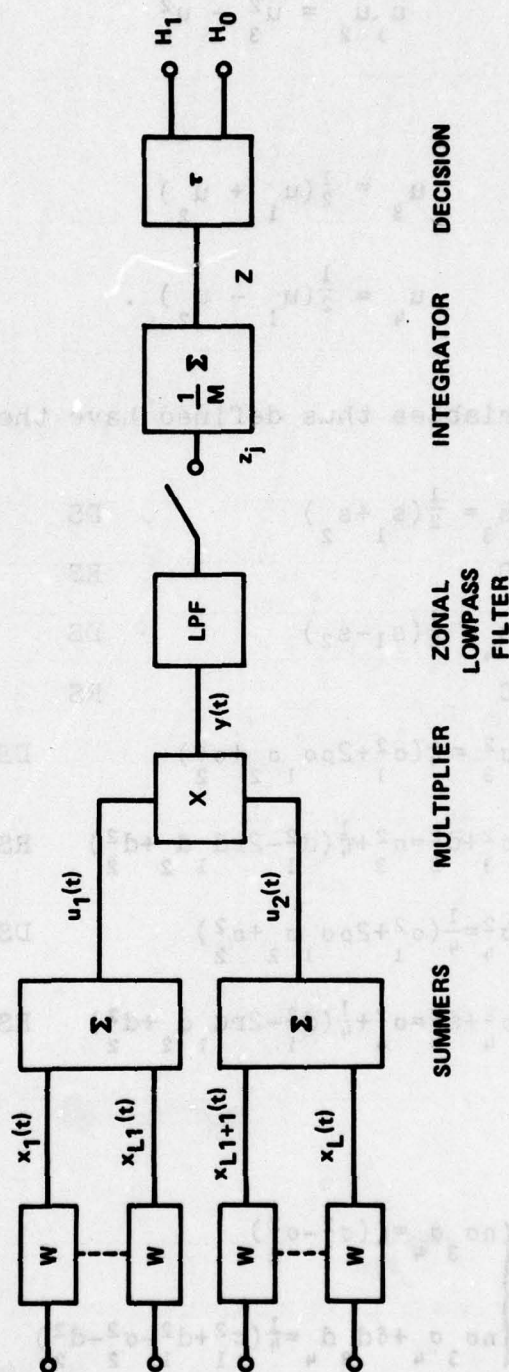


FIG. 3-1. CORRELATION DETECTOR MODEL

The product can be written

$$u_1 u_2 = u_3^2 - u_4^2 \quad (3-5)$$

where

$$\begin{aligned} u_3 &= \frac{1}{2}(u_1 + u_2) \\ u_4 &= \frac{1}{2}(u_1 - u_2) \end{aligned} \quad (3-6)$$

The two new Gaussian variables thus defined have the moments

$$\begin{aligned} E\{u_3\} &= \begin{cases} s_3 = \frac{1}{2}(s_1 + s_2) & \text{DS} \\ 0 & \text{RS} \end{cases} \\ E\{u_4\} &= \begin{cases} s_4 = \frac{1}{2}(s_1 - s_2) & \text{DS} \\ 0 & \text{RS} \end{cases} \\ \text{Var}\{u_3\} &= \begin{cases} \sigma_3^2 = \frac{1}{4}(\sigma_1^2 + 2\rho\sigma_1\sigma_2 + \sigma_2^2) & \text{DS} \\ \sigma_3^2 + d_3^2 = \sigma_3^2 + \frac{1}{4}(d_1^2 - 2rd_1d_2 + d_2^2) & \text{RS} \end{cases} \\ \text{Var}\{u_4\} &= \begin{cases} \sigma_4^2 = \frac{1}{4}(\sigma_1^2 - 2\rho\sigma_1\sigma_2 + \sigma_2^2) & \text{DS} \\ \sigma_4^2 + d_4^2 = \sigma_4^2 + \frac{1}{4}(d_1^2 - 2rd_1d_2 + d_2^2) & \text{RS} \end{cases} \end{aligned} \quad (3-7)$$

and

$$\begin{aligned} \text{Cov}\{u_3, u_4\} &= \begin{cases} \rho\sigma_3\sigma_4 = \frac{1}{4}(\sigma_1^2 - \sigma_2^2) & \text{DS} \\ \rho\sigma_3\sigma_4 + d_3d_4 = \frac{1}{4}(\sigma_1^2 + d_1^2 - \sigma_2^2 - d_2^2) & \text{RS} \end{cases} \end{aligned} \quad (3-9)$$

In the lowpass case the detector output is

$$z = \frac{1}{M} \sum_{i=1}^M [u_3^2(t_i) - u_4^2(t_i)]$$

$$\Delta z_1 - z_2, \quad M=2WT \quad (3-10)$$

where for deterministic signals

$$\left\{ \begin{array}{l} \frac{2WTz_1}{\sigma_3^2} \text{ is } \chi'^2(2WT, 2WTh_3^2) \\ \frac{2WTz_2}{\sigma_4^2} \text{ is } \chi'^2(2WT, 2WTh_4^2) \end{array} \right. \quad \text{DS} \quad (3-11)$$

and for random signals

$$\frac{2WTz_1}{\sigma_3^2 + d_3^2} \text{ and } \frac{2WTz_2}{\sigma_4^2 + d_4^2} \text{ are } \chi^2(2WT). \quad \text{RS} \quad (3-12)$$

Thus the detector output is the difference of two scaled, correlated (central or noncentral) chi-squared random variables. However, from (3-9), if the input noise power is the same in each channel ($\sigma_1 = \sigma_2 = \sigma$), these output variables are uncorrelated (and independent) for deterministic signals; for Gaussian signals, the same effect results if $\sigma_1^2 + d_1^2 = \sigma_2^2 + d_2^2$.

In the narrowband case the detector output is

$$\begin{aligned}
 &= \frac{1}{M} \sum_{i=1}^M \left[\frac{u_{3ci}^2 + u_{3si}^2}{2} - \frac{u_{4ci}^2 + u_{4si}^2}{2} \right] \\
 &= \frac{1}{2M} \sum_{i=1}^M (U_{31}^2 - U_{41}^2)
 \end{aligned}$$

$$z_1 - z_2, M=WT, \quad (3-13)$$

where U_3 and U_4 are the envelopes of u_3 and u_4 . As in the instance of the square-law detector, with an appropriate change in the interpretations of h_3^2 and h_4^2 , the "sum" and "difference" channel SNR's, the narrowband correlation detector output components z_1 and z_2 are distributed in the same way as in the lowpass case (as indicated in (3-11) and (3-12)).

When the conditions for independence of z_1 and z_2 are met, as described above, then the SNR's become

$$h_3^2 = \frac{1}{2(1+\rho)} [h_1^2 + h_2^2 + 2h_1 h_2 \cos(\theta_1 - \theta_2)]$$

DS

$$h_4^2 = \frac{1}{2(1-\rho)} [h_1^2 + h_2^2 - 2h_1 h_2 \cos(\theta_1 - \theta_2)]. \quad (3-14)$$

3.2 Probability Distribution.

The functional form of the distribution of the correlation detector output z , in the case of no post-detection integration ($M=1$), has been developed in complete generality for the assumed model [13,19]. This form is very complex and far from being "closed". A great

simplification, however, occurs if the equal input variance conditions discussed above are assumed, so that z_1 and z_2 are independent. Using those assumptions, in Appendix B it is shown that the probability density function of z becomes, for deterministic signals,

$$p(z) = \frac{M}{\sigma^2} \left(\frac{1-\rho}{4} \right)^{2M-1} \exp \left\{ -M(h_3^2 + h_4^2) \right\} \\ \times \sum_{n=0}^{\infty} \sum_{m=0}^{\infty} \frac{1}{n!m!} [M(1-\rho)h_3^2/2]^n [M(1+\rho)h_4^2/2]^m \quad \text{DS} \quad (3-15) \\ (M=WT)$$

$$\times \begin{cases} \exp \left\{ -2Mz/\sigma^2(1-\rho) \right\} G_{M+n-1}^{M+m-1} [4Mz/\sigma^2(1-\rho^2)], & z \geq 0 \\ \exp \left\{ 2Mz/\sigma^2(1-\rho) \right\} G_{M+m-1}^{M+n-1} [-4Mz/\sigma^2(1-\rho^2)], & z < 0 \end{cases}$$

where

$$G_n^m(x) \triangleq \sum_{k=0}^n \binom{n+m-k}{m} \frac{x^k}{k!} \quad (3-16)$$

are polynomials whose properties are discussed in [13]. For Gaussian signals, the pdf is obtained by setting $h_3^2 = h_4^2 = 0$ in (3-15). Using

$$\psi \equiv \rho_{n+s} = \frac{\rho \sigma_1 \sigma_2 + r d_1 d_2}{\sigma^2 + d^2} = \frac{\rho + r h_1 h_2}{\sqrt{(1+h_1^2)(1+h_2^2)}} \quad (3-17)$$

and

$$\sigma_1^2 + d_1^2 = \sigma_2^2 + d_2^2 = \sigma^2 + d^2 = \sigma^2(1+h^2),$$

(3-15) becomes

$$p(z) = \frac{M}{\sigma^2 (1+h^2)} \left(\frac{1-\psi^2}{4} \right)^{M-1} G_{M-1}^{M-1} \left[\frac{4M|z|}{\sigma^2 (1+h^2) (1-\psi^2)} \right]$$

RS

$$\times \begin{cases} \exp \{-2Mz/\sigma^2 (1+h^2) (1+\psi)\} & , \quad z \geq 0 \\ \exp \{2Mz/\sigma^2 (1+h^2) (1-\psi)\} & , \quad z < 0. \end{cases} \quad (M=WT) \quad (3-18)$$

In [15], the following integral is derived:

$$\int_{\tau}^{\infty} dx e^{-bx} G_r^s(x) = \frac{1}{b} e^{-b\tau} \sum_{K=0}^s \binom{r+s-K}{s} \left(\frac{c}{b} \right)^K e_K(b\tau) , \quad (3-19)$$

where the incomplete exponential function $e_K(\cdot)$ is given in (2-16).

Thus the probability of detection for the correlation detector is

$$P_D(\tau) = \left(\frac{1+\rho}{2} \right) \left(\frac{1-\rho}{4} \right)^{M-1} \exp \{-M(h_3^2 + h_4^2) - 2M\tau/\sigma^2 (1+\rho)\}$$

DS

$$\times \sum_{n=0}^{\infty} \sum_{m=0}^{\infty} \frac{1}{n!m!} [M(1-\rho)h_3^2/2]^n [M(1+\rho)h_4^2/2]^m$$

$$\times \sum_{K=0}^{n+M-1} \binom{2M+n+m-2-K}{m+M-1} \left(\frac{2}{1-\rho} \right)^K e_K[2M\tau/\sigma^2 (1+\rho)] \quad (3-20)$$

(M = WT)

3-3 Receiver Operating Characteristics.

The computer program presented in Figure 3-2 was used to calculate a truncated version of (3-20). False alarm thresholds are first computed according to the procedure diagrammed in Figure 3-3, which illustrates the case of $\alpha=10^{-4}$ and $\rho=0$. A number of values of the threshold thus obtained are listed in Table 3-1 for different α and WT.

An impression of the rate of converge of the distribution of the detector output to that of a Gaussian variable can be gained from Table 3-2, in which thresholds from Table 3-1, normalized by

$$\sqrt{\text{Var}\{z\}} = \sigma^2 \sqrt{(1+\rho)/2M}, \quad (3-22)$$

are compared to their Gaussian counterparts taken from Table 26.6 of [1].

Having computed false alarm thresholds corresponding to various values of α , the method of Figure 3-4 was employed to compute $P_D = \gamma$ for fixed α and WT, and for input SNR varied when the signal is deterministic. For computation, the case for which there is no inter-channel noise correlation ($\rho=0$) and for which the signals are of equal phase and power ($S_1=S_2=S$, $\theta_1=\theta_2$) was selected. For this case, $h_3^2=2h^2$ and $h_4^2=0$, where h^2 is the input SNR in each channel. The resulting ROC are given in Figures 3-5 and 3-6 for $\alpha=10^{-2}$ and 10^{-4} , respectively.

EXAMPLE 3-1. Problem: Find the input SNR required to achieve a detection probability of .95 when α is constrained to be 1% for a correlation detector whose bandwidth is 0.1 Hz and the integration


```

60 H3=2*H/(1+RO)
70 H4=0
71 IF H3>0 THEN 73
72 L2 = 0
73 IF H4>0 THEN 75
74 L1 = 0
75 C9=CO
80 UO=.5*M*(1+RO)*H4
90 VO=.5*M*(1-RO)*H3
110 Y=2*M*X/(1+RO)
120 S=0
130 U1=1
135 CO=C9
140 FOR N=0 TO L1
150 IF N=0 THEN 180
160 U1=U1*UO/N
170 CO=CO*(2*M+N-2)/(N+M-1)
180 V1=1
190 CL=CO
200 FOR J=0 TO L2
210 IF J=0 THEN 240
220 V1=V1*VO/J
230 C1=C1*(2*M+N+J-2)/(M+J-1)
240 W1=W8=1
250 C2=C1
260 FOR K=0 TO M+J-1
270 IF K=0 THEN 310
280 W8=W8*Y/K
290 W1=W1+W8
300 C2=C2*(M+J-K)/(2*M+N+J-1-K)
310 S=S+W1*U1*V1*C2*(2/(1-RO))K
320 NEXT K
350 NEXT J
400 NEXT N
410 S=S*EXP(-Y-M*(H3+H4))
420 S=S*(1+RO)*(1-RO+2)M-1
430 S=S*2/4+M

```

Mnemonics: $RO \equiv \rho$, $.Y \equiv \frac{2Mx}{1+\rho}$, $H3 \equiv h_3^2$, $H4 \equiv h_4^2$,

$W1 \equiv e_k(Y)$, $U1 \equiv [M(1+\rho)h_3^2/2]^N/N!$,

$V1 \equiv [M(1-\rho)h_3^2/2]^J/J!$, $C2 = \binom{2M+N+J-2-K}{M+N-1}$

$$S = \frac{2}{4^m} (1+RO)(1-RO^2)^{M-1} \exp [-Y-M(H3+H4)]$$

$$\times \sum_{N=0}^{L1} \sum_{J=0}^{L2} \sum_{K=0}^{M+J-1} W1 \cdot U1 \cdot V1 \cdot C2 \left(\frac{2}{1-RO} \right)^K$$

FIGURE 3-2
Program to Compute Correlation Detector Probabilities

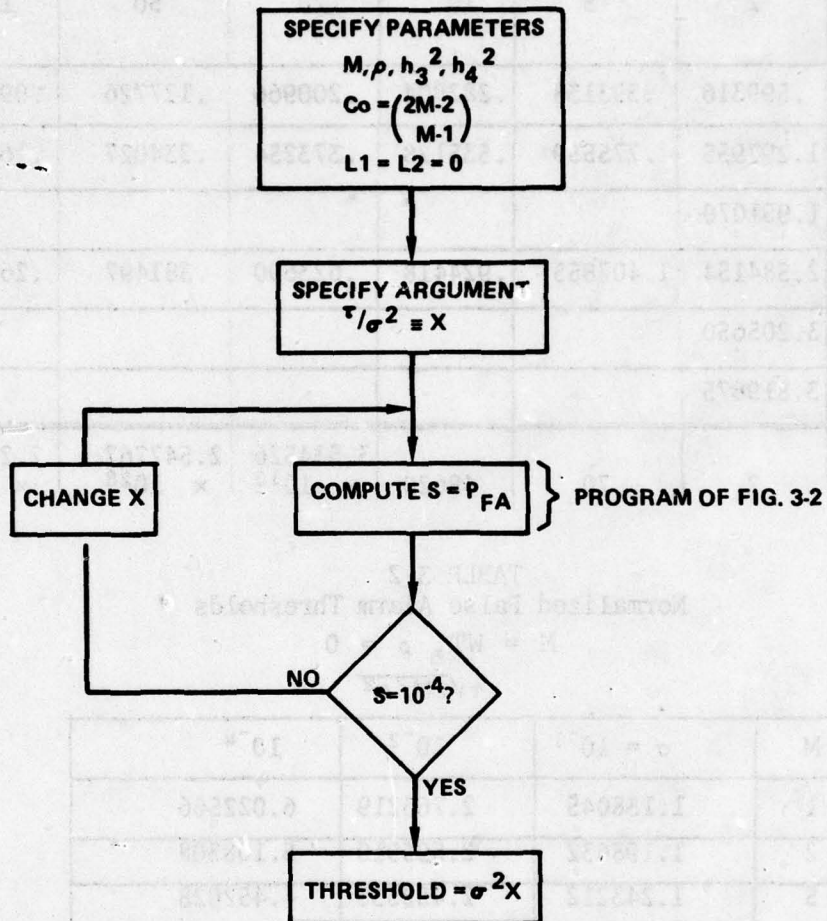


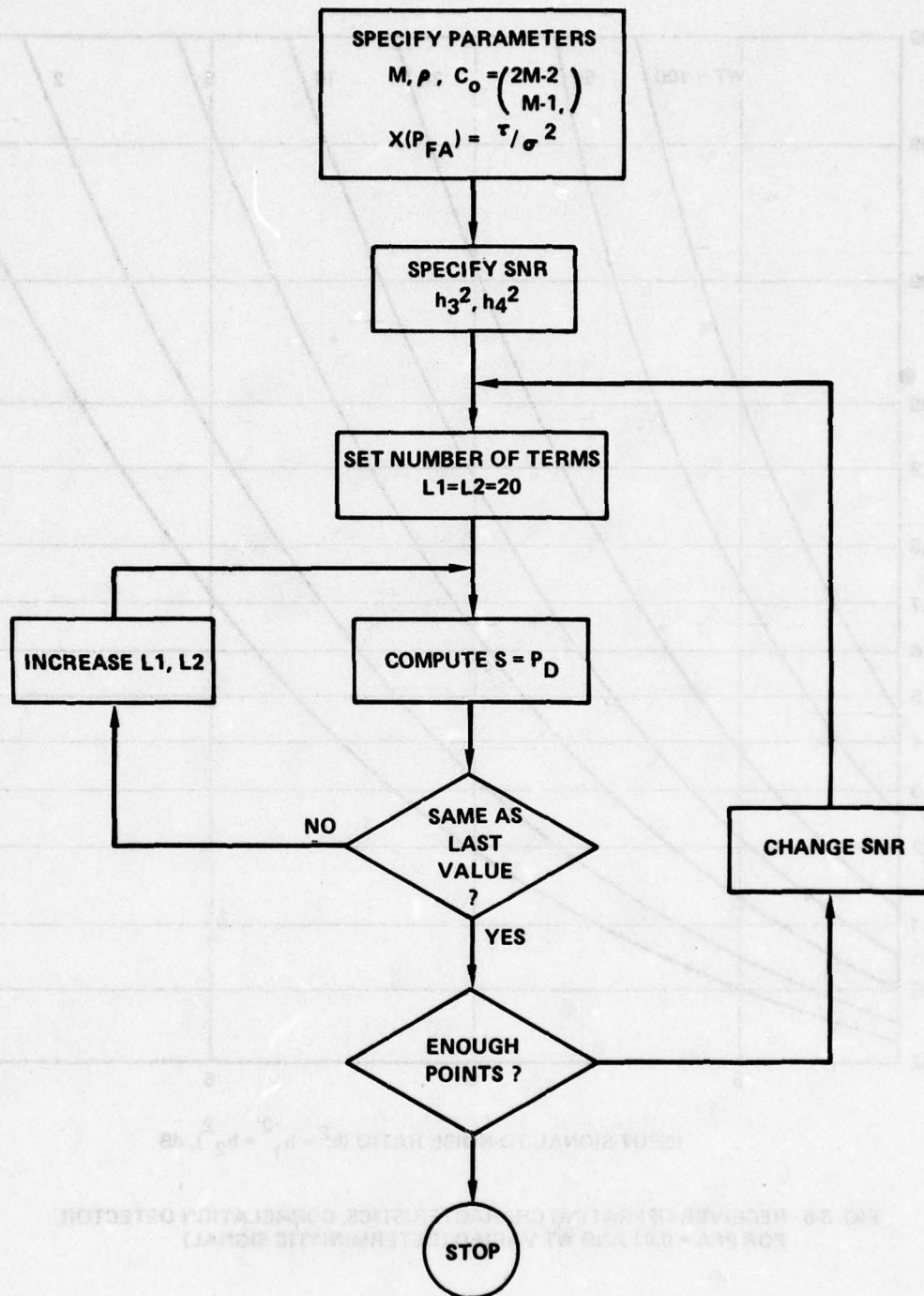
FIG. 3-3. PROCEDURE TO COMPUTE FALSE ALARM THRESHOLDS.

TABLE 3-1
False Alarm Thresholds $M = WT, \rho = 0$ τ/α^2

$P_{FA} \equiv \alpha$	$M=1$	2	5	10	20	50	100
10^{-1}	.804719	.599316	.393138	.282004	.200966	.127726	.090467
10^{-2}	1.956012	1.297955	.775559	.535128	.373254	.234027	.164992
10^{-3}	3.107304	1.951070					
10^{-4}	4.258597	2.584154	1.407855	.924418	.623690	.381497	.266446
10^{-5}	5.409889	3.205650					
10^{-6}	6.561182	3.819675					
$\left(\frac{2M-2}{M-1}\right)$	1	2	70	48620	3.534526×10^{10}	2.547767×10^{28}	2.275093×10^{58}

TABLE 3-2
Normalized False Alarm Thresholds $M = WT, \rho = 0$ $\tau\sqrt{2M}/\alpha^2$

M	$\sigma = 10^{-1}$	10^{-2}	10^{-4}
1	1.138045	2.766219	6.022566
2	1.198632	2.595910	5.168308
5	1.243212	2.452533	4.452028
10	1.261160	2.393165	4.134123
20	1.271021	2.360664	3.944562
50	1.277260	2.340270	3.814970
100	1.279397	2.333339	3.768116
∞ (Gaussian)	1.28155	2.32635	3.71902

FIG. 3-4. METHOD FOR COMPUTING P_D .

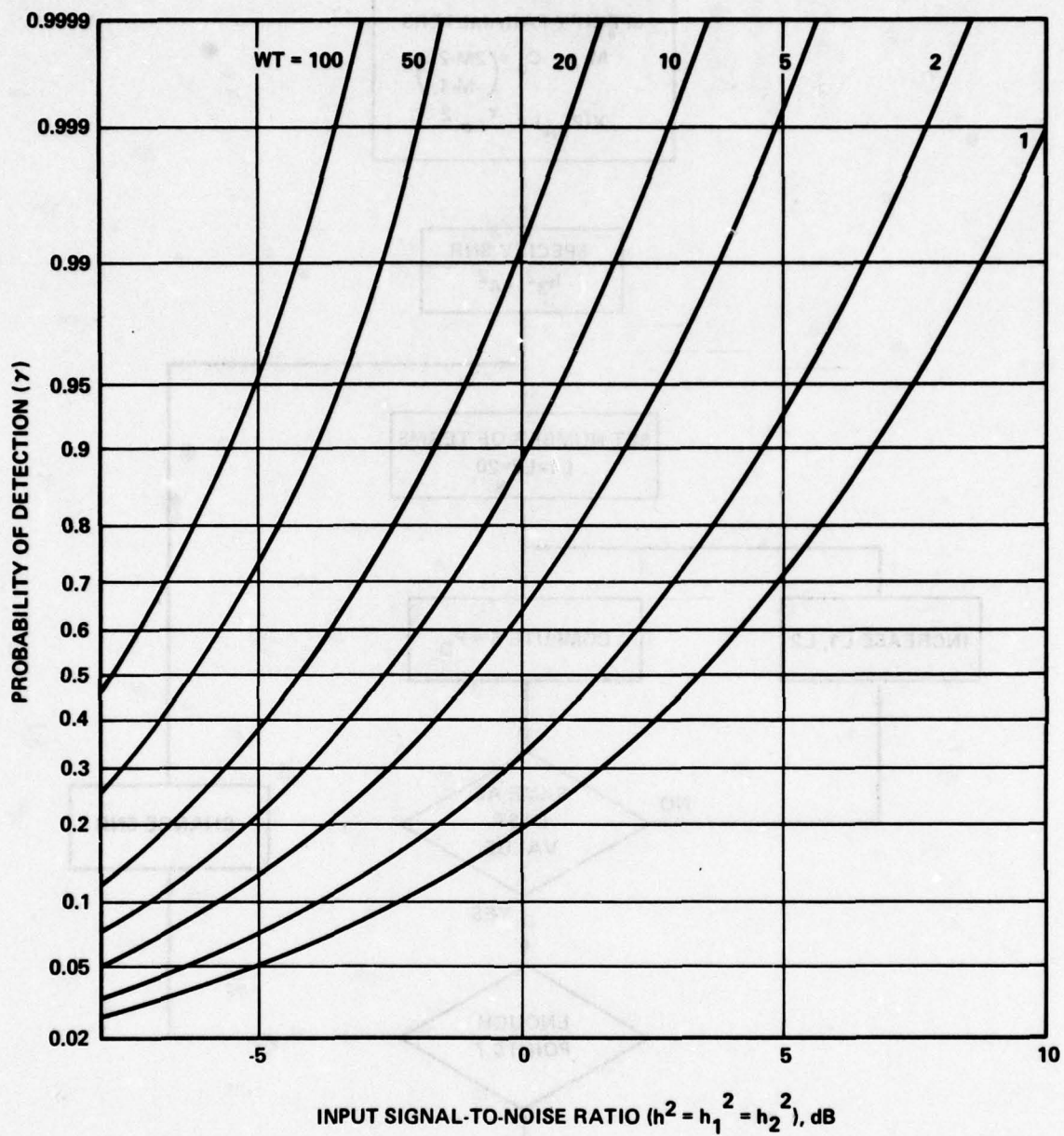


FIG. 3-5 RECEIVER OPERATING CHARACTERISTICS, CORRELATION DETECTOR, FOR $PFA = 0.01$ AND WT VARIED (DETERMINISTIC SIGNAL)

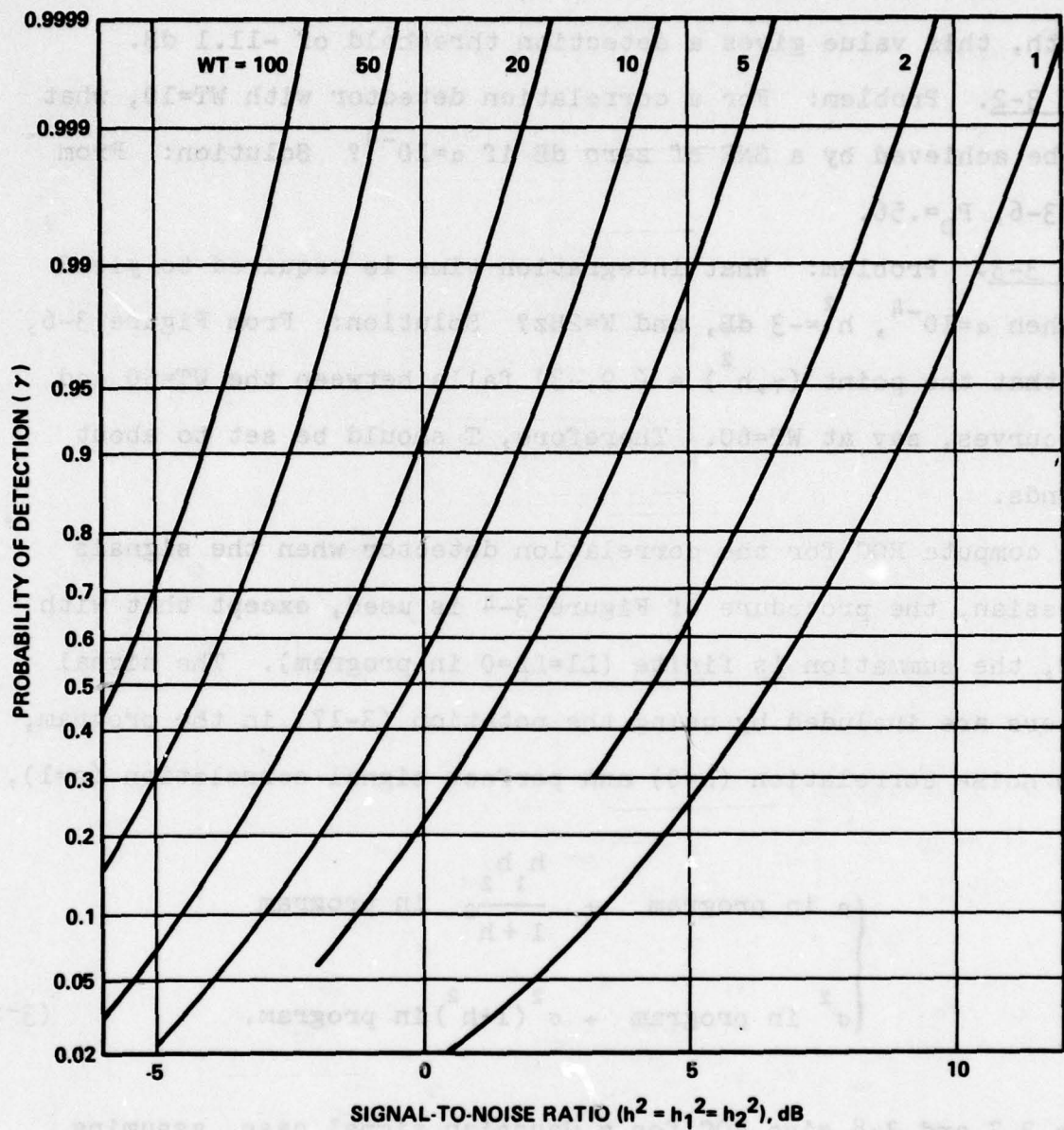


FIG. 3-6 RECEIVER OPERATING CHARACTERISTICS, CORRELATION DETECTOR,
FOR PFA = 0.0001 AND WT VARIED (DETERMINISTIC SIGNAL)

time is 200 seconds. Solution: From Figure 3-5, the $WT=20$ curve, we find that $\gamma=.95$ corresponds to $h^2=-1.1$ dB. Referred to one hertz bandwidth, this value gives a detection threshold of -11.1 dB.

EXAMPLE 3-2. Problem: For a correlation detector with $WT=10$, what P_D can be achieved by a SNR of zero dB if $\alpha=10^{-4}$? Solution: From Figure 3-6, $P_D=.56$.

EXAMPLE 3-3. Problem: What integration time is required to yield $P_D=.9$ when $\alpha=10^{-4}$, $h^2=-3$ dB, and $W=2$ Hz? Solution: From Figure 3-6, we see that the point $(\gamma, h^2) = (.9, -3)$ falls between the $WT=50$ and $WT=100$ curves, say at $WT=60$. Therefore, T should be set to about 30 seconds.

To compute ROC for the correlation detector when the signals are Gaussian, the procedure of Figure 3-4 is used, except that with $h_3=h_4=0$, the summation is finite ($L1=L2=0$ in program). The signal parameters are included by using the notation (3-17) in the program, with no noise correlation ($\rho=0$) and perfect signal correlation ($r=1$), or

$$\left\{ \begin{array}{l} \rho \text{ in program} \rightarrow \frac{h_1 h_2}{1+h} \text{ in program} \\ \sigma^2 \text{ in program} \rightarrow \sigma^2 (1+h^2) \text{ in program.} \end{array} \right. \quad (3-23)$$

Figures 3-7 and 3-8 give ROC for a Gaussian signal case, assuming $h_1=h_2=h$, when $\alpha=10^{-2}$ and 10^{-4} .

EXAMPLE 3-4. Problem: What increase in input SNR is required to maintain $P_D=.95$ for a correlation detector with Gaussian signals and noise, if P_{FA} is decreased from 10^{-2} to 10^{-4} , and $WT=2$?

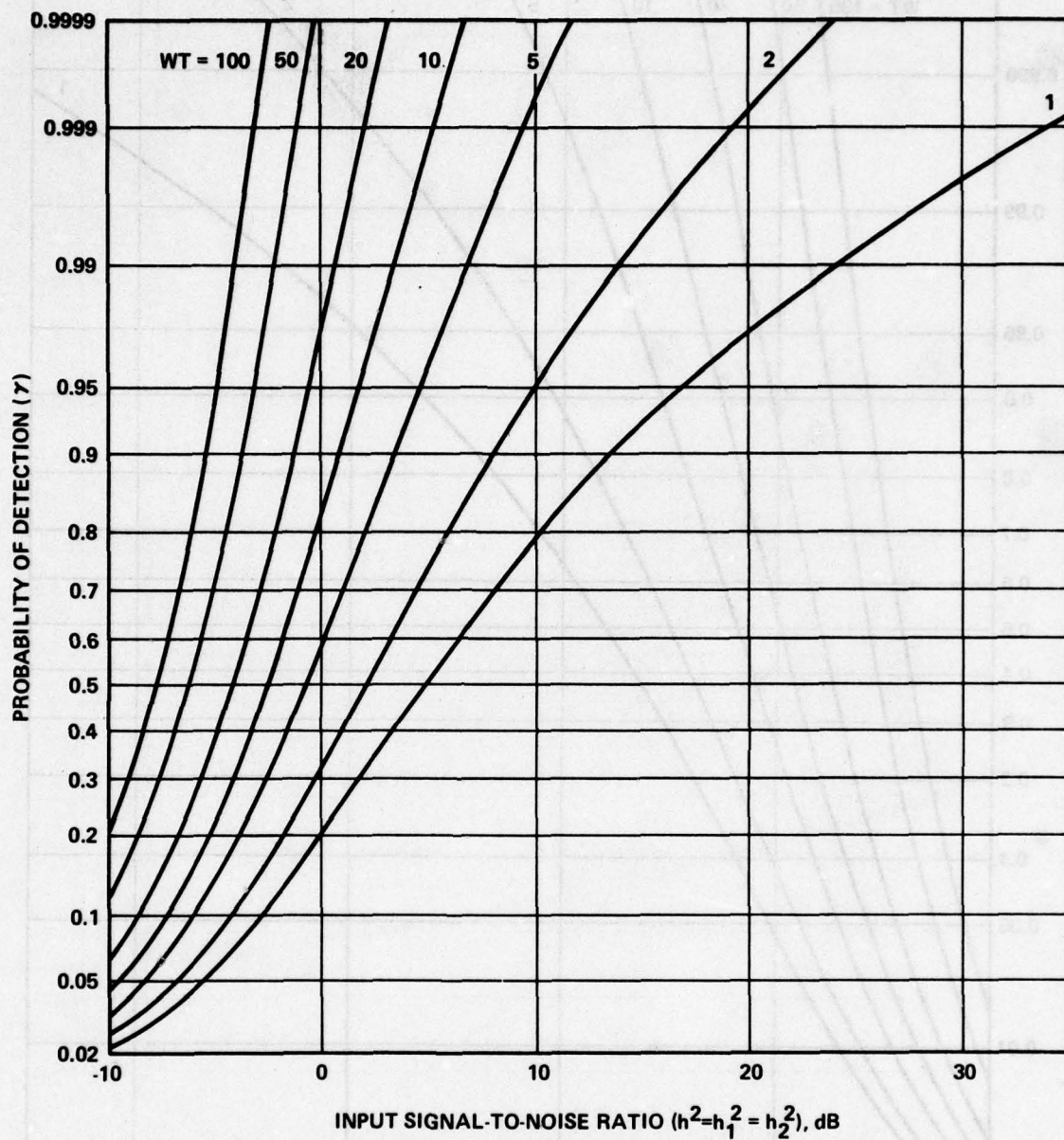


FIG. 3-7 RECEIVER OPERATING CHARACTERISTICS, CORRELATION DETECTOR, FOR PFA = 0.01 AND WT VARIED (RANDOM SIGNAL)

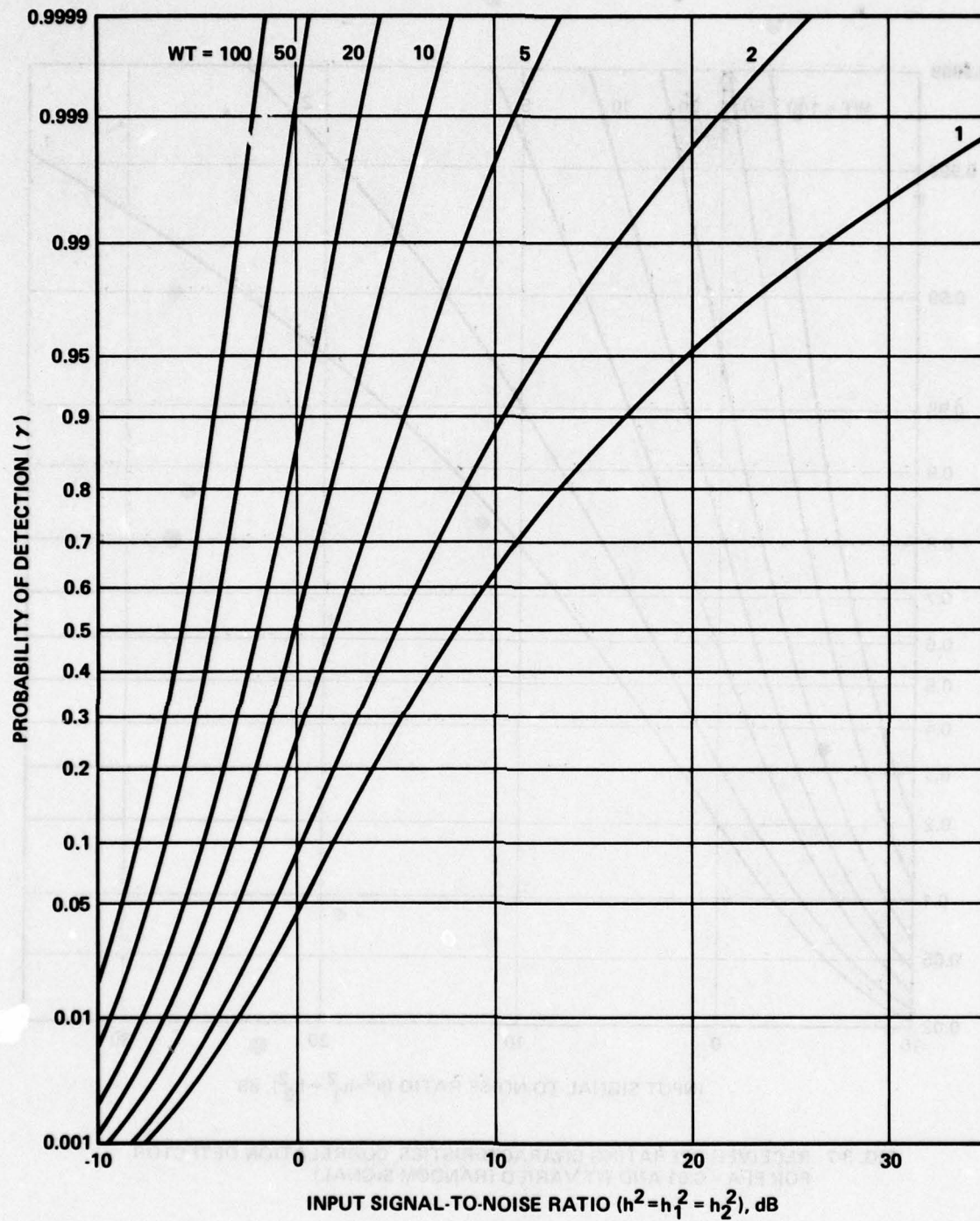


FIG. 3-8. RECEIVER OPERATING CHARACTERISTICS, CORRELATION DETECTOR, FOR PFA = 0.0001 AND WT VARIED (RANDOM SIGNAL).

Solution: From Figure 3-7, $h^2 = 9.8$ dB for $WT = 2$ and $\gamma = .95$, in Figure 3-8, for the same WT and γ ; $h^2 = 12.3$ dB. Thus an increase of 2.5 dB is required.

EXAMPLE 3-5. Problem: How does the detection performance of a correlator compare with that of a "sum and square" detector with two Gaussian inputs? Solution: Assuming that the signals are perfectly correlated ($r=1$), the noises are independent ($\rho=0$), and that the SNR's in the channels are equal, the SNR at the input to the square-law device is twice that in the input channels. Thus we may use Figures 2-4 and 2-5 if we subtract 3 dB from the SNR indicated. Table 3-3 summarizes the comparison to be made, using data from Figures 2-4, 2-5, 3-7, and 3-8. From the comparison, we observe that the square-law is better (requires a smaller SNR) than the correlation detector for the case modeled, but only by about 1 dB or less, typically.

TABLE 3-3

Detector Performance Comparison

$P_D = .95$						WT
$P_{FA} = 10^{-2}$			$P_{FA} = 10^{-4}$			
$h^2(\text{correl})$	$h^2(\text{SQ.L})$	Δh^2	$h^2(\text{correl})$	$h^2(\text{SQ.L})$	Δh^2	
16.8	16.5	0.3	19.7	19.5	0.2	1
9.8	9.5	0.3	12.3	12.1	0.2	2
4.5	3.8	0.7	6.5	6.1	0.4	5
1.7	1.0	0.7	3.4	2.8	0.6	10
-0.6	-1.5	0.9	0.9	0.2	0.7	20
-3.2	-4.3	1.1	-1.8	-2.7	0.9	50
-4.9	-6.2	1.3	-3.6	-4.7	1.1	100
$P_D = .9$						
13.6	13.4	0.2	16.6	16.4	0.2	1
8.0	7.7	0.3	10.5	10.3	0.2	2
3.4	2.7	0.7	5.4	5.0	0.4	5
0.8	0.1	0.7	2.6	2.1	0.5	10
-1.3	-2.2	0.9	0.3	-0.4	0.7	20
-3.8	-4.8	1.0	-2.3	-3.2	0.9	50
-5.5	-6.7	1.2	-4.0	-5.1	1.1	100
$P_D = .5$						
4.8	4.5	0.3	8.1	7.9	0.2	1
2.1	1.7	0.4	5.0	4.8	0.2	2
-0.7	-1.3	0.6	1.8	1.5	0.3	5
-2.5	-3.2	0.7	-0.2	-0.7	0.5	10
-4.2	-5.1	0.9	-1.8	-2.6	0.8	20
-6.2	-7.3	1.1	-4.2	-5.0	0.8	50
-7.8	-9.0	1.2	-5.8	-6.8	1.0	100

CHAPTER 4
INCOHERENT POWER DETECTOR

4.1 Detector Configuration

A third class of quadratic detector which can be analyzed conveniently is that in which the inputs are squared and then summed, as illustrated in Figure 4-1. The output of the lowpass filter is, in the lowpass detector bandwidth case,

$$y(t) = \sum_{i=1}^L x_i^2(t), \quad (4-1)$$

where the inputs $\{x_i\}$ are correlated and have different variances in general. If they were independent and of equal variance, the sum would be distributed $\chi^2(L)$ and the detector output, $\chi^2(LM)$.

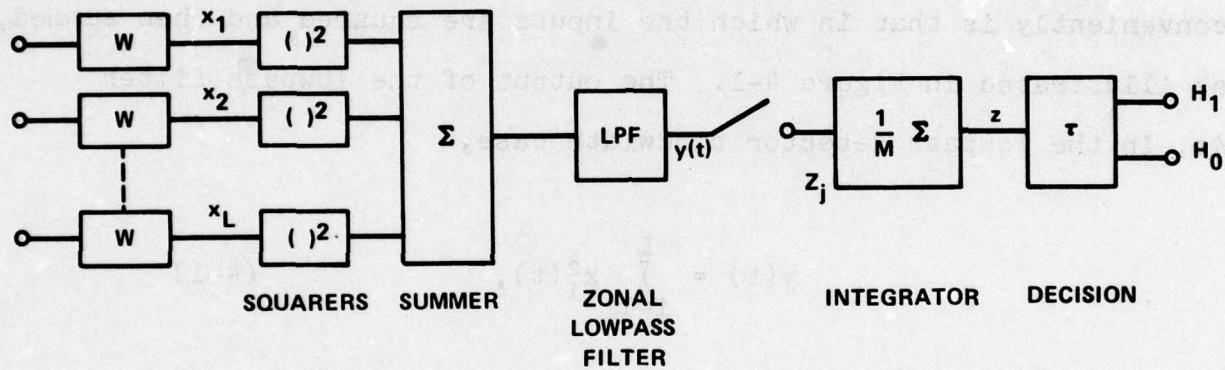


FIG. 4-1. DETECTOR CONFIGURATION

Rather than treat this specialized case, we shall maintain the generality and restrict the number of inputs to $L=2$, the cases of larger dimension being encompassed by the approach given in Part II.

For $L=2$, then

$$\begin{aligned} y &= x_1^2 + x_2^2 \\ &= 2(u_3^2 + u_4^2), \end{aligned} \quad (4-2)$$

where u_3 and u_4 are the sum and difference terms defined before in (3-6), with the moments given in (3-7), (3-8), and (3-9). The detector output is

$$\begin{aligned} z &= \frac{2}{M} \sum_{j=1}^M [u_3^2(t_j) + u_4^2(t_j)] \\ &\triangleq z_1 + z_2. \end{aligned} \quad (4-3)$$

For both lowpass and narrowband detector cases,

$$\left\{ \begin{array}{l} \frac{WTz_1}{\sigma_3^2} \text{ is } \chi'^2(2WT, 2WTh_3^2) \\ \frac{WTz_1}{\sigma_4^2} \text{ is } \chi'^2(2WT, 2WTh_4^2), \end{array} \right. \quad \text{DS} \quad (4-4)$$

so that z is the weighted sum of correlated noncentral chi-squared random variables.

4.2 Receiver Operating Characteristics

The pdf for the output of the square and sum detector with two inputs is developed in Appendix C. From (C-14), the probability of detection is

$$P_D = \left(\frac{1+\rho}{1-\rho}\right)^{WT} \exp\left\{-WT\left[\frac{\tau}{\sigma^2(1+\rho)} + h_3^2 + h_4^2\right]\right\} \quad \text{DS}$$

$$\times \sum_{n=0}^{\infty} \sum_{m=0}^{\infty} \sum_{K=0}^{\infty} [WTh_4^2 \left(\frac{1+\rho}{1-\rho}\right)]^n (WTh_3^2)^m \left(\frac{-2\rho}{1-\rho}\right)^K \frac{(n+WT)_K}{n!m!K!} e_{m+n+K+2WT-1} \left[\frac{WT\tau}{\sigma^2(1+\rho)}\right]$$

(4-5)

where the equal input noise variance assumption has been made. The corresponding false alarm probability is

$$P_{FA} = \left(\frac{1+\rho}{1-\rho}\right)^{WT} \exp\left\{\frac{-WT\tau}{\sigma^2(1+\rho)}\right\} \sum_{K=0}^{\infty} \left(\frac{-2\rho}{1-\rho}\right)^K \binom{K+WT-1}{K} e_{K+2WT-1} \left[\frac{WT\tau}{\sigma^2(1+\rho)}\right],$$

$$-1 < \rho < 1/3$$

$$= \left(\frac{1-\rho}{1+\rho}\right)^{WT} \exp\left\{\frac{-WT\tau}{\sigma^2(1-\rho)}\right\} \sum_{K=0}^{\infty} \left(\frac{2\rho}{1+\rho}\right)^K \binom{K+WT-1}{K} e_{K+2WT-1} \left[\frac{WT\tau}{\sigma^2(1-\rho)}\right],$$

$$-\frac{1}{3} < \rho < 1.$$

(4-6)

For deterministic signals, the computer program of Figure 4-2 was written to compute (4-5) when the input SNR's are equal and the signals are in phase. The program was used according to a strategy very analogous to that diagrammed in Figures 3-3 and 3-4. False alarm thresholds for $\alpha=10^{-2}$ and 10^{-4} are given in Table 4-1, and ROC for the same α are shown in Figures 4-3 and 4-4 for deterministic signals.

EXAMPLE 4-1. Problem: How do the three types of detectors we have considered compare as to minimum detectable signal ($P_D=.5$, $\alpha=10^{-4}$) as W_T varies, for two channels of uncorrelated noise and a deterministic signal common to the channels? Solution: Using Figures 2-7, 3-6, and 4-4, the comparison in Figure 4-5 was constructed, showing that in this instance the coherent power or square-law detector is consistently "best" and the incoherent is consistently "worst", although the difference in MDS is at most 1.6 dB.

For the Gaussian signal case, (4-6) was computed using $\rho=h^2/(1+h^2)$ and replacing σ^2 with $\sigma^2(1+h^2)$ in the program, as done previously for the correlation detector. Figures 4-6 and 4-7 provide the ROC for the two-input sum and square detector when $\alpha=10^{-2}$ and 10^{-4} respectively.

EXAMPLE 4-2. Problem: Perform the same comparison as in Example 4-1 for Gaussian signals. Solution: Using data from Figures 2-5, 3-8, and 4-7, the comparison plotted in Figure 4-8 shows much the same result as in the deterministic signal case.


```

80 DO=2*M*H/(1+RO)
82 AO=-2*RO/(1-RO)
85 IF DO>0 THEN 100
86 L1=0
100 Y=X*M/(1+RO)
105 S=0
110 D1=1
120 FOR I=0 TO L1
130 A1=BO=B1=CO=1
140 IF I=0 THEN 160
150 D1=D1*DO/I
160 FOR J=1 TO I+2*M-1
170 BO=BO*Y/J
180 B1=B1+BO
190 NEXT J
194 S1=B1
195 IF RO>0 THEN 200
197 L2=1
200 FOR K=1 TO L2
210 A1=A1*AO/K
230 BO=BO*Y/(K+2*M-1+I)
240 B1=B1+BO
245 CO=CO*(M+K-1)
250 S1=S1+A1*CO*B1
260 NEXT K
265 S=S+S1*D1
270 NEXT I
275 S=S*EXP(-Y-DO)*((1+RO)/(1-RO))+M

```

$$H \equiv h^2$$

$$RO \equiv \rho$$

$$X \equiv \tau/\sigma^2$$

$$M \equiv WT$$

FIGURE 4-2

Program to Compute Square-And-Sum Detector Probabilities

TABLE 4-1

False Alarm Thresholds, Square and Sum Detector

WT	Threshold, τ/σ^2	Normalized threshold $(\tau/\sigma^2 - 2)\sqrt{\frac{WT}{2}}$		
	$\alpha = 10^{-2}$	10^{-4}	10^{-2}	10^{-4}
1	6.638352	11.756371	3.2798	6.8988
2	5.02256	7.95691	3.0226	5.9569
5	3.75662	5.23860	2.7775	5.1207
10	3.18454	4.10311	2.6487	4.7027
20	2.80822	3.39456	2.5558	4.4100
50	2.49445	2.83060	2.4723	4.1530
100	2.34362	2.56828	2.4298	4.0254
Gaussian	--	--	2.3264	3.7190

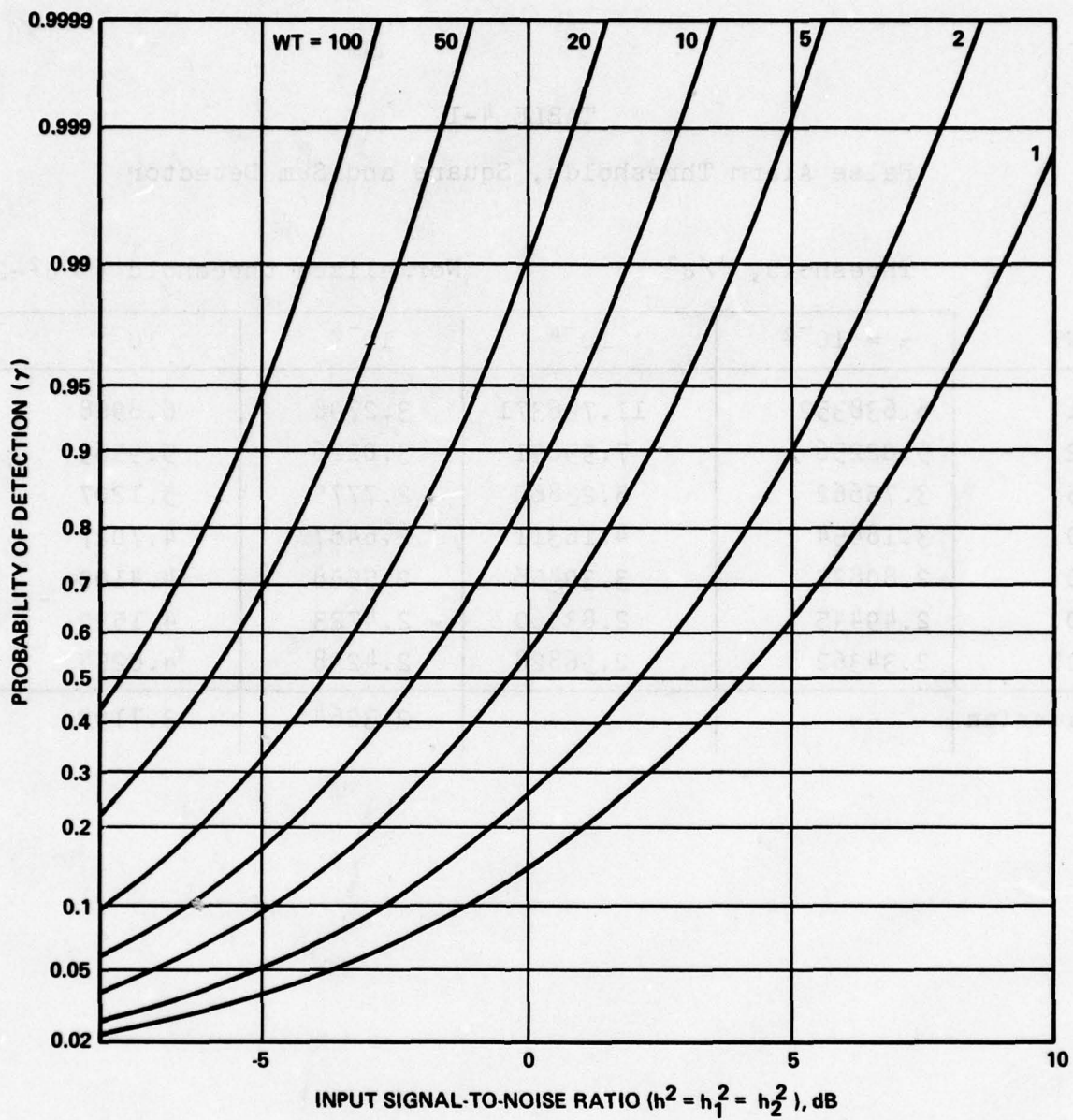


FIG. 4-3. RECEIVER OPERATING CHARACTERISTICS, INCOHERENT DETECTOR, FOR PFA = 0.01 AND WT VARIED (DETERMINISTIC SIGNAL)

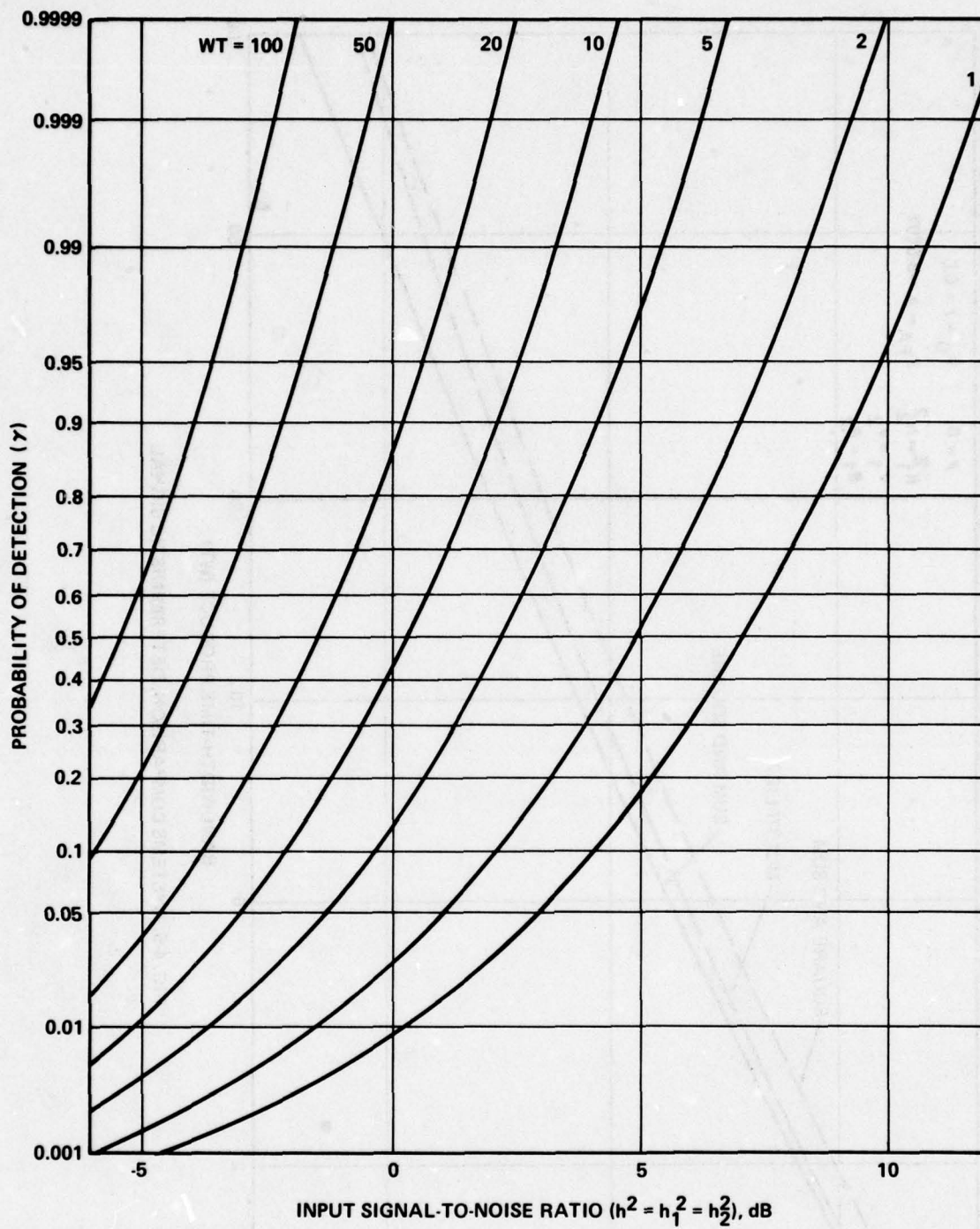


FIG. 4.4. RECEIVER OPERATING CHARACTERISTICS, INCOHERENT DETECTOR, FOR PFA = 0.0001 AND WT VARIED (DETERMINISTIC SIGNAL)

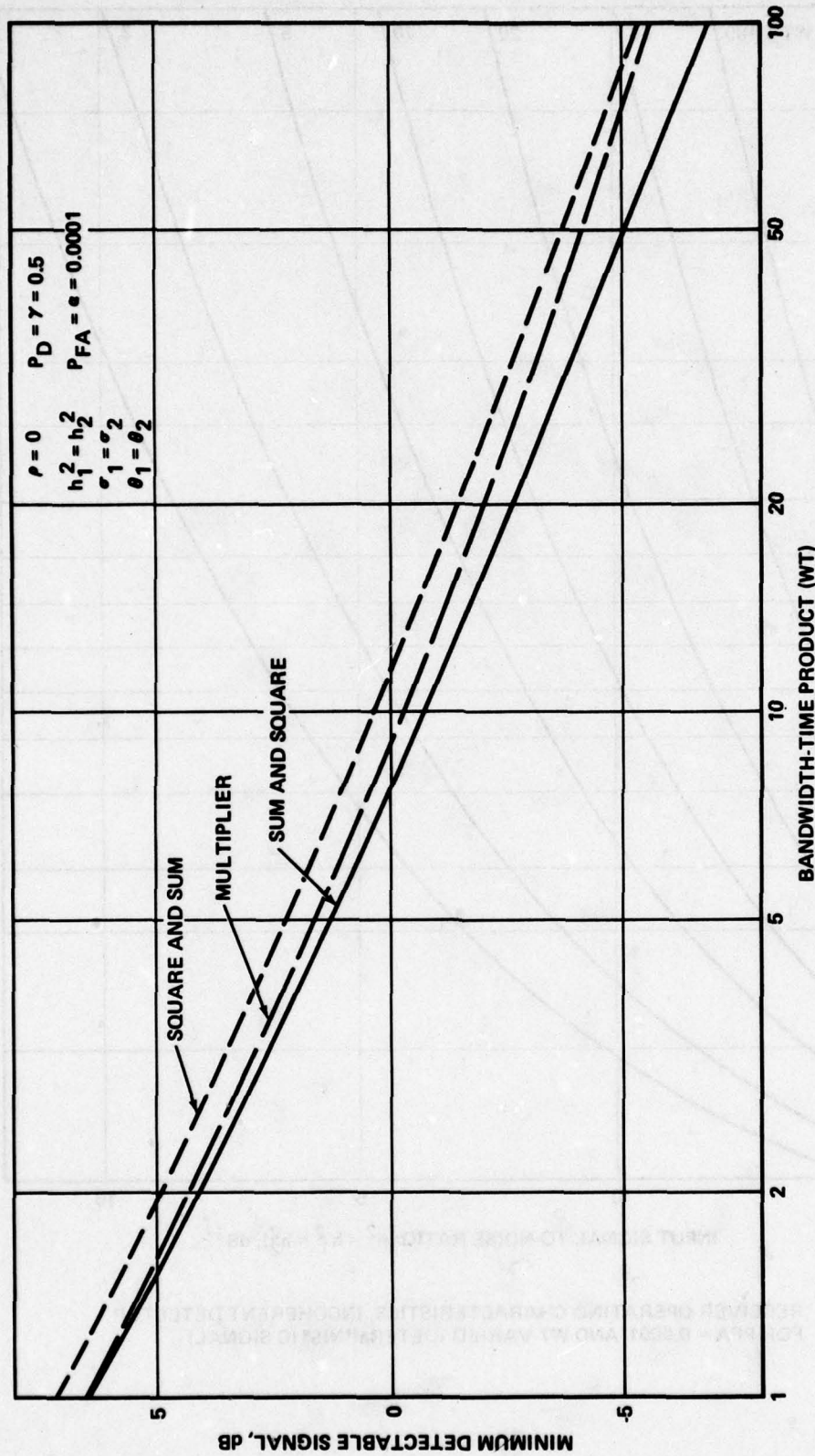


FIG. 4.5. SYSTEMS COMPARISON, DETERMINISTIC SIGNAL

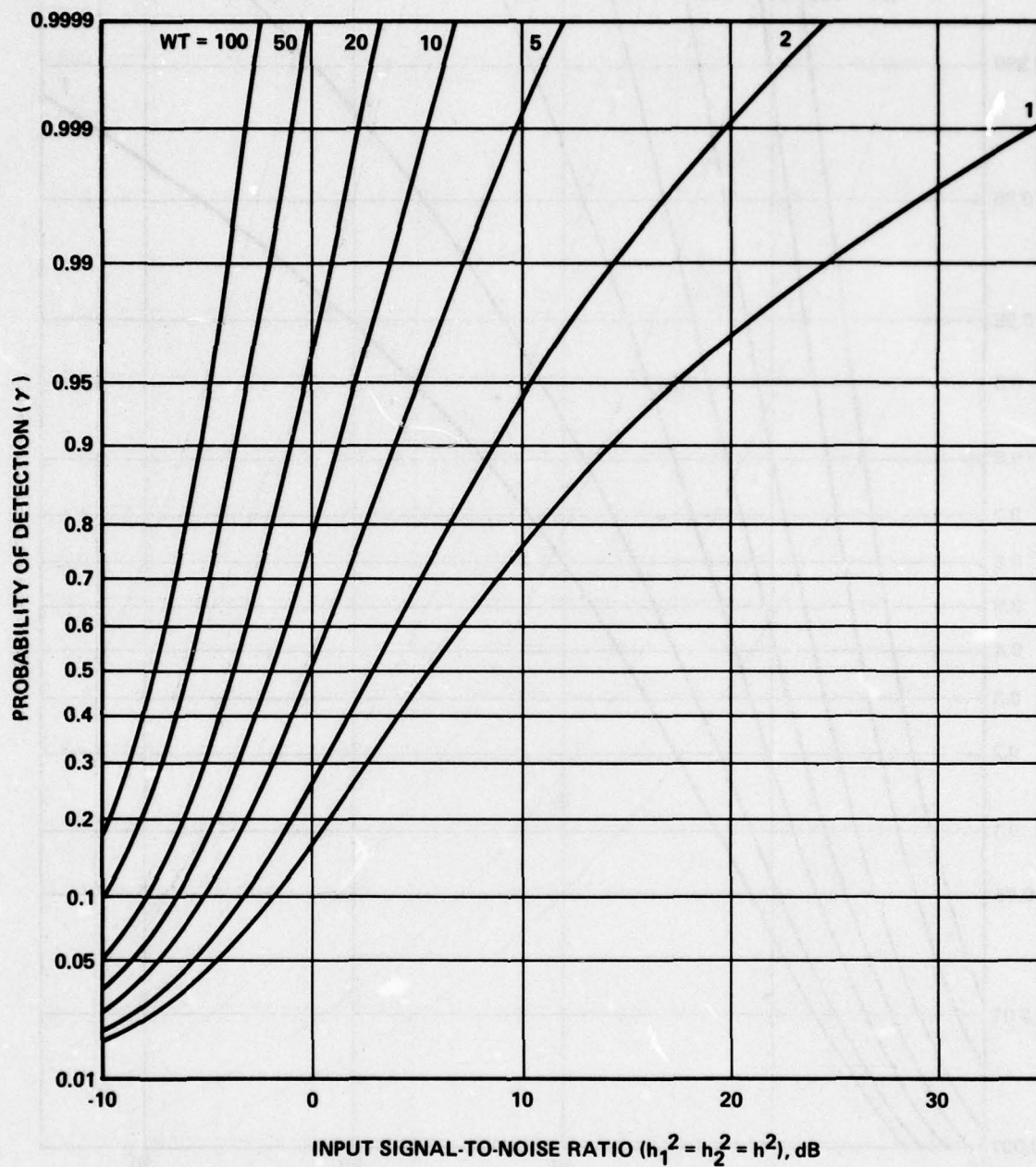


FIG. 4-6 RECEIVER OPERATING CHARACTERISTICS, INCOHERENT DETECTOR,
FOR PFA = 0.01 AND WT (RANDOM SIGNAL)

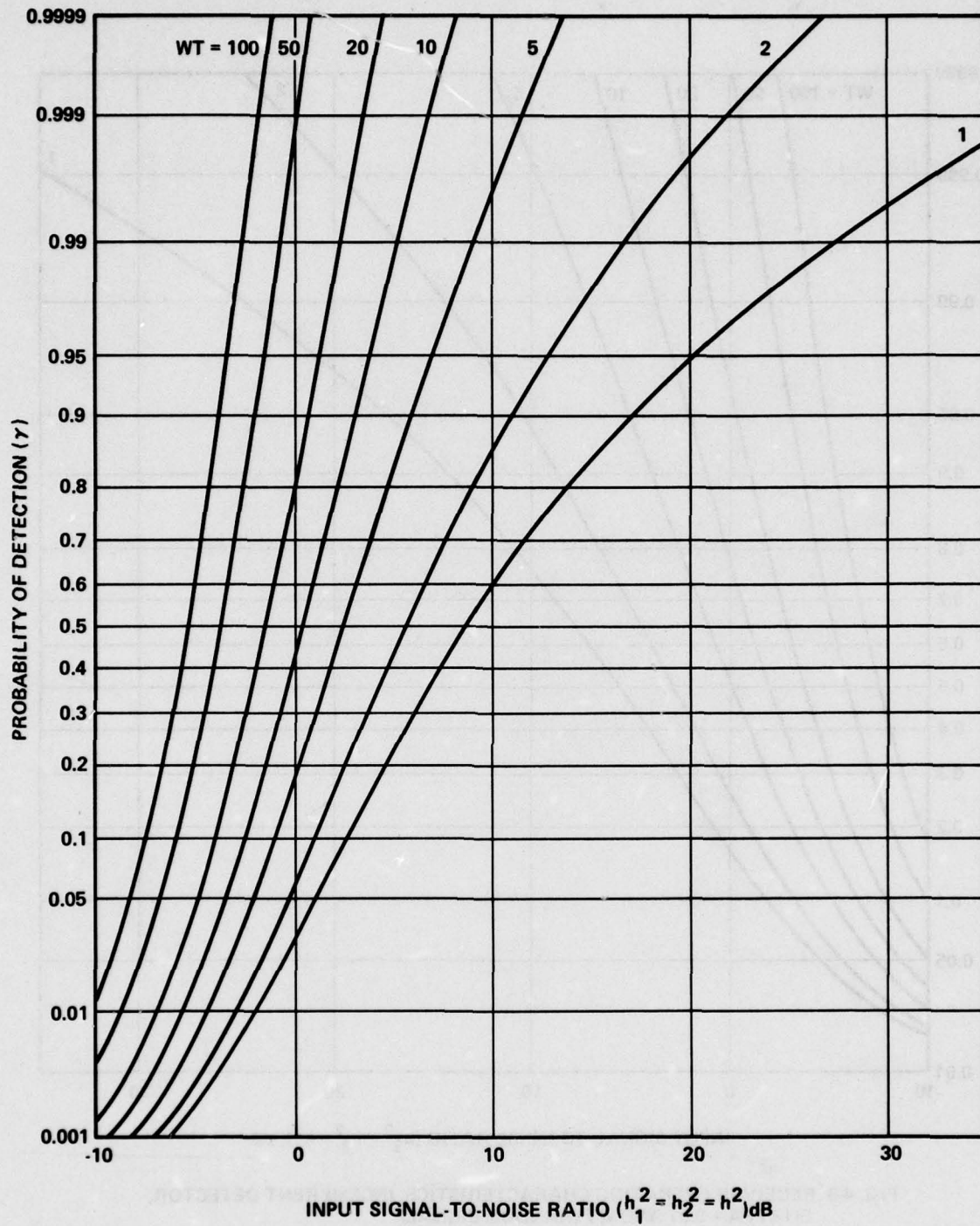


FIG. 4-7 RECEIVER OPERATING CHARACTERISTICS, INCOHERENT DETECTOR, FOR PFA = 0.0001 AND WT VARIED (RANDOM SIGNAL)

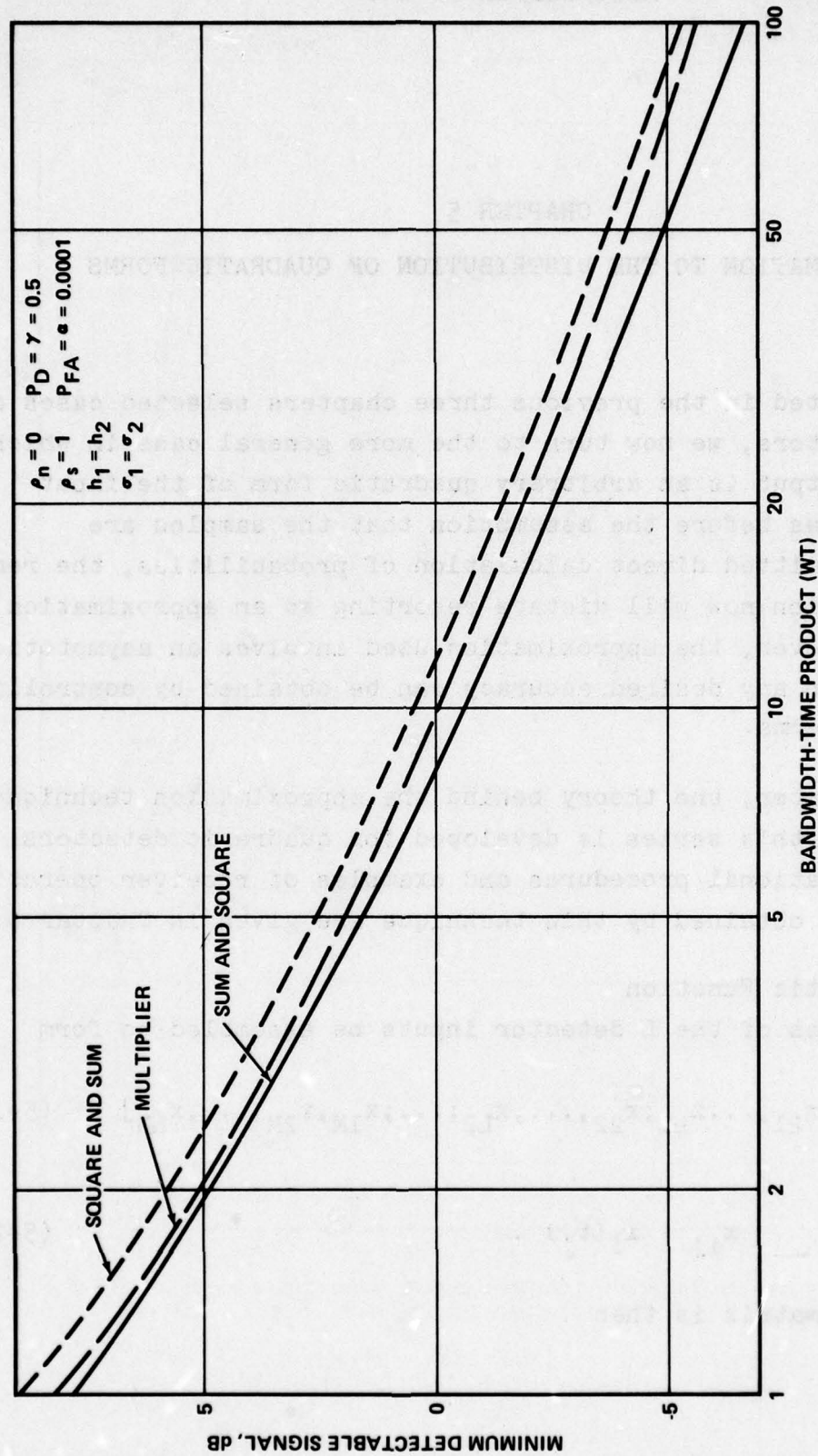


FIG. 4-8 SYSTEMS COMPARISON, RANDOM SIGNAL

CHAPTER 5

APPROXIMATION TO THE DISTRIBUTION OF QUADRATIC FORMS

Having treated in the previous three chapters selected cases of quadratic detectors, we now turn to the more general case in which the detector output is an arbitrary quadratic form of the input samples. Whereas before the assumption that the samples are independent permitted direct calculation of probabilities, the removal of that assumption now will dictate resorting to an approximation technique. However, the approximation used involves an asymptotic series, in which any desired accuracy can be obtained by controlling the number of terms.

In this chapter, the theory behind the approximation technique known as Edgeworth's series is developed for quadratic detectors. Specific computational procedures and examples of receiver operating characteristics obtained by this technique are given in Chapter 6.

5.1 Characteristic Function

Let M samples of the L detector inputs be assembled to form a vector:

$$\xi' \triangleq [x_{11}, x_{21}, \dots, x_{L1}; x_{12}, \dots, x_{L2}; \dots; x_{1M}, x_{2M}, \dots, x_{LM}] \quad (5-1)$$

where

$$x_{1j} \equiv x_1(t_j) . \quad (5-2)$$

The covariance matrix is then

$$E\{\xi\xi'\} = \begin{bmatrix} \Sigma_0 & \Sigma_1 & \Sigma_2 & \cdot & \cdot & \cdot & \cdot & \Sigma_{M-1} \\ \Sigma_1 & \Sigma_0 & \Sigma_1 & \cdot & \cdot & \cdot & \cdot & \Sigma_{M-2} \\ \cdot & \cdot & \cdot & \cdot & \cdot & \cdot & \cdot & \cdot \\ \cdot & \cdot & \cdot & \cdot & \cdot & \cdot & \cdot & \cdot \\ \cdot & \cdot & \cdot & \cdot & \cdot & \cdot & \cdot & \cdot \\ \cdot & \cdot & \cdot & \cdot & \cdot & \cdot & \cdot & \cdot \\ \Sigma_{M-1} & \Sigma_{M-2} & \Sigma_{M-3} & \cdot & \cdot & \cdot & \cdot & \Sigma_0 \end{bmatrix} = \Sigma_{(LM \times LM)} \quad (5-3)$$

where each sub-matrix is $L \times L$ and

$$\begin{aligned} \Sigma_K &= ||E\{x_1(t)x_j(t+K\Delta t)\}|| \\ &= ||R_{1j}(K\Delta t)||, \end{aligned} \quad (5-4)$$

$R_{1j}(\tau)$ being the cross-correlation function between input channels 1 and j . If a deterministic signal vector μ is defined analogous to ξ in (5-1), the joint probability density function for the components of ξ is given by

$$p(\xi) = [(2\pi)^{LM} \det \Sigma]^{-1/2} \exp\left\{-\frac{1}{2}(\xi-\mu)' \Sigma^{-1}(\xi-\mu)\right\} \quad (5-5)$$

in the lowpass detector case, and by

$$p(\xi) = [(2\pi)^{LM} \det \Sigma]^{-1} \exp\left\{-\frac{1}{2}(\xi_c - \mu_c)' \Sigma_c^{-1}(\xi_c - \mu_c) - \frac{1}{2}(\xi_s - \mu_s)' \sum_{s=1}^{L-1} (\xi_s - \mu_s)\right\} \quad (5-6)$$

in the narrowband case.

Adopting the detector model of Figure 1-1, we postulate a detector output of the form

$$z = \frac{1}{M} \sum_{i=1}^M \xi_i' Q \xi_i, \quad (Q \text{ } L \times L) \quad (5-7)$$

with

$$\xi_i' = (x_{1i}, x_{2i}, \dots, x_{Li}) \quad (5-8)$$

Alternately, this output can be written

$$z = \xi' Q_M \xi \quad \text{or} \quad \frac{1}{2} \xi_c' Q_m \xi_c + \frac{1}{2} \xi_s' Q_m \xi_s \quad (5-9)$$

(lowpass) (narrowband)

in which

$$Q_M = \frac{1}{M} \begin{bmatrix} Q & O_L & O_L & \dots & O_L \\ O_L & Q & O_L & \dots & O_L \\ \vdots & \vdots & \vdots & \ddots & \vdots \\ O_L & O_L & O_L & \dots & Q \end{bmatrix} \quad (5-10)$$

an $LM \times LM$ block diagonal matrix. (O_L denotes an $L \times L$ null matrix.)

The characteristic function for the distribution of the detector output z is given by

$$\begin{aligned} \phi_z(ip) &= E\{ipz\} = E\{ip \xi' Q_m \xi\} \quad (\text{lowpass}) \\ &= E\left\{\frac{ip}{2} \xi_c' Q_m \xi_c\right\} E\left\{\frac{ip}{2} \xi_s' Q_m \xi_s\right\} \quad (\text{narrowband}) \end{aligned} \quad (5-11)$$

Using the results of Middleton [18, Chapter 17], who likes to refer to this distribution "generalized χ^2 ," we have

$$\phi_z(ip) = (\det A)^{-1/2} \exp\left\{-\frac{1}{2} \mu' \Sigma^{-1} (I_{LM} - A^{-1}) \mu\right\} \quad (5-12)$$

in the lowpass case, and

$$\phi_z(ip) = (\det A)^{-1} \exp\left\{-\frac{1}{2} \mu_c' \Sigma^{-1} (I_{LM} - A^{-1}) \mu_c - \frac{1}{2} \mu_s' \Sigma^{-1} (I_{LM} - A^{-1}) \mu_s\right\} \quad (5-13)$$

in the narrowband case, using

$$A \triangleq \begin{cases} I_{LM} - 2ip\Sigma Q_m, & \text{lowpass} \\ I_{LM} - ip\Sigma Q_m, & \text{narrowband} \end{cases} \quad (5-14)$$

Now, although these expressions are exact, the corresponding probability density functions

$$p_z(z) = \frac{1}{2\pi} \int_{-\infty}^{\infty} dp \phi_z(ip) e^{-ipz} \quad (5-15)$$

are "intractable" except for $LM = 1, 2$ and the degenerate case where $Q_m = \sigma^2 I_{LM}$, according to [18]. Thus another approach is taken.

5.2 Asymptotic expansion for the pdf.

We use Middleton's formula,

$$I_{LM} - A^{-1} = - \sum_{m=1}^{\infty} \frac{(2ip)^m}{m} (\{Q_M\}^m) \quad (5-16)$$

(lowpass)

and the relation

$$\det A = \exp \left\{ - \sum_{m=1}^{\infty} \frac{(2ip)^m}{m} \text{tr}[(\{Q_M\}^m)] \right\} \quad (5-17)$$

(lowpass)

where

$$\text{tr}[C] = \sum_i c_{ii} \quad (5-18)$$

is the trace of the matrix C. Thus we can write the characteristic function as

$$\phi_z(ip) = \exp \left\{ \sum_{m=1}^{\infty} a_m (ip)^m \right\} \quad (5-19)$$

with

$$a_m = 2^{m-1} \{ \mu' \sum^{-1} (\{Q_M\}^m) \mu + \frac{1}{m} \text{tr}[(\{Q_M\}^m)] \} \quad (5-20)$$

for a lowpass detector, and

$$a_m = \frac{1}{2} \{ \mu_c \sum^{-1} (\{Q_M\}^m) \mu_c + \mu_s' \sum^{-1} (\{Q_M\}^m) \mu_s + \frac{2}{m} \text{tr}[(\{Q_M\}^m)] \} \quad (5-21)$$

for a narrowband detector.

For small correlation between time samples ($\psi^M \ll 1$) and a lowpass sampling rate twice that of the corresponding narrowband detector, it is shown in Appendix D that (5-20) and (5-21) are equivalent.

Putting together (5-15) and 5-19), we have the asymptotic expansion with respect to the number of variables LM

$$\begin{aligned}
 p_z(z) &\approx \frac{1}{2\pi} \int_{-\infty}^{\infty} dp \exp \{-ipz + \sum_{m=1}^{\infty} a_m (ip)^m\} \\
 &= \frac{1}{2\pi} \int_{-\infty}^{\infty} dp \exp\{-ip(z - a_1) - p^2 a_2\} \exp \left\{ \sum_{m=3}^{\infty} a_m (ip)^m \right\} \\
 &= \frac{1}{2\pi\sqrt{2a_2}} \int_{-\infty}^{\infty} dp \exp\left\{-ip \left(\frac{z-a_1}{\sqrt{2a_2}} \right) - p^2/2\right\} \exp\left\{ \sum_{m=3}^{\infty} b_m (ip)^m \right\} \quad (5-22)
 \end{aligned}$$

where

$$b_m = a_m / (2a_2)^{m/2}. \quad (5-23)$$

Now, the first term in the integrand by itself would yield

$$\begin{aligned}
 \frac{1}{2\pi\sqrt{2a_2}} \int_{-\infty}^{\infty} dp \exp\left\{-ip \left(\frac{z-a_1}{\sqrt{2a_2}} \right) - p^2/2\right\} &= (2\sqrt{\pi a_2})^{-1} \exp\left\{-\frac{(z-a_1)^2}{4a_2}\right\} \\
 &= \frac{1}{\sqrt{2a_2}} \phi \left(\frac{z-a_1}{\sqrt{2a_2}} \right), \quad (5-24)
 \end{aligned}$$

in which $\phi(x)$ is the pdf of a Gaussian variable with zero mean and unit variance. The second factor in the integrand of (5-22) can be recognized as a power series:

$$\begin{aligned}
 \exp\left\{ \sum_{m=3}^{\infty} b_m (ip)^m \right\} &= \sum_{k=0}^{\infty} \frac{1}{k!} \left[\sum_{m=3}^{\infty} b_m (ip)^m \right]^k \\
 &= 1 + \sum_{m=3}^{\infty} b_m (ip)^m + \frac{1}{2} \sum_{m=3}^{\infty} \sum_{n=3}^{\infty} b_m b_n (ip)^{m+n} \\
 &\quad + \dots
 \end{aligned}$$

$$= 1 + \sum_{m=3}^{\infty} c_m (1p)^m. \quad (5-25)$$

Since the integral (5-22) is actually a Fourier transform, we recall that

$$F^{-1}\{(1p)^k F[g(z)]\} = (-1)^k g^{[k]}(z). \quad (5-26)$$

Thus we find that

$$\begin{aligned} p_z(z) &= \frac{1}{\sqrt{2a_2}} \left\{ \phi\left(\frac{z-a_1}{\sqrt{2a_2}}\right) + \sum_{m=3}^{\infty} (-1)^m c_m \phi^{[m]}\left(\frac{z-a_1}{\sqrt{2a_2}}\right) \right. \\ &= \frac{1}{\sqrt{2a_2}} \phi\left(\frac{z-a_1}{\sqrt{2a_2}}\right) \left\{ 1 + \sum_{m=3}^{\infty} c_m \text{He}_m\left(\frac{z-a_1}{\sqrt{2a_2}}\right) \right\}, \end{aligned} \quad (5-27)$$

$\text{He}_m(\cdot)$ being the Hermite polynomial.

Accurate representation of the density function by means of the asymptotic expansion (5-27) requires that terms be arranged in order of magnitude with respect to dimension LM. Truncation of the series then yields an error no larger than the absolute value of the first discarded term [16, § 0.33].

A truncation of (5-27) accurate to $O\left[\frac{1}{(LM)^{6.5}}\right]$ is the finite series,

$$\begin{aligned} p_z(z) &= \frac{1}{\sqrt{2a_2}} \phi(z') \left\{ 1 + b_3 \text{He}_3(z') + [b_4 \text{He}_4(z') + \frac{1}{2} b_3^2 \text{He}_6(z')] \right. \\ &+ [b_5 \text{He}_5(z') + b_3 b_4 \text{He}_7(z') + \frac{1}{6} b_3^3 \text{He}_9(z')] \\ &+ [b_6 \text{He}_6(z') + (\frac{1}{2} b_4^2 + b_3 b_5) \text{He}_8(z') + \frac{1}{2} b_3^2 b_4 \text{He}_{10}(z') \\ &+ \frac{1}{24} b_3^4 \text{He}_{12}(z')], \end{aligned} \quad (5-28)$$

where bracketed terms are of the same order of magnitude, and

$$z' \equiv (z - a_1) / \sqrt{2a_2}. \quad (5-29)$$

5.3 Asymptotic expansion for the probability integral.

The probability integral (or complementary cumulative distribution function) for the output of the quadratic detector is

$$P(\tau) = \Pr\{z > \tau\}$$

$$= \int_{\tau}^{\infty} dz p_z(z)$$

or

$$P(\tau) = \sqrt{2a_2} \int_{\frac{\tau - a_1}{\sqrt{2a_2}}}^{\infty} dx P_z(x\sqrt{2a_2} + a_1)$$

$$\begin{aligned} &= Q(\tau') + \phi(\tau') \{ b_3 \text{He}_2(\tau') + [b_4 \text{He}_3(\tau') + \frac{1}{2} b_3^2 \text{He}_5(\tau')] \\ &\quad + [b_5 \text{He}_4(\tau') + b_3 b_4 \text{He}_6(\tau') + \frac{1}{6} b_3^3 \text{He}_8(\tau')] \\ &\quad + [b_6 \text{He}_5(\tau') + (\frac{1}{2} b_4^2 + b_3 b_5) \text{He}_7(\tau') + \frac{1}{2} b_3^2 b_4 \text{He}_9(\tau') \\ &\quad + \frac{1}{24} b_3^4 \text{He}_{11}(\tau')] \}, \end{aligned} \quad (5-30)$$

again for convenience using

$$\tau' = (\tau - a_1) / \sqrt{2a_2}. \quad (5-31)$$

CHAPTER 6

COMPUTING R.O.C. FOR GENERAL QUADRATIC FORMS

Although sufficient information is provided in the previous chapter to compute receiver operating characteristics for the more general cases of quadratic detectors, it is appropriate to document some of computational techniques which have been used with success. In this chapter these techniques are described and illustrated with example calculations, and results similar to those in Chapters 2-4 are given also.

6.1 Generation of Expansion Coefficients

A general outline of the procedures followed in this chapter is diagrammed in Figure 6-1. As indicated in the figure, the first task is compute the expansion coefficients used in (5-28) and (5-30), based on signal, noise, and detector parameters. The remainder of the procedures are useful for computing any distribution for which these coefficients have been generated.

From (5-21) and (5-23), expansion coefficients for narrow-band detectors are given by

$$a_m = 2^{m-1} \{ \mu_c' Q_M ([Q_M])^{m-1} \mu_c + \mu_s' Q_M ([Q_M])^{m-1} \mu_s + \frac{2}{m} \text{tr} [([Q_M])^m] \} \quad (6-1)$$

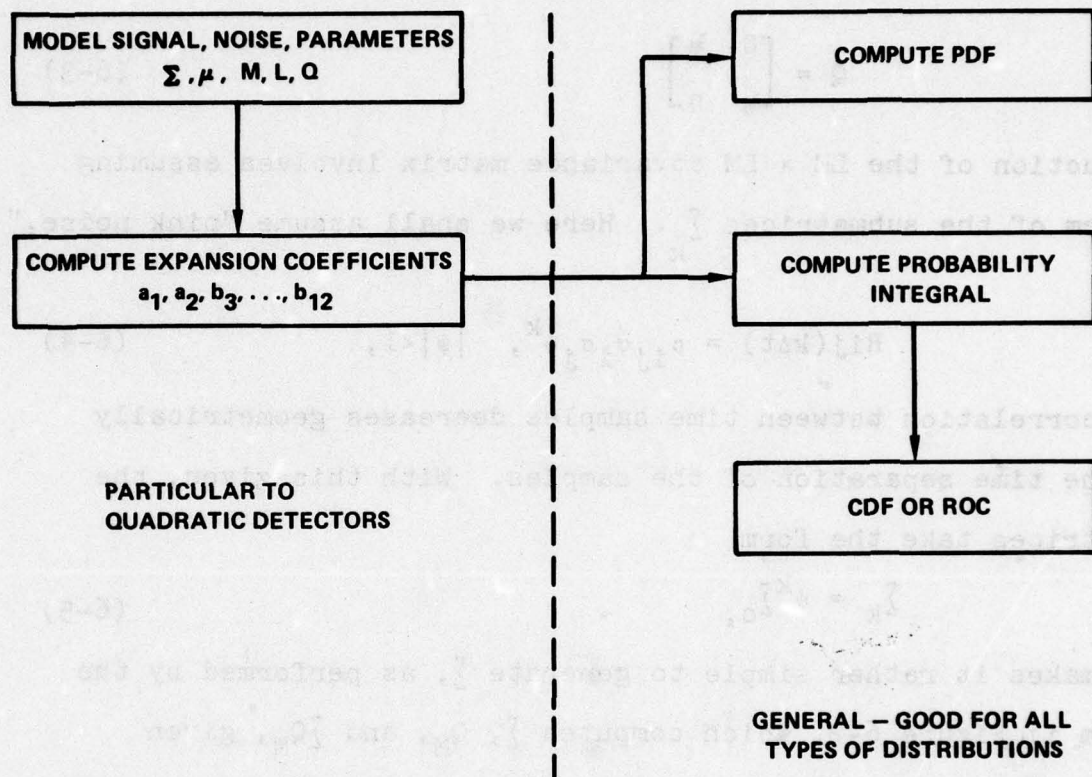


FIG. 6-1. OUTLINE OF COMPUTATION PROCEDURES.

$$b_m = a_m / (2a_2)^{m/2}, \quad m \geq 3, \quad (6-2)$$

where Σ and Q_M take the form shown in (5-3) and (5-10), respectively.

To begin, the user chooses values for L , M , Σ , and Q .

The $L \times L$ matrix Q is chosen to reflect the detector configuration.

For example, for a (two-input) correlator,

$$Q = \begin{bmatrix} 0 & \frac{1}{2} \\ \frac{1}{2} & 0 \end{bmatrix}. \quad (6-3)$$

Construction of the $LM \times LM$ covariance matrix involves assuming the form of the submatrices Σ_k . Here we shall assume "pink noise," or

$$R_{ij}(k\Delta t) = \rho_{ij} \sigma_i \sigma_j \psi^k, \quad |\psi| < 1, \quad (6-4)$$

where correlation between time samples decreases geometrically with the time separation of the samples. With this given, the sub-matrices take the form

$$\Sigma_k = \psi^k \Sigma_0, \quad (6-5)$$

which makes it rather simple to generate Σ , as performed by the program in Figure 6-2, which computes Σ , Q_M , and ΣQ_M , given L , M , Q , Σ_0 , and ψ . Figure 6-3 illustrates the output of the program for $L = M = 2$, Q as in (6-3), $\psi = .1$, and

$$\Sigma_0 = \begin{bmatrix} 1 & \frac{1}{2} \\ \frac{1}{2} & 1 \end{bmatrix}. \quad (6-6)$$

Once the signal components μ_c and μ_s are specified, computation of the expansion coefficients is straightforward. For the stationary signal case, which was assumed throughout

```

5    BASE1
10   DIM Q(40,40),Z(40,40),V(10,10),W(10,10)
15   DIM R(40,40)
20   M=2
30   L=2
40   W(1,1)=W(2,2)=1 } L
60   W(1,2)=W(2,1)=.5 } L
80   P=.1
90   V(1,1)=V(2,2)=0 } Q
100  V(1,2)=V(2,1)=.5 } Q
105  MAT Z=ZER(L*M,L*M)
106  MAT Q=ZER(L*M,L*M)
107  MAT R=ZER(L*M,L*M)
110  FOR I=0 TO M-1
120  FOR J=1 TO L
130  FOR K=1 TO L
140  J1=J+I*L
150  K1=K+I*L
160  Z(J1,K1)=W(J,K)
170  Q(J1,K1)=V(J,K)/M
180  FOR I1=1 TO M-1-I
190  K2=K1+I1*L
200  Z(J1,K2)=(P+I1)*Z(J,K)
210  Z(K2,J1)=Z(J1,K2)
220  NEXT I1
230  NEXT K
240  NEXT J
250  NEXT I
260  PRINT "          MATRIX Z"
270  PRINT
280  MAT PRINT Z
290  PRINT"          MATRIX Q"
300  PRINT
310  MAT PRINT Q
320  MAT R=Z*Q
330  PRINT"          MATRIX Z*Q"
340  PRINT
350  MAT PRINT R
500  STOP
600  END

```

FIGURE 6-2

Program to Construct Matrices

MATRIX Z

$$\begin{bmatrix} 1 & .5 & .1 & .05 \\ .5 & 1 & .05 & .1 \\ .1 & .05 & 1 & .5 \\ .05 & .1 & .5 & 1 \end{bmatrix} \quad \Sigma$$

MATRIX Q

$$\begin{bmatrix} 0 & .25 & 0 & 0 \\ .25 & 0 & 0 & 0 \\ 0 & 0 & 0 & .25 \\ 0 & 0 & .25 & 0 \end{bmatrix} \quad Q_M$$

MATRIX Z*Q

$$\begin{bmatrix} .125 & .25 & .0125 & .025 \\ .25 & .125 & .025 & .0125 \\ .0125 & .025 & .125 & .25 \\ .025 & .0125 & .25 & .125 \end{bmatrix} \quad \Sigma Q_M$$

FIG. 6-3 EXAMPLE OF COMPUTED MATRICES.

chapters 2-4,

$$\left. \begin{aligned} u_{c1} &= S_j \cos \theta_j \\ u_{s1} &= S_j \sin \theta_j \end{aligned} \right\} \begin{aligned} i &= j + nL \\ j &= 1, 2, \dots, L \\ n &= 0, 1, 2, \dots, M-1 \end{aligned} \quad (6-7)$$

If, as a reference case, we suppose that

$$\left. \begin{aligned} S_j &= S \\ \theta_j &= \theta \end{aligned} \right\} \text{all } j, \quad (6-8)$$

then (6-1) takes the simple form

$$a_m = 2^{m-1} \{ S^2 \mu' Q_m (\sum Q_m)_{\mu}^{m-1} + \frac{2}{m} \text{tr} [(\sum Q_m)^m] \} \quad (6-9)$$

with

$$\mu' = (1, 1, \dots, 1). \quad (\text{LM elements}) \quad (6-10)$$

The program of Figure 6-4 implements the expressions (6-9) and (6-2), and for the simple matrices of Figure 6-3, gives the expansion coefficients listed in Table 6-1.

EXAMPLE 6-1. Problem: Find the expansion coefficients for a sum-and-square detector with four inputs and $WT = 10$, assuming no signal, an intersample correlation factor of $\psi = .12$, and an input covariance matrix

$$\Sigma_0 = \begin{bmatrix} 1 & .24 & .05 & .01 \\ .24 & 1.5 & .3 & .05 \\ .05 & .3 & 1.5 & .24 \\ .01 & .05 & .24 & 1 \end{bmatrix}. \quad (6-11)$$

Solution: For this configuration,

$$Q = \begin{bmatrix} 1 & 1 & 1 & 1 \\ 1 & 1 & 1 & 1 \\ 1 & 1 & 1 & 1 \\ 1 & 1 & 1 & 1 \end{bmatrix}, \quad (6-12)$$

```

5  BASE1
10  DIM O(40,40),Z(40,40),V(10,10),W(10,10)
15  DIM R(40,40),U(40,1),Y(40,1),F(1,40),A(12)
16  DIM I(1,1)
20  M=2
30  L=2
35  L1=L*M
40  W(1,1)=W(2,2)=1
60  W(1,2)=W(2,1)=.5
80  P=.1
85  S=1
90  V(1,1)=V(2,2)=0
100 V(1,2)=V(2,1)=.5
105 MAT Z=ZER(L*M,L*M)
106 MAT Q=ZER(L*M,L*M)
107 MAT R=ZER(L*M,L*M)
110 FOR I=0 TO M-1
120   FOR J=1 TO L
130     FOR K=1 TO L
140       J1=J+I*L
150       K1=K+I*L
160       Z(J1,K1)=W(J,K)
170       Q(J1,K1)=V(J,K)/M
180       FOR I1=1 TO M-1-I
190         K2=K1+I1*L
200         Z(J1,K2)=(P+I1)*Z(J,K)
210         Z(K2,J1)=Z(J1,K2)
220       NEXT I1
230     NEXT K
240   NEXT J
250 NEXT I
260 MAT R=Z*Q
270 MAT U=CON(L1,I)
280 MAT Y=CON(L1,I)
290 MAT Y=Q*U
300 MAT F=COV(1,L1)
305 MAT F=TRN(Y)
310 MAT Z=(1)*R
320 MAT Q=IDN(L1,L1)
330 FOR K=1 TO 12
340   MAT Y=Q*U
350   MAT T=F*Y
360   A(K)=0
370   FOR J=1 TO L1
380     A(K)=A(K)+Z(J,J)
390   NEXT J
400   A(K)=S*I(1,1)+2*A(K)/K
405   A(K)=A(K)/2
410   IF K 3 THEN 430
420   A(K)=A(K)/(2*A(2))+(K/2)
430   MAT Q=(1)*Z
440   MAT Z=Q*R
450   PRINT K,A(K)
460 NEXT K
500 STOP
600 END

```

FIGURE 6-4

Program to Compute Narrowband Coefficients

TABLE 6-1

EXAMPLE NARROWBAND CORRELATOR COEFFICIENTS

$$\sigma_1^2 = \sigma_2^2 = 1, \rho = .5, \psi = .1, S_1 = S_2 = 1, \theta_1 = \theta_2; L=M=2$$

<u>m</u>	<u>a_m or b_m</u>
1	1
2	.364062 } a _{1, 2}
3	.193056
4	8.62109E-2
5	3.91863E-2
6	1.82383E-2
7	8.57530E-3
8	4.06278E-3
9	1.93408E-3
10	9.23871E-4
11	4.42390E-4
12	2.12217E-4

TABLE 6-2

EXAMPLE SQUARE-LAW COEFFICIENTS COVARIANCE MATRIX GIVEN BY
(6-11); $\psi = .12, L=4, M=10$

<u>m</u>	<u>a_m or b_m</u>
1	6.78
2	2.35877 } a _{1, 2}
3	.10948
4	2.75998E-2
5	7.57808E-3
6	2.20737E-3
7	6.71795E-4
8	2.11502E-4
9	6.83994E-5
10	2.26049E-5
11	7.60434E-6
12	2.59604E-6

and in the program of Figure 6-3 is defined by the statements

```
90 MAT V = CON(4,4)
100 (deleted).
```

The covariance matrix is entered by the statements

```
40 MAT W = ZER(4,4)
60 MAT READ W
510 DATA 1, .24, .05, .01
520 DATA .24, 15, .3, .05
530 DATA .05, .3, 1.5, .24
540 DATA .01, .05, .24, 1
```

Other changes to the program required are

```
20 M = 10
30 L = 4
80 P = .12
85 S = 0.
```

The coefficients, as computed by the program, are given in Table 6-2.

As a quick check, note that the mean value of the detector output, given by a_1 , agrees with the correct value, which in this case can easily be calculated by summing all the elements of \sum_0 . Finally, since $\psi^M \ll 1$, these results apply for both lowpass and narrowband detectors.

6.2 Computation of PDF and CDF

After obtaining the coefficients for the asymptotic expansion (5-19) for the characteristic function of the detector output's probability distribution, it is straightforward to compute either the probability density function, using (5-28) or the cumulative distribution function using (5-30). Common to both of these expressions are the Hermite polynomials, which are given by

$$\left. \begin{aligned} \text{He}_n(x) &= (-1)^n \left[\frac{d^n}{dx^n} \phi(x) \right] / \phi(x) \\ &= x \text{He}_{n-1}(x) - (n-1) \text{He}_{n-2}(x), \\ &\text{with } \text{He}_0(x) = 1, \text{He}_1(x) = x. \end{aligned} \right\} \quad (6-13)$$

Continuing the example of the correlator with λ_0 given by (6-6) and Q by (6-3) and with $h_1^2 = h_2^2 = 1$ ($S = \sqrt{2}$ in (6-8)) and $\psi = .1$, Figure 6-5 shows the detector output PDF for different values of M , the number of samples. Two effects are evident in the figure as M increases: the variance of the distribution decreases (the peak becomes narrower), and the distribution begins to approach symmetry about the mean value ($= 1.5$), indicating a slow convergence to a Gaussian distribution. These effects are perhaps more obvious in Figure 6-6, in which the probability integral (5-30) is plotted, using the following approximation [1] for the Gaussian probability integral:

$$Q(x) = \begin{cases} \phi(x) [d_1 y + d_2 y^2 + d_3 y^3], & x \geq 0 \\ 1 - Q(-x), & x < 0 \end{cases} \quad (6-14)$$

with

$$y = 1/(1 + .33267x)$$

$$d = .4361836$$

$$d_1 = -.1201676$$

$$d_2 = .9372980.$$

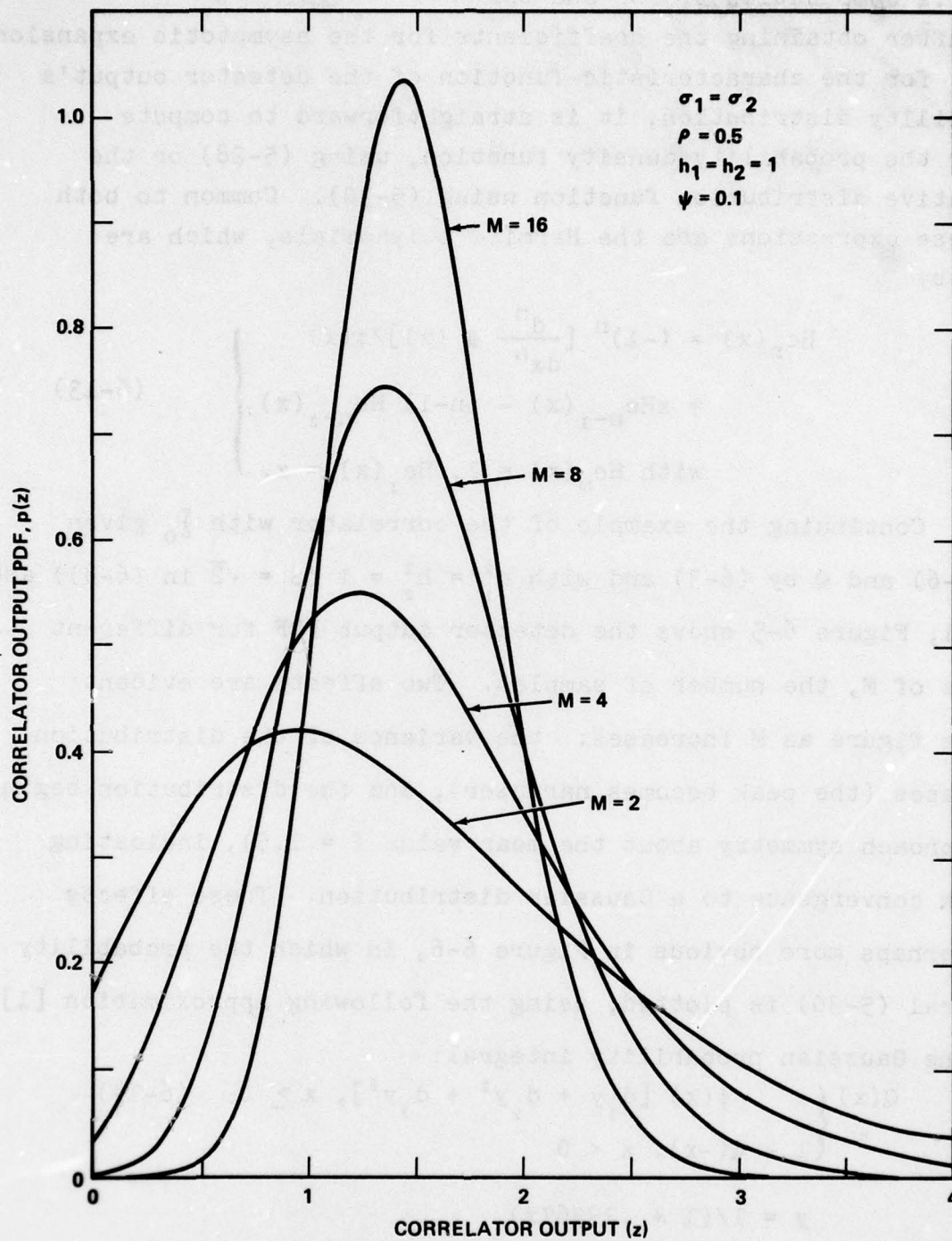


FIG. 6-5. CORRELATOR PROBABILITY DENSITY FUNCTION.

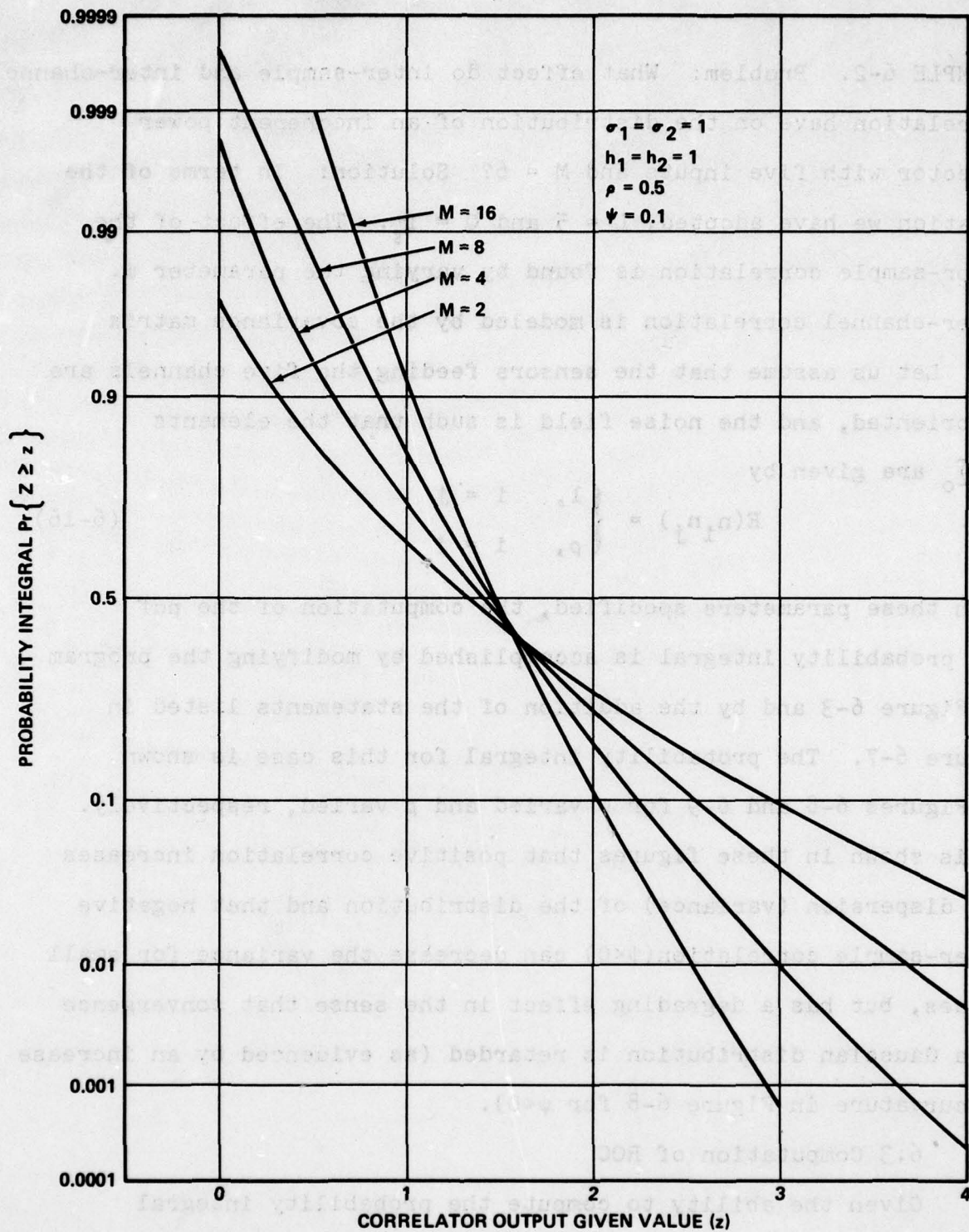


FIG. 6-6. CORRELATOR PROBABILITY INTEGRAL

EXAMPLE 6-2. Problem: What effect do inter-sample and inter-channel correlation have on the distribution of an incoherent power detector with five inputs and $M = 6$? Solution: In terms of the notation we have adopted, $L = 5$ and $Q = I_5$. The effect of the inter-sample correlation is found by varying the parameter ψ . Inter-channel correlation is modeled by the covariance matrix Σ_0 . Let us assume that the sensors feeding the five channels are so oriented, and the noise field is such that the elements of Σ_0 are given by

$$E(n_i n_j) = \begin{cases} 1, & i = j \\ \rho, & i \neq j \end{cases} \quad (6-16)$$

With these parameters specified, the computation of the pdf and probability integral is accomplished by modifying the program of Figure 6-3 and by the addition of the statements listed in Figure 6-7. The probability integral for this case is shown in Figures 6-8 and 6-9 for ψ varied and ρ varied, respectively. It is shown in these figures that positive correlation increases the dispersion (variance) of the distribution and that negative inter-sample correlation ($\psi < 0$) can decrease the variance for small values, but has a degrading effect in the sense that convergence to a Gaussian distribution is retarded (as evidenced by an increase in curvature in Figure 6-8 for $\psi < 0$).

6.3 Computation of ROC

Given the ability to compute the probability integral for the types of quadratic detectors we have been considering, it is relatively simple to obtain receiver operating characteristics

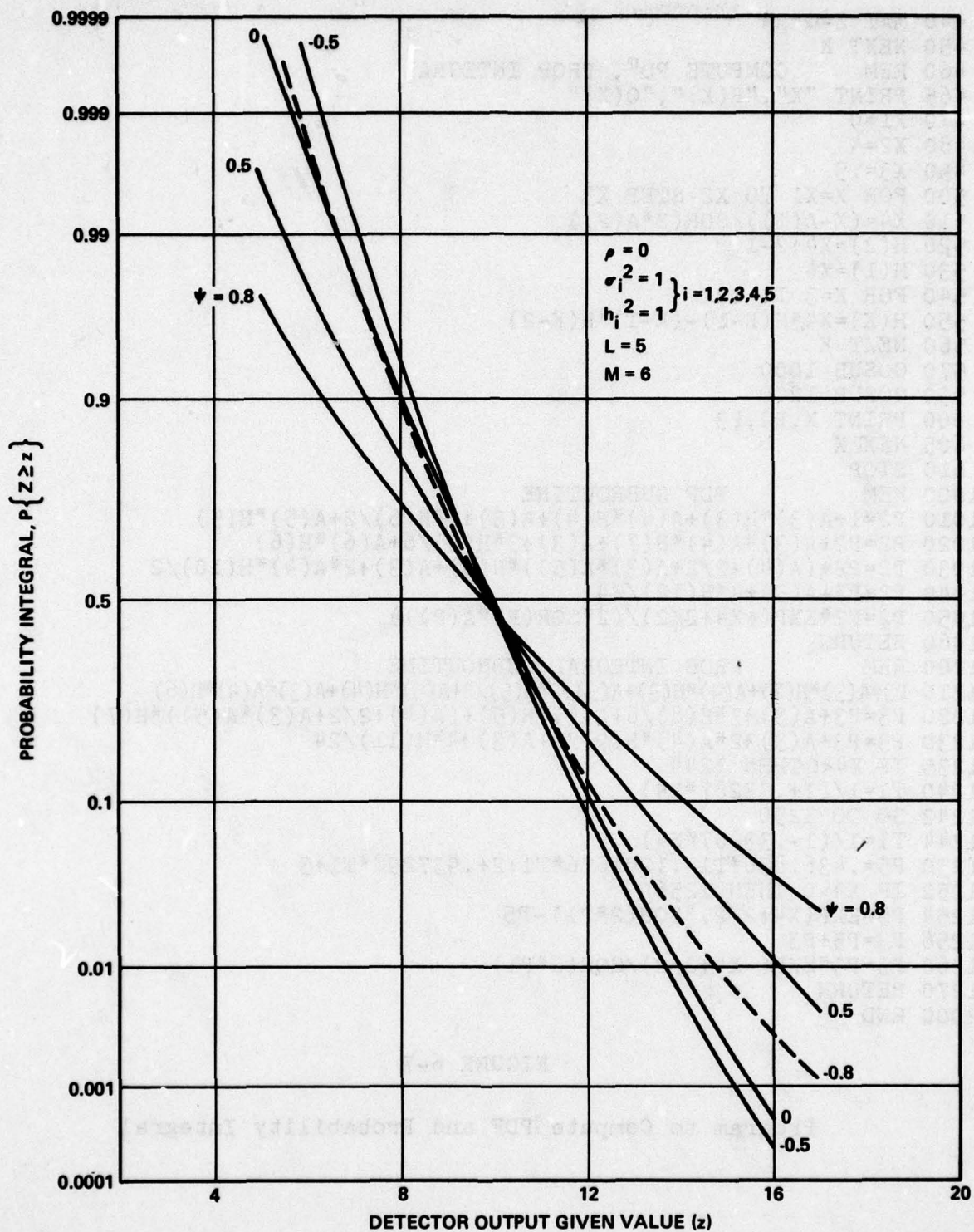

```

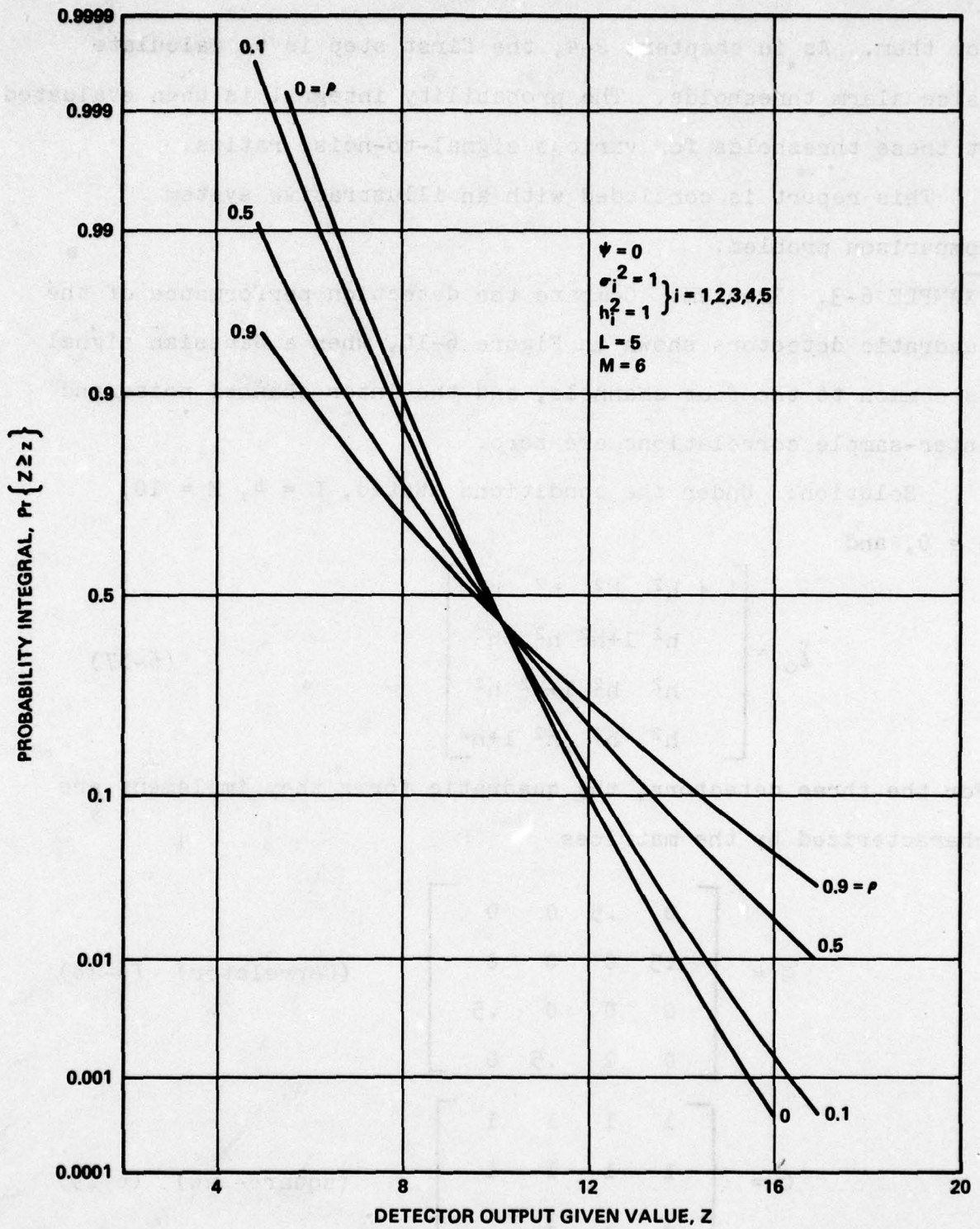
440 MAT Z=Q*R
450 NEXT K
460 REM      COMPUTE PDF, PROB INTEGRAL
465 PRINT "X","P(X)","Q(X)"
470 X1=0
480 X2=4
490 X3=.5
500 FOR X=X1 TO X2 STEP X3
510 X4=(X-A(1))/SOR(2*A(2))
520 H(2)=X4+2-1
530 H(1)=X4
540 FOR K=3 TO 12
550 H(K)=X4*H(K-1)-(K-1)*H(K-2)
560 NEXT K
570 GOSUB 1000
590 GOSUB 1200
600 PRINT X,P2,P3
605 NEXT X
610 STOP
1000 REM      PDF SUBROUTINE
1010 P2=1+A(3)*H(3)+A(4)*H(4)+A(3)+2*H(6)/2+A(5)*H(5)
1020 P2=P2+A(3)*A(4)*H(7)+A(3)+3*H(9)/6+A(6)*H(6)
1030 P2=P2+(A(4)+2/2+A(3)*A(5))*H(8)+A(3)+2*A(4)*H(10)/2
1040 P2=P2+A(3)+4*H(12)/24
1050 P2=P2*EXP(+X4+2/2)/(2*SQR(P1*A(2)))
1060 RETURN
1200 REM      PROB INTEGRAL SUBROUTINE
1210 P3=A(3)*H(2)+A(4)*H(3)+A(3)+2*H(5)/2+A(5)*H(4)+A(3)*A(4)*H(6)
1220 P3=P3+A(3)+3*H(8)/6+A(6)*H(5)+(A(4)+2/2+A(3)*A(5))*H(7)
1230 P3=P3+A(3)+2*A(4)*H(9)/2+A(3)+4*H(11)/24
1235 IF X4<0 THEN 1244
1240 T1=1/(1+.33267*X4)
1242 GO TO 1250
1244 T1=1/(1-.33267*X4)
1250 P5=.4361836*T1-.1201676*T1+2+.937298*T1+3
1252 IF X4>0 THEN 1256
1254 P5=EXP(X4+2/2)*SQR(2*P1)-P5
1256 P3=P5+P3
1260 P3=P3*EXP(-X4+2/2)/SQR(2*P1)
1270 RETURN
2000 END

```

FIGURE 6-7

Program to Compute PDF and Probability Integral

FIG. 6-8. INCOHERENT DETECTOR PROBABILITY INTEGRAL, ψ VARIED

FIG. 6-9 INCOHERENT DETECTOR PROBABILITY INTEGRAL, ρ VARIED

for them. As in chapters 2-4, the first step is to calculate false alarm thresholds. The probability integral is then evaluated at these thresholds for various signal-to-noise ratios.

This report is concluded with an illustrative system comparison problem.

EXAMPLE 6-3. Problem: Compare the detection performance of the quadratic detectors shown in Figure 6-10, when a Gaussian signal is common to the four channels, and the inter-channel noise and inter-sample correlations are zero.

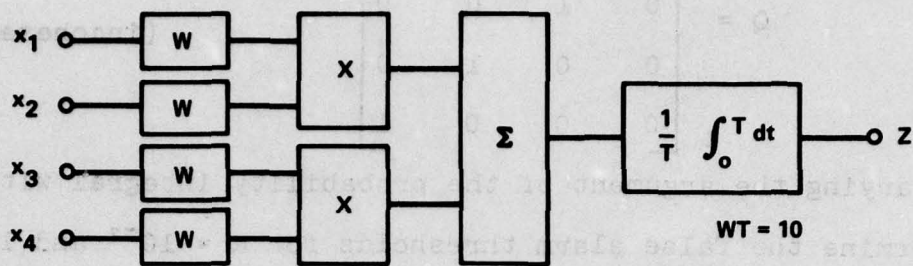
Solution: Under the conditions stated, $L = 4$, $M = 10$, $\psi = 0$, and

$$\Sigma_0 = \begin{bmatrix} 1 + h^2 & h^2 & h^2 & h^2 \\ h^2 & 1 + h^2 & h^2 & h^2 \\ h^2 & h^2 & 1 + h^2 & h^2 \\ h^2 & h^2 & h^2 & 1 + h^2 \end{bmatrix} \quad (6-17)$$

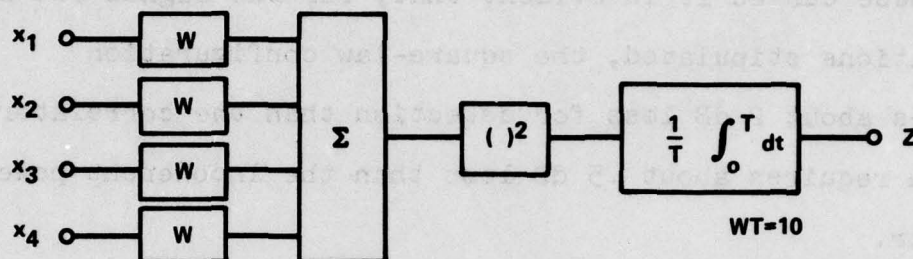
For the three detectors, the quadratic forms they implement are characterized by the matrices

$$Q = \begin{bmatrix} 0 & .5 & 0 & 0 \\ .5 & 0 & 0 & 0 \\ 0 & 0 & 0 & .5 \\ 0 & 0 & .5 & 0 \end{bmatrix} \quad (\text{Correlator}) \quad (6-18)$$

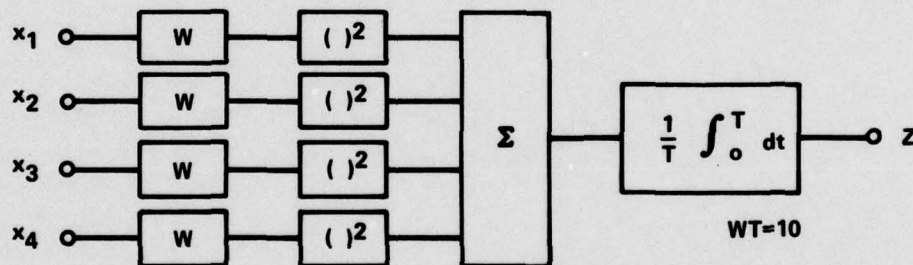
$$Q = \begin{bmatrix} 1 & 1 & 1 & 1 \\ 1 & 1 & 1 & 1 \\ 1 & 1 & 1 & 1 \\ 1 & 1 & 1 & 1 \end{bmatrix} \quad (\text{square-law}) \quad (6-19)$$



CORRELATE-AND-SUM.



CONVENTIONAL SQUARE-LAW



INCOHERENT POWER DETECTOR

FIG. 6-10. FOUR-INPUT DETECTORS

$$Q = \begin{bmatrix} 1 & 0 & 0 & 0 \\ 0 & 1 & 0 & 0 \\ 0 & 0 & 1 & 0 \\ 0 & 0 & 0 & 1 \end{bmatrix} \quad \begin{array}{l} \text{(incoherent)} \\ (6-20) \end{array}$$

After varying the argument of the probability integral with $h^2=0$ to determine the false alarm thresholds for $\alpha = 10^{-2}$ and 10^{-4} for the three detectors; These values of argument were fixed while h^2 was varied, producing the ROC's of Figure 6-11 and 6-12. From these curves it is evident that, for the signal and noise correlations stipulated, the square-law configuration requires about 2 dB less for detection than the correlator, which in turn requires about .5 dB less than the incoherent power detector.

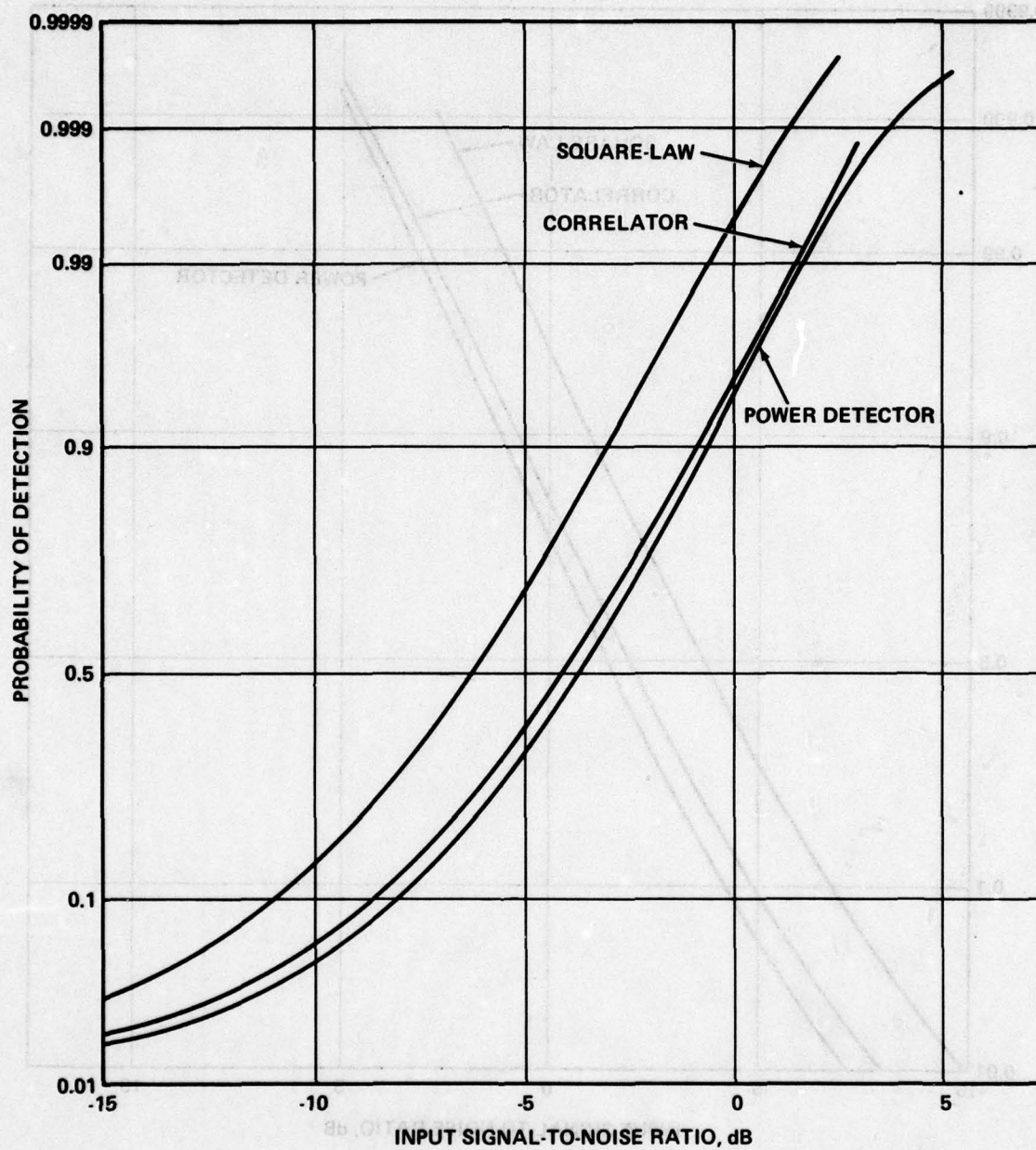


FIG. 6-11 FOUR-INPUT DETECTOR COMPARISON, PFA = 0.01, RANDOM SIGNAL (WT = 10)

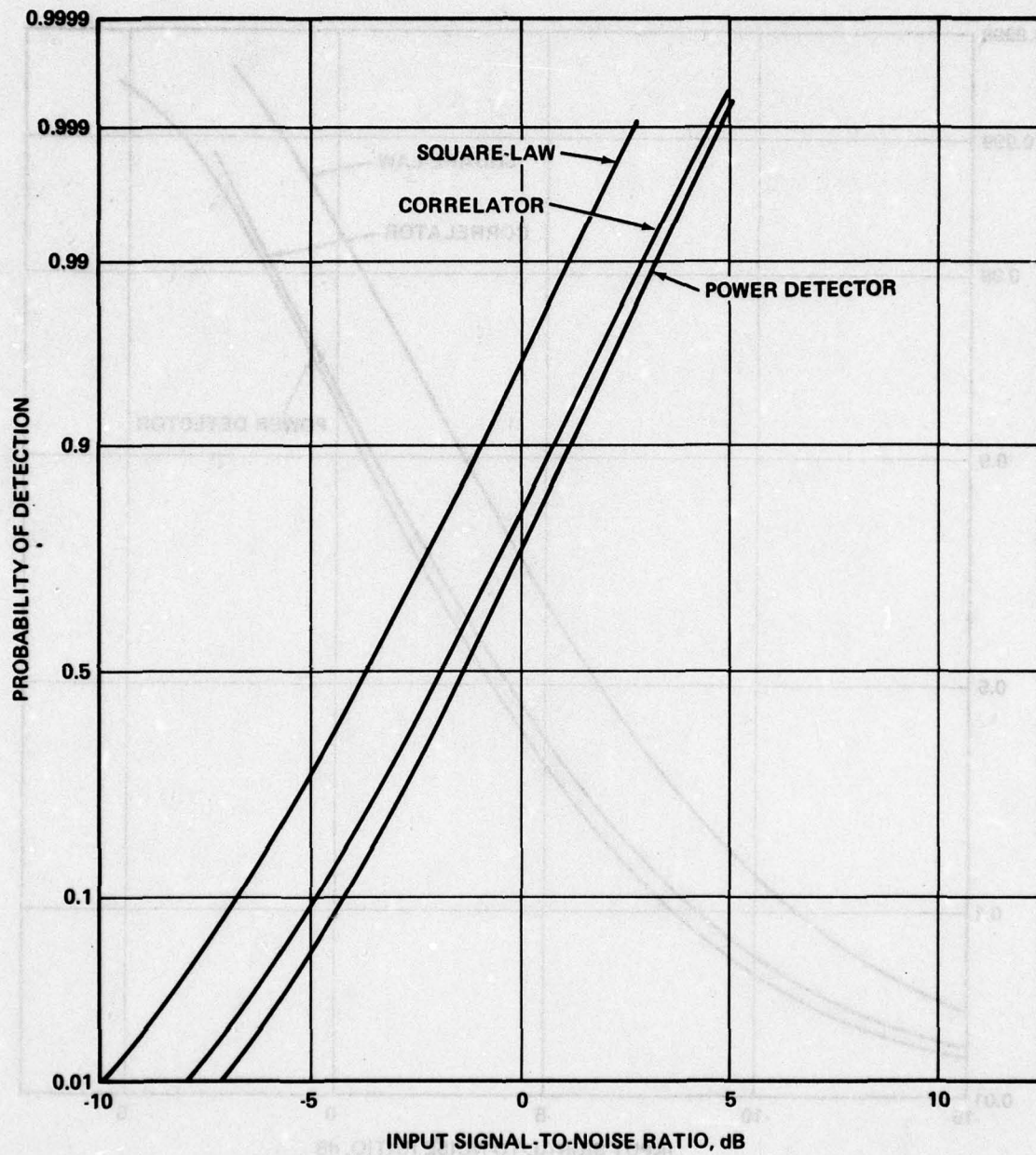


FIG. 6-12. FOUR-INPUT DETECTOR COMPARISON, PFA = 0.0001, RANDOM SIGNAL (WT = 10)

REFERENCES

1. M. Abramowitz and I. Stegun, eds., Handbook of Mathematical Functions, National Bureau of Standards Applied Mathematics Series, #55, Government Printing Office, Washington, 1970.
2. G. A. Campbell "Probability Curves Showing Poisson's Exponential Summations," Bell System Technical Journal, Vol. 2 (1923), pp. 95-113.
3. C. Hodgman, ed., C.R.C. Standard Mathematical Tables, twelfth edition, Chemical Rubber Publishing Company, Cleveland, 1959.
4. C. N. Pryor, "Calculation of the Minimum Detectable Signal for Practical Spectrum Analyzers," Naval Ordnance Laboratory Technical Report TR 71-92, 2 August 1971.
5. E. Fix, "Tables of Noncentral χ^2 ," Publications in Statistics, Vol. 1(1949), University of California Press, Berkeley, pp. 15-19.
6. G. E. Haynam et. al., "Tables of the Cumulative Non-Central Chi-Square Distribution," in Selected Tables in Mathematical Statistics, American Mathematical Society, Providence, Rhode Island, 1973 (2nd printing), pp. 1-78.
7. J. I. Marcum, "Table of Q Functions," Project Rand Research Memorandum RM-338, The Rand Corporation, Santa Monica, CA 1950.
8. D. E. Bailey and N. C. Randall, "Nomograph Determines Probability of Detecting Signals in Noise," Electronics, March 17, 1961.
9. H. Urkowitz, "Energy Detection of Unknown Deterministic Signals," Proceedings of the IEEE, Vol. 55 (April, 1967), pp. 523-531.
10. S. V. Smirnov and M. K. Potapov, "Nomogram for the χ^2 Probability and Function," Theory of Probability, Vol. VI (1961), Society for Industrial and Applied Math (Translation of Russian Journal).

11. P. B. Patnaik, "The Noncentral χ^2 and F Distributions and Their Applications," Biometrika, Vol. 36 (1949), pp. 202-232.
12. M. Sankaran, "Approximations to the Non-Central Chi-Square Distribution," Biometrika, Vol. 50 (1963), pp. 199-204.
13. L. E. Miller and J. S. Lee, "The Probability Density Function for the Output of an Analog Cross-Correlator with Correlated Bandpass Inputs," IEEE Transactions on Information Theory, IT-20, July, 1974, pp. 433-440.
14. T. Jayachandran and D. R. Barr, "On the Distribution of a Difference of Two Scaled Chi-Square Random Variables," American Statistician, pp. 29-30, December, 1970.
15. L. E. Miller, "Signal Detection and Bearing Estimation Capabilities of Multiplicative Array Processors," Ph.D. dissertation, The Catholic University of America, Washington, DC 1973 (University Microfilms #73-21, 104).
16. I. S. Gradshteyn and I. M. Ryzhik, Table of Integrals Series and Products, Fourth edition, Academic Press, New York, 1965.
17. K. S. Miller, Multidimensional Gaussian Distributions, Wiley, New York, 1964.
18. D. Middleton, Introduction to Statistical Communication Theory, McGraw-Hill, New York, 1960.
19. L. C. Andrews, "The Probability Density Function for the Output of a Cross-Correlator With Bandpass Inputs," IEEE Transactions on Information Theory, Vol. IT-19, pp 13-19, (January, 1973).

APPENDIX A

APPROXIMATION TO THE NONCENTRAL χ^2 DISTRIBUTION

In [12] it is shown that when the noncentral chi-squared random variable X , with ν degrees of freedom and noncentrality parameter λ , is transformed into the variable Y by the relation

$$Y = \sqrt{X - \frac{1}{2}(\nu - 1)}, \quad (\text{A-1})$$

the variable Y very closely approximates a Gaussian variable with unit variance and mean equal to

$$E(Y) = \sqrt{\lambda + \frac{1}{2}(\nu - 1)}. \quad (\text{A-2})$$

Thus, the probability integral for X is approximately

$$Q(x | \nu, \lambda) \approx Q(\sqrt{x - \frac{1}{2}(\nu - 1)} - \sqrt{\lambda + \frac{1}{2}(\nu - 1)}), \quad (\text{A-3})$$

where $Q(x)$ is the Gaussian probability integral. Defining a normalized detection threshold d_Y analogous to the false alarm threshold d_α , we have

$$d_Y = \sqrt{\chi^2_{1-\alpha} - \frac{1}{2}(2WT - 1)} - \sqrt{2WTh^2 + \frac{1}{2}(2WT - 1)} \quad (\text{A-4})$$

or

$$h^2 = \frac{2WT-1}{4WT} + \frac{1}{2WT} [\sqrt{\chi^2_{1-\alpha} - WT + \frac{1}{2}} - d_Y]^2. \quad (\text{A-5})$$

From (2-13),

$$\chi^2_{1-\alpha} = 2\sqrt{WT}d_\alpha + 2WT, \text{ and}$$

$$h^2(\gamma, \alpha, WT) = \frac{d_\alpha}{\sqrt{WT}} + \frac{d_\alpha^2 + 1}{2WT} + \frac{d_Y}{\sqrt{WT}} \sqrt{\frac{2d_\alpha}{WT} + 1 + \frac{1}{2WT}} \quad (\text{A-6})$$

AD-A050 477

NAVAL SURFACE WEAPONS CENTER WHITE OAK LAB SILVER SP--ETC F/G 17/9
COMPUTING R.O.C. FOR QUADRATIC DETECTORS.(U)

OCT 76 L E MILLER

NSWC/WOL/TR-76-148

UNCLASSIFIED

2 OF 2

AD
A050 477



NL

END

DATE
FILMED

3-78

DDC

The accuracy of this approximation to the noncentral chi-squared distribution was checked against the table of [6] for $\alpha = 10^{-2}$, with the result

ν	λ	γ	$\gamma_{\text{approx.}}$	%dev.
2	8.190	.5	.4986	-.28
	13.881	.8	.7998	-.02
	27.415	.99	.9902	+.02
4	10.232	.5	.4974	-.52
	16.749	.8	.7997	-.04
	31.794	.99	.9904	+.04
10	14.126	.5	.4961	-.77
	22.177	.8	.7995	-.07
	40.021	.99	.9905	+.05
20	18.451	.5	.4957	-.87
	28.162	.8	.7994	-.08
	49.027	.99	.9907	+.07
40	24.542	.5	.4955	-.90
	36.550	.8	.7993	-.08
	61.572	.99	.9908	+.08
100	36.614	.5	.4958	-.83
	53.103	.8	.7994	-.08
	86.175	.99	.9908	+.08

APPENDIX B

DERIVATION OF CORRELATOR PDF

As indicated in the text, the output of the correlation detector with deterministic signal input is the difference of two scaled noncentral chi-squared variables:

$$z = z_1 - z_2 \quad (B-1)$$

where, using $M = WT$

$$\frac{2Mz}{\sigma_3^2} \text{ is } \chi'^2(2M, 2Mh_3^2) \quad (B-2)$$

$$\frac{2Mz}{\sigma_4^2} \text{ is } \chi'^2(2M, 2Mh_4^2).$$

Under the simplifying assumption of equal input noise power $\sigma_1 = \sigma_2 = \sigma$, z_1 and z_2 are independent, and

$$\begin{aligned} \frac{4Mz}{\sigma^2} &= (1 + \rho) \left(\frac{2Mz}{\sigma_3^2} \right) - (1 - \rho) \left(\frac{2Mz}{\sigma_4^2} \right) \\ &\triangleq (1 + \rho)v_1 - (1 - \rho)v_2. \end{aligned} \quad (B-3)$$

The characteristic function for the distribution of a non-central chi-squared variable V with $2v$ degrees of freedom and noncentrality parameter λ is, from [11],

$$\begin{aligned}
\phi_v(ip | v, \lambda) &\triangleq E\{e^{ipv}\} \\
&= \frac{\exp[ip\lambda/(1-2ip)]}{(1-2ip)^v} \\
&= e^{-\lambda/2} \sum_{n=0}^{\infty} \frac{(\lambda/2)^n}{n!} \frac{1}{(1-2ip)^{v+n}}
\end{aligned}$$

Therefore, the characteristic function for the distribution of

$$v = 4Mz/\sigma^2$$

is

$$\phi_v(ip) = E\{e^{ip(1+\rho)v_1}\} E\{e^{-ip(1-\rho)v_2}\} \quad (B-5)$$

$$= \exp\{-M(h_3^2 + h_4^2)\} \sum_{n=0}^{\infty} \sum_{m=0}^{\infty} \frac{(Mh_3^2)^n}{n!} \frac{(Mh_4^2)^m}{m!} \quad (B-6)$$

$$\times \frac{1}{[1-2ip(1+\rho)]^{M+n}} \frac{1}{[1+2ip(1-\rho)]^{M+m}}$$

Making use of an expression in [14], we may write

$$\begin{aligned}
&[1-2ip(1+\rho)]^{-M-n} [1+2ip(1-\rho)]^{M-m} \\
&= \sum_{j=1}^{n+M} \binom{2M+m+n-1-j}{M+m-1} \left(\frac{1+\rho}{2}\right)^{M+m} \left(\frac{1-\rho}{2}\right)^{M+n-j} \frac{1}{[1-2ip(1+\rho)]^j} \\
&\quad (B-7)
\end{aligned}$$

$$+ \sum_{k=1}^{m+M} \binom{2M+m+n-1-k}{M+n-1} \left(\frac{1-\rho}{2}\right)^{M+n} \left(\frac{1+\rho}{2}\right)^{M+m-k} \frac{1}{[1+2ip(1-\rho)]^k}.$$

This expression allows a representation of the pdf of v in terms of chi-squared pdf's:

$$p_V(v) = \frac{1}{2} \left(\frac{1-\rho^2}{4} \right)^{M-1} \exp\{-M(h_3^2 + h^2 \sum_{n=0}^{\infty} \sum_{m=0}^{\infty} \frac{[M(1-\rho)h_3^2/2]^n [M(1-\rho)h^2/2]^m}{n! m!}\}$$

$$\times \left\{ \begin{array}{l} \sum_{j=0}^{n+m-1} \binom{2M+m+n-2-j}{M+m-1} \left(\frac{2}{1-\rho} \right)^j p_{\chi^2} \left(\frac{v}{1+\rho} | 2+2j \right), v \geq 0 \\ \sum_{k=0}^{m+M-1} \binom{2M+m+n-2-k}{M+m-1} \left(\frac{2}{1-\rho} \right)^k p_{\chi^2} \left(\frac{-v}{1-\rho} | 2+2k \right), v < 0, \end{array} \right. \quad (B-8)$$

where

$$p_{\chi^2}(x|2v) \equiv e^{-x/2} \frac{(x/2)^{v-1}}{2\Gamma(v)}, \quad x \geq 0. \quad (B-9)$$

Alternately, to get the double infinite series into a more recognizable form, such as

$$\sum_{n=0}^{\infty} \sum_{m=0}^{\infty} \frac{a_n b_m}{n! m!} f_{mn}(v), \quad (B-10)$$

we define the polynomials

$$G_r^s(x) \triangleq \sum_{k=0}^r \binom{r+s-k}{s} \frac{x^k}{k!} \quad (\text{B-11})$$

whose properties are summarized in [13]. This allows the pdf of the detector output to be written as

$$\begin{aligned} p_z(z) &= \frac{4M}{\sigma^2} p_v\left(\frac{4Mz}{\sigma^2}\right) \\ &= \frac{M}{\sigma^2} \left(\frac{1-\rho^2}{4}\right)^{M-1} \exp\{-M(h_3^2 + h_4^2)\} \\ &\times \sum_{n=0}^{\infty} \sum_{m=0}^{\infty} \frac{[M(1-\rho)h_3^2/2]^n}{n!} \frac{[M(1+\rho)h_4^2/2]^m}{m!} \end{aligned} \quad (\text{B-12})$$

$$\times \begin{cases} \exp\{-2Mz/\sigma^2(1+\rho)\} G_{M+n-1}^{M+m-1} [4Mz/\sigma^2(1-\rho^2)], & z \geq 0 \\ \exp\{2Mz/\sigma^2(1-\rho)\} G_{M+m-1}^{M+n-1} [-4Mz/\sigma^2(1-\rho^2)], & z < 0. \end{cases}$$

APPENDIX C

DERIVATION OF SQUARE-AND-SUM PDF

As shown in the text, the output of the incoherent or square-and-sum detector with two deterministic signal inputs can be considered the sum of two scaled noncentral chi-squared variables:

$$z = z_1 + z_2 \quad (C-1)$$

where, using $M = WT$,

$$\frac{Mz_1}{\sigma^2_3} \text{ is } \chi'^2(2M, 2Mh^2_3) \quad (C-2)$$

$$\frac{Mz_2}{\sigma^2_4} \text{ is } \chi'^2(2M, 2Mh^2_4).$$

Under the simplifying assumption of equal input noise power, $\sigma_1 = \sigma_2 = \sigma$, z_1 and z_2 are independent, and

$$\frac{2Mz}{\sigma^2} = (1 + \rho) \frac{Mz_1}{\sigma^2_3} + (1 - \rho) \frac{Mz_2}{\sigma^2_4} \quad (C-3)$$

$$\Delta (1 + \rho)v_1 + (1 - \rho)v_2.$$

The joint pdf of v_1 and v_2 is

$$p_1(v_1, v_2) = \frac{1}{4} e^{-(\lambda_1 + \lambda_2 + v_1 + v_2)/2} \left[\frac{v_1 v_2}{\lambda_1 \lambda_2} \right]^{\frac{M-1}{2}} \\ \times I_{M-1}(\sqrt{\lambda_1 v_1}) I_{M-1}(\sqrt{\lambda_2 v_2}), v_1, v_2 > 0 \quad (C-4)$$

where

$$\lambda_1 = 2Mh_3^2$$

$$\lambda_2 = 2Mh_4^2$$

(C-5)

$I_K(x)$ is the modified Bessel function of the first kind, of order K .

Consider the following change of variables:

$$v_1 = \frac{x}{1+\rho} + \frac{(1-\rho)y}{2} \quad x = (1+\rho)v_1 + (1-\rho)v_2 \geq 0 \\ \text{or} \quad v_2 = -\frac{(1+\rho)y}{2} \quad y = \frac{-2v_1}{1+\rho}, \frac{-2x}{1-\rho} \leq y \leq 0. \quad (C-6)$$

Then the pdf of x and y is

$$p_2(x, y) = \frac{1}{4} p_1\left[\frac{x}{1+\rho} + \frac{(1-\rho)y}{2}, -\frac{(1+\rho)y}{2}\right] \\ = (1/8) \exp\left\{-\frac{1}{2}[\lambda_1 + \lambda_2 + \rho y - \frac{x}{1+\rho}]\right\} \left\{\frac{-y[(1-\rho^2)y+2x]}{4\lambda_1\lambda_2}\right\}^{\frac{M-1}{2}} \\ \times I_{M-1}\left\{\sqrt{\lambda_1\left[\frac{x}{1+\rho} + \frac{(1-\rho)y}{2}\right]}\right\} I_{M-1}\left\{\sqrt{-\frac{(1+\rho)y\lambda_2}{2}}\right\} \quad (C-7)$$

for $x \geq 0$ and $-\frac{2x}{1-\rho^2} \leq y \leq 0$.

Since $x \equiv \frac{2Mz}{\sigma^2}$ is the variable of interest, we obtain its pdf by integrating out y :

$$\begin{aligned}
 p_3(x) &= \int_{-\frac{2x}{1-\rho^2}}^0 \text{dyp}_2(x, y) = \int_0^{\frac{2x}{1-\rho^2}} \text{dyp}_2(x, -y) \\
 &= f_1(x) \int_0^{\alpha} dy e^{-\rho y} [y(y - \alpha)]^{\frac{M-1}{2}} \quad (C-8) \\
 &\quad \times I_{M-1}\left\{\sqrt{\lambda_1 \frac{(1-\rho)}{2}} [\alpha - y]\right\} I_{M-1}\left\{\sqrt{\frac{(1+\rho)\lambda_2}{2}} y\right\},
 \end{aligned}$$

using $\alpha = \frac{2x}{1-\rho^2}$ and

$$f_1(x) = \frac{1}{8} \left[\frac{-(1-\rho^2)}{4\lambda_1\lambda_2} \right]^{\frac{M-1}{2}} \exp\{-\frac{1}{2}[\lambda_1\lambda_2 + \frac{x}{1+\rho}]\} \quad (C-9)$$

By expanding the Bessel functions into their series representations, we have

$$\begin{aligned}
 p_3(x) &= f_2(x) \sum_{n=0}^{\infty} \sum_{m=0}^{\infty} \frac{[(1-\rho)\lambda_1/8]^n}{n!(n+M-1)!} \frac{[(1+\rho)\lambda_2/8]^m}{m!(m+M-1)!} \\
 &\quad \times \int_0^{\alpha} dy e^{-\rho y/2} y^{m+M-1} (\alpha - y)^{n+M-1}, \quad (C-10)
 \end{aligned}$$

with

$$f_2(x) = \left[\frac{-\lambda_1\lambda_2(1-\rho^2)}{256} \right]^{\frac{M-1}{2}} f_1(x). \quad (C-11)$$

From [16], formula 3.383.1, we learn that

$$\int_0^{\alpha} dy e^{-\rho y/2} y^{m+M-1} (\alpha - y)^{n+M-1} \quad (C-12)$$

$$= \frac{(m+M-1)!(n+M-1)!}{(m+n+2M-1)!} \alpha^{m+n+2M-1} {}_1F_1[m+M; m+n+2M; -\rho\alpha/2],$$

where ${}_1F_1(\)$ is the confluent hypergeometric function. After substituting into (C-10), we obtain the pdf of the detector output Z:

$$p_Z(z) = \frac{2M}{\sigma^2} P_s \left(\frac{2Mz}{\sigma^2} \right)$$

$$= \frac{M}{\sigma^2(1+\rho)} \frac{Mz}{\sigma^2(1+\rho)} \frac{1+\rho}{1-\rho} \exp\left\{-M \frac{z}{\sigma^2(1+\rho)} + h_3 + h_4\right\}$$

$$\sum_{n=0}^{\infty} \sum_{m=0}^{\infty} \frac{[Mh_4^2(1+\rho)/(1-\rho)]^n}{n!} \frac{(Mh_3^2)^m}{m!} \frac{[Mz/\sigma^2(1+\rho)]^{n+m}}{(n+m+2M-1)!}$$

$$\times {}_1F_1[M+n; 2M+m+n; -2\rho Mz/\sigma^2(1-\rho^2)], z \geq 0. \quad (C-13)$$

This expression can be shown to be a special case of that given in [17], page 59.

By expanding the hypergeometric function, the probability integral is found to be

$$P(\tau) = \int_{\tau}^{\infty} p_Z(z) dz = \left(\frac{1+\rho}{1-\rho} \right)^M \exp\left\{-M \left[\frac{\tau}{\sigma^2(1+\rho)} + h_3^2 + h_4^2 \right]\right\}$$

(expression continued)

$$\times \sum_{n=0}^{\infty} \sum_{m=0}^{\infty} \sum_{k=0}^{\infty} \frac{1}{n!m!k!} \left[M h_4^2 \left(\frac{1+\rho}{1-\rho} \right) \right] (M h_3^2)^m \left(\frac{-2\rho}{1-\rho} \right)^k (n+M)_k \quad (C-14)$$

$$\times e_{m+n+k+2M-1} \{M\tau/\sigma^2(1+\rho)\}, \tau \geq 0.$$

Special cases. (1) For $h_3^2 = h_4^2 = 0$,

$$P(\tau) = \left(\frac{1+\rho}{1-\rho} \right)^M e^{-M\tau/\sigma^2(1+\rho)} \sum_{k=0}^{\infty} \left(\frac{-2\rho}{1-\rho} \right)^k e_{k+2M-1} \{M\tau/\sigma^2(1+\rho)\},$$

$-1 < \rho < \frac{1}{3}$

or

$$P(\tau) = \left(\frac{1-\rho}{1+\rho} \right)^M e^{-M\tau/\sigma^2(1-\rho)} \sum_{k=0}^{\infty} \left(\frac{2\rho}{1+\rho} \right)^k e_{k+2M-1} \{M\tau/\sigma^2(1-\rho)\}$$

$-\frac{1}{3} < \rho < 1.$

(2) For $\rho = 0$ (input noise uncorrelated),

$$P(\tau) = \exp\left\{-M\left(\frac{\tau}{\sigma^2} + h_3^2 + h_4^2\right)\right\} \sum_{n=0}^{\infty} \sum_{m=0}^{\infty} \frac{(M h_3^2)^n}{n!} \frac{(M h_4^2)^m}{m!} e_{m+n+2M-1} \{M\tau/\sigma^2\}$$

(C-17)

APPENDIX D

EQUIVALENCE OF LOWPASS AND NARROWBAND DISTRIBUTIONS

Given a narrowband detector sampling rate of B samples per second and a lowpass detector sampling rate of 2B samples per second. For T seconds, the number of samples M in the expression for the narrowband expansion coefficients (5-21) is $M = BT$, and for the lowpass coefficients $M = 2BT$ in (5-20).

For $M = 2BT$, from (5-3) and (5-10),

$$\sum_{(2BT)} = \left[\begin{array}{c|c} \sum_{(BT)} & \psi^{BT} \sum_{(BT)} \\ \hline \psi^{BT} \sum_{(BT)} & \sum_{(BT)} \end{array} \right] \quad (D-1)$$

and

$$Q_{2BT} = \frac{1}{2} \left[\begin{array}{c|c} Q_{BT} & Q_{(BT)} \\ \hline Q_{(BT)} & Q_{BT} \end{array} \right] \quad (D-2)$$

Now, if we write

$$\left(\sum_{(2BT)} Q_{2BT} \right)^m = \frac{1}{2^m} \left[\begin{array}{c|c} e_m \left(\sum_{(BT)} Q_{BT} \right)^m & f_m \left(\sum_{(BT)} Q_{(BT)} \right)^m \\ \hline f_m \left(\sum_{(BT)} Q_{(BT)} \right)^m & e_m \left(\sum_{(BT)} Q_{BT} \right)^m \end{array} \right] \quad (D-3)$$

it is true that

$$\begin{pmatrix} e_m \\ f_m \end{pmatrix} = \begin{bmatrix} 1 & \psi^{BT} \\ \psi^{BT} & 1 \end{bmatrix} \begin{pmatrix} e_{m-1} \\ f_{m-1} \end{pmatrix}$$

$$= \begin{bmatrix} 1 & \psi^{BT} \\ \psi^{BT} & 1 \end{bmatrix}^{m-1} \begin{pmatrix} 1 \\ \psi^{BT} \end{pmatrix}, \quad (D-4)$$

since $e_1 = 1$ and $f_1 = \psi^{BT}$. Thus e_m is of the order $1 + O(\psi^{BT})$, and f_m is $O(\psi^{BT})$, with the consequence

$$\text{tr} \left[\left(\Sigma_{(2BT)} Q_{2BT} \right)^m \right] = \frac{1}{2^{m-1}} \text{tr} \left[\left(\Sigma_{(B)} Q_{BT} \right)^m \right] \times [1 + O(\psi^{BT})]. \quad (D-5)$$

Therefore, under the assumptions made here, the noise power terms in (5-20) and (5-21) are equivalent for $\psi^{BT} \ll 1$.

Equal signal power for the two cases of bandwidth is represented by

$$\mu_1(t_j) = A_1(t_j) \cos[wt_j + \theta_1(t_j)] \quad (\text{narrowband})$$

$$\mu_1(t_j) = \frac{1}{\sqrt{2}} A_1(t_j). \quad (\text{lowpass})$$

If the signals are stationary over the entire integration period, then

$$\mu_{(2BT)} \left[\frac{\mu_{(BT)}}{\mu_{(BT)}} \right], \quad (D-7)$$

and also

$$\begin{aligned}
 & \mu'_{(2BT)} Q_{2BT} \left(\sum_{(2BT)} Q_{2BT} \right)^{M-1} \mu_{(2BT)} \\
 &= \frac{1}{2^{m-1}} \mu'_{(BT)} Q_{BT} \left(\sum_{(BT)} Q_{BT} \right)^{m-1} \mu_{(BT)} \\
 &\times (e_{m-1} + f_{m-1}). \tag{D-8}
 \end{aligned}$$

Thus, in the sense of (D-6) the signal terms in (5-20) and (5-21) are equivalent to order $O(\psi^{BT})$ for the assumptions which have been made.

DISTRIBUTION LIST

Commander
 Naval Ocean Systems Center
 San Diego, CA 92132
 303 (Hanna, Marsh)
 2522 (Hodgkiss)
 Library

Commanding Officer
 ARPA Research Center
 Unit 1
 Moffett Field, CA 94035
 Richard Trueblood
 Library

Commander
 Naval Underwater Systems Center
 New London, CT 06320
 G. C. Carter
 Library

Dr. C. Nicholas Pryor
 Technical Director
 Naval Underwater Systems Center
 Newport, Rhode Island 02840
 Library

Commanding Officer
 Naval Research Laboratory
 Washington, DC 20390
 Library

Commanding Officer
 Naval Air Development Center
 Warminster, PA 18974
 Library
 J. Howard, Code 205

Page

2
1
11
11
1
1

2

1

1
1

Page

University of Rhode Island
 Providence, RI 02903
 Dr. D. Tufts

1

Chief
 Office of Naval Research
 800 N. Quincy Street
 Arlington, VA 22217
 A. Sykes (222)

1

TRW
 Washington Operations Division
 7600 Colshire Drive
 McLean, VA 22101
 Dr. William Richter

1

Director
 Applied Research Laboratory
 P. O. Box 30
 State College, PA 16801
 Paul Kurtz
 Carter Ackerman

1

1

California Institute of Technology
 Pasadena, CA 91109
 Information Science 286-80 (Sheby)

1

Rockwell International, Space Division
 12214 Lakewood Boulevard
 Downey, CA 90241
 Ching-Quo Ho (SF12)

1

The Catholic University of America
 Washington, DC 20017
 Dr. T. Smits (EE)

1

Lincoln Laboratory
 Massachusetts Institute of Technology
 Lexington, MA 02173
 D. A. Shnidman

1

University of Texas at Austin
 Austin, TX 78712
 Prof. C. W. Horton

1

Bell Labs
 Whippany, New Jersey 07981
 G. H. Robertson

1

Technology Service Corp.
Santa Monica, CA 90401
R. L. Mitchell

Institute for Defense Analysis
400 Army-Navy Drive
Arlington, VA 22202
Library

The Energystics Corporation
4410 Executive Boulevard
Ft. Wayne, Indiana 46808

Magnavox Corporation
4624 Executive Boulevard
Ft. Wayne, Indiana 46808
R. Wagar

Purdue University
West Lafayette, Indiana 47906
Engineering Library

Rensselaer Polytechnic Institute
Troy, New York 12190
Library

Florida Technological University
Orlando, Florida 32716
L. C. Andrews

The Mitre Corporation
1820 Dolley Madison Boulevard
McLean, VA 22101

J. S. Lee Associates
11111 South Glen Road
Potomac, MD 20854

Naval Postgraduate School
Monterey, CA 93940
Library

Systems Control, Inc.
Palo Alto, CA 94306
J. LaPointe, Jr.

General Electric Co.
Aircraft Equipment Division
Utica, NY 13503
J. J. Gusselin

Tracor, Inc.
6500 Tracor Lane
Austin, TX 78721
F. Weidmann

Manager, ASW Systems Project Office
Department of the Navy
Washington, DC 20360
R. W. Bryant (ASW-132)
R. Delaney (ASW-138)

Commander
Naval Air Systems Command
Washington, DC 20361
E. Benson (AIR 53302F)

Planning Systems, Inc.
7900 West-Park Drive
Suite 507
McLean, VA 22101
Attn: Mr. Spooner

Defense Documentation Center
Cameron Station
Alexandria, Virginia 22314

1

1

1

1

1

12

TO AID IN UPDATING THE DISTRIBUTION LIST
FOR NAVAL SURFACE WEAPONS CENTER, WHITE
OAK LABORATORY TECHNICAL REPORTS PLEASE
COMPLETE THE FORM BELOW:

TO ALL HOLDERS OF NSWC/WOL TR 76-148
by L. E. Miller, Code 03-22

DO NOT RETURN THIS FORM IF ALL INFORMATION IS CURRENT

A. FACILITY NAME AND ADDRESS (OLD) (Show Zip Code)

WHITE OAK LABORATORY
NAVAL SURFACE WEAPONS CENTER
CONTINUED

NEW ADDRESS (Show Zip Code)

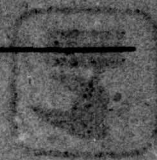
NAVY-NAVY WEAPONS CENTER

NAVY-NAVY WEAPONS CENTER

B. ATTENTION LINE ADDRESSES:

NAVY-NAVY WEAPONS CENTER
NAVY-NAVY WEAPONS CENTER
NAVY-NAVY WEAPONS CENTER

NAVY-NAVY WEAPONS CENTER
NAVY-NAVY WEAPONS CENTER



C.

☐ REMOVE THIS FACILITY FROM THE DISTRIBUTION LIST FOR TECHNICAL REPORTS ON THIS SUBJECT.

D.

NUMBER OF COPIES DESIRED